IMPACTS OF CLIMATE CHANGE ON RAINFED MAIZE PRODUCTION IN RIFT VALLEY LAKES BASINS OF ETHIOPIA; HAWASSA AS CASE STUDY

MSc.THESIS

BY

KINDE NEGESSA DISASA

HAWASSA UNIVERSITY, HAWASSA, ETHIOPIA

JUNE, 2017

IMPACTS OF CLIMATE CHANGE ON RAINFED MAIZE PRODUCTION IN RIFT VALLEY LAKES BASINS OF ETHIOPIA; HAWASSA AS CASE STUDY

A THESIS SUBMITTED TO THE SCHOOL OF WATER RESOURCES ENGINEEERNG, INSTITUTE OF TECHNOLOGY,

SCHOOL OF GRADUATE STUDIES

HAWASSA UNIVERSITY,

HAWASSA, ETHIOPIA

IN THE PARTIAL FULFILLMENT OF THE REQUIREMENTS FOR THE DEGREE OF

MASTER OF SCIENCE IN IRRIGATION AND DRAINAGE ENGINEERING

BY

KINDE NEGESSA DISASA

ADVISOR: SIRAK TEKLEAB (PhD)

CO-ADVISOR: ALEMAYEHU MULUNEH (PhD)

HAWASSA UNIVERSITY

SCHOOL OF GRADUATE STUDIES

ADVISORS' APPROVAL SHEET

(Submission Sheet-1)

This is to certify that the thesis entitled "**Impact Of Climate Change On Rainfed Maize Production In Rift Valley Lakes Basins Of Ethiopia; Hawassa As Case Study**" submitted in partial fulfillment of the requirements for the degree of **Masters** in science with specialization in **Irrigation and Drainage Engineering,** the Graduate Program of the **School of Water Resources Engineering,** and has been carried out by **Kinde Negessa** Id. No. **PGIDE 002/07**, under our supervision. Therefore we recommend that the student has fulfilled the requirements and hence hereby can submit the thesis to the school.

Sirak Tekleab (PhD)	_____	_____/____/___
Name of major advisor	Signature	Date
Alemayehu Muluneh (PhD)	_____	___/_____/___
Name of co-advisor	Signature	Date

HAWASSA UNIVERSITY

SCHOOL OF GRADUATE STUDIES

EXAMINERS' APPROVAL SHEET-2

(Submission Sheet-3)

As members of the Board of Examiners of the final Master's degree open defense, we certify that we have read and evaluated the thesis prepared by **Kinde Negessa** under the title "Impact Of Climate Change On Rainfed Maize Production In Rift Valley Lakes Basins Of Ethiopia; Hawassa As Case Study" and recommend that it be accepted as fulfilling the thesis requirement for the degree of **Masters** of science in **Water Resources Engineering** with **Specialization** in **Irrigation and Drainage Engineering.**

_____	_____	____/___/____
Name of Chairperson	Signature	Date
_____	_____	___/___/_____
Name of Major Advisor	Signature	Date
_____	_____	___/___/_____
Name of Co-advisor	Signature	Date
_____	_____	___/___/_____
Name of Internal Examiner	Signature	Date
_____	_____	___/___/_____
Name of External Examiner	Signature	Date

Final approval and acceptance of the thesis is in contingent upon the submission of the final copy of the thesis to the School of Graduate Studies (SGS) through the School Graduate Committee (SGC) of the candidate's school.

Thesis Approved by

_____	_____	_____/____/_____
SGCs	Signature	Date

Certification of the Final Thesis

I hereby certify that all the corrections and recommendations suggested by the Board of Examiners are incorporated into this Final Thesis entitled 'Impact of Climate Change on Rainfed Maize Production in Rift Valley Lakes Basins of Ethiopia; Hawassa As Case Study' by **Kinde Negessa**.

_____	_____	____/____/_____
Name of the Designate	Signature	Date

DECLARATION

I hereby, declare that the thesis entitled **"Impact Of Climate Change On Rainfed Maize Production In Rift Valley Lakes Basins Of Ethiopia; Hawassa As Case Study",** submitted to partial fulfillment for the Degree of Master of science with specialization in **Irrigation and Drainage Engineering** in Hawassa University is my own original work and has not been submitted earlier to any other institution for award of any type of academic degree. I also declare that no chapter of this document is in whole lifted and incorporated in this report from any earlier work done by others.

Therefore, I declare that this thesis is a work of my research investigations and findings. Sources of information I have used for this work have been properly acknowledged by inside citations and listed under reference.

Name: Kinde Negessa!

Signature _____

Date _____/_____/_____

ACKNOWLEDGMENTS

Above all, I Praise the name of all Almighty God Jesus for keeping me from all uncertainties, difficulties and brought me to the triumph and for his compassion for all what I have ever achieved.

My sincere gratitude goes to my thesis advisor Dr. Sirak Tekleab and my co-advisor Dr. Alemayehu Muluneh for their perpetual support and for entrusting me with the responsibility to carry out this research. Their guidance and support go through from preparing my research proposal till carrying out my research. I am thankful to Dr. Mulugeta Dadi for his close advice and support during research method course study.

Many thanks and long life hope go to my mother Likitu Fakansa and my father Negessa Disasa because they are reason for what I am today and where I am today, and My brother Amsalu Negessa paid many sacrifices for my success by encouraging and supporting me throughout my life.

My heartfelt thanks also go to Mr. Mesele Hailu Maize Research Sub Center Director at Hawassa branch, workers in National Meteorological Agency, workers in Southern Agricultural Research Institute and Agronomist working in Sidama zone for providing me proper data.

I would like to express my sincere gratitude to my financiers, Federal Democratic Republic of Ethiopia Ministry of Water, Irrigation and Electricity (MoWIE) and Oromia Water Works Construction Enterprise (OWWCE) giving me this full scholarship opportunity to advance my knowledge and skills. Finally I would like to say thank you to all my friends working in Oromia Water Works Construction Enterprise for their financial help and stand beside me throughout my research.

I love you all, May the Almighty God Jesus always bless you! Your success is my ambition!

LIST OF ABBREVIATION AND ACRONYMS

B: Biomass

$C0_2$: Atmospheric carbon dioxide concentration

CC: Canopy Cover

CDFs: Cumulative Distribution Functions

CERES: Crop Environment Resource Synthesis

CSA: Central Statistical Agency

DJF: December, January, February

DP: Discussion Paper

DSSAT: Decision Support System for Agro technology Transfer

Dr: Root zone depletion

E: Soil evaporation

EEA: Ethiopian Economy Association

EEPRI: Ethiopian Economy Policy Research Institute

EfD: Environment for Development

ETo: Reference evapotranspiration

FAO: Food and Agriculture Organization of the United Nations

FDRE: Federal Democratic Republic of Ethiopia

GCM: Global Circulation Model

GDD: Growing Degree Day

GDP: Gross Domestic Product

GHG: Green House Gas

Gs: Stomata conductance

HI: Harvest Index

IFPRI: International Food Policy Research Institute

ILRI: International Livestock Research Institute

IPPC: Intergovernmental Panel for Climate Change

I: Irrigation

JJA: June, July, August

Kcb: Crop Transpiration Coefficient

Ke : Crop evaporation

Kr: Reduction coefficient

Ks: Stress coefficient

KS: Kolmogorov-Smirnov

LAI: Leaf Area Index

LARS-WG: Long Ashton Research Station Weather Generator

MAE: Mean Absolute Error

MAM: March, April, May

MoA: Ministry of Agriculture

MOTP: Mean Observed Temperature-Precipitation

MoWR: Ministry of Water Resources

NAPA: Climate Change National Adaptation Programme of Action

NWP: Numerical Weather Prediction

NMA: National Meteorological Agency

OECD: - Organization for Economic Cooperation and Development

OWWCE: Oromia Water Works and Construction Enterprise

PASDEP: Plan for Accelerated Sustainable Development to End Poverty

PDFs: Probability Distribution Functions

RMSE: Root Mean Square Error

SDPRP: Sustainable Development and Poverty Reduction Program

SDSM: Statistical Down Scaling Model

SEI: Stock ham Environment Institute

SNNPR: South Nations Nationalities and Peoples Region

SNNPRS-RSA: South Nations Nationalities and Peoples Regional State-Regional Statistical Abstract.

SON: September, October, November

SRA: Scenario A

SRB: Scenario B

SRES: Special Report on Emission Scenarios

SSA: Sub-Saharan Africans

SWAP: Soil-Water-Atmosphere-Plant model

T_n: Minimum air temperature

T_r: Canopy transpiration

T_x: Maximum air temperature

UDS: United States Dollar

USDA: US Department of Agriculture

USGCRP: United States Global Change Research Program

WG: Weather Generator

WP:-Water productivity

WUE:-Water Use Efficiency

TABLE OF CONTENTS

Content **Page**

LIST OF TABLES

LIST OF FIGURES

LIST OF TABLES IN APPENDICES

LIST OF FIGURES IN APPENDICES

ABSTRACT

Agriculture is mainstay of Ethiopian economy. Developing country like Ethiopia suffers from effects of climate change, due to their limited economic capability to build irrigation projects to reduce climate change impact on crop production. This study evaluates climate change impact on rainfed maize production in rift valley lakes basins of Ethiopia. First, outputs of 15 General Circulation Models (GCMs) under two emission scenarios (SRA1B and SRB1) are statistically downscaled by using LARS-WG software. Probability assessment of bounded range with known distributions is used to deal with the uncertainties of GCMs' outputs. These GCMs outputs are weighted by considering the ability of each model to simulate historical records. The study result indicates that LARS-WG 5.5 model is more uncertain to simulate future mean rainfall than generating maximum and minimum mean temperatures hereby GCMs weight difference for rainfall mean is 0.83 whereas weight difference for minimum and maximum mean temperatures is 0.09. AquaCrop, version 4 developed by FAO that simulates the crop yield response to water deficit conditions, is employed to assess potential rainfed maize production in the study area with and without climate change. The study results indicate minimum and maximum temperatures absolute increase in the range of 0.34 ^{0}C to 0.58^{0}C, 0.94^{0}C to 1.8^{0}C and 1.42^{0}C to 3.2^{0}C and 0.32^{0}C to 0.56^{0}C, 0.91^{0}C to 1.8^{0}C and 1.34^{0}C to 3.035^{0}C respectively in the near-term (2020s), mid-term (2055s) and long-term (2090s) under both emission scenarios. The expected percentage change of rainfall during these three time periods considering this GCMs weight difference into account ranges from -2.3 to 7%, 0.375 to 15.83% and 2.625 to 31.1%. Maize yields are expected to increase with the range of 3.63% to 7%, 5.39% to 14.08%, and 6.83% to 15.61%, during the same time periods. Unlike many studies in the world this study result show that maize yield increased in coming three time periods under both emission scenarios. Due to rainfall increase with temperature increase maize yield is expected to increase in future for this study area by using only rainfall. In conclusion, the results indicate that climate change will respond positively to climate change impact on maize yield production for this district if all field management, soil fertility and crop variety improved; but since there is rainfall variability among the seasons planting date should be scheduled well to combat water stress on crops.

Keywords: *Climate change, GCM, IPCC AR4, LARS-WG, Uncertainty, Probabilistic prediction, AquaCrop, Yield.*

CHAPTER ONE

1. INTRODUCTION

1.1. Background of the study

"Agriculture is the mainstay of the Ethiopian Economy". This statement has almost become a cliché for development professionals in Ethiopia. The Report on the Ethiopian Economy, Volume IV (EEA/EEPRI, 2005) stated, for example: "…agriculture is the mainstay of the Ethiopian economy and the most volatile sector mainly due to its dependence on rain and the seasonal shocks that are frequently observed". As things stand, our children and grandchildren will be repeating this refrain for generations to come. Yet, the sector has been unable to realize its potential and contribute significantly to economic development.

According to PASDEP, (2006); in the Ethiopian context, agriculture is proving to be the most complex sector to understand. On the one hand, it contributes the largest share to GDP, export trade and earnings, and employs 84% of the population. On the other hand, despite such socio-economic importance, the performance of the sector is very low due to many natural and manmade factors. As a result, Ethiopia is characterized by large food self-sufficiency gap at national level and food insecurity at household level (EEA/ EEPRI, 2005). Agriculture, as is the case in much of the developing world, is still the largest sector in the Ethiopian economy contributing to about 50 percent to GDP and estimated to provide employment to most of the 85 percent of the country's population that reside in rural areas.

According to IPPC, (2007) climate change is considered to be the biggest challenge facing by the mankind in the twenty first century. The change in the climate mean state within a certain time period is referred to as climate variability which can be more detrimental than the climate change. Both climate variability and change can lead to severe impacts on different major sectors of the world such as water resources, agriculture, energy and tourism. Previous research on climate change impacts on crop production in different parts of the world agrees with the assertion that climate change has major implications for agricultural production in general and for maize yield in particular. Ethiopian agriculture is also affected by climate change either positively or negatively. In the United States and other developed nations, extensive studies on the impacts of climate change on agricultural production have been carried out (Cai et al.,

2009). There has been relatively little research in developing nations although recently, a few papers have been published (Schmidhuber and Tubiello, 2005, Chen et al. 2013, Herrero et al.2010). Yet, developing countries like Ethiopia are the ones which could suffer more from the effects of climate change, due to their limited economic capability for constructing irrigation projects to reduce climate change impact on crop production which based on rainfed and adaptive capacity. Being one of the least developed countries, Ethiopia's crop production can be affected by climate change impacts. Nevertheless, little is known about such impacts to date. Climate change is likely to affect the productivity of Africa's diverse agricultural and pastoral systems over the coming century. As these sectors underpin rural economic development, employing over 60% of the labor force, this poses a threat to rural livelihoods development and food security across the continent (FAO, 2002). Previous work, such as IPCC AR4 and other reviews has identified a potentially wide range (positive and negative) of impacts on agriculture at continental and some national levels. Studies highlight Africa's high level of vulnerability relative to other world regions, due to a large dependence on rainfed agriculture, low levels of development and adaptive capacity to existing climate variability.

In East Africa large water bodies and varied topography give rise to a range of climatic conditions, from a humid tropical climate along the coastal areas to arid low-lying inland elevated plateau regions across Ethiopia, Kenya, Somalia and Tanzania. The presence of the Indian Ocean to the east, and Lake Victoria and Lake Tanganyika, as well as high mountains such as Kilimanjaro and Kenya induce localized climatic patterns in this region (Herrero et al. 2010).

Gebreegziabher et al**.** (2011) conducted research on climate change and Ethiopian economy and they explained that agriculture in Ethiopia is heavily dependent on rain. In addition to its low adaptive capacity, its geographical location and topography make the country highly vulnerable to the adverse impacts of climate change. Results indicate that, over a 50-year period, the projected reduction in agricultural productivity may lead to 30 percent less average income, compared with the possible outcome in the absence of climate change. Understanding the potential economy-wide impacts of climate change for a given country is critical for designing national adaptation strategies, as well as formulating effective global climate-policy agreements. Developing countries particularly need to tailor adaptation policies to offset the

specific impacts they anticipate. Quantifying the impact of climate change on the overall economy can be crucial in guiding appropriate policy. Report from federal democratic republic of Ethiopia ministry agriculture, (2011) titled on Agriculture Sector Programme of Plan on Adaptations to Climate Change show that climate change is a key concern to Ethiopia in our time and need to be tackled in a state of emergency. It has brought an escalating burden to already existing environmental concerns of the country including deforestation, serious soil erosion and loss of top soil and land degradation which in turn have adversely impacted agricultural productivity. This phenomenon is occurring throughout the country and affecting every community although it may assume diverging degrees from place to place as the country has varied landscape featured by contrasting altitudinal ranges.

Small holder farmers and pastoralists of Ethiopia are continuously in a state of challenging state of affairs because of climate change impacts. This situation has forced them to make constant exertion to adapt to the unpredictable climate. In the near past, the community is severely challenged by the negative impacts of climate change and the community's ability to endure these changes is constrained by lack of infrastructure, inadequate institutional and financial capacity. Ethiopia, one of the world's centers of genetic diversity in crop germ plasm McCann, (2001), produces more of maize than any other crop (CSA, 2010). The area under maize cultivation in 2009/2010 was 1.69 million hectares from which 37.8 million quintals of maize were produced which was higher than that of any other cereal crop. From the country's total grain production, maize shares more than 27 percent (Samuel, 2006).

The study conducted in northwestern Turkey, indicates that winter wheat yields may decline by more than 20% due to climate change causing shorter growth periods and reduced precipitation Ozdogan, (2011). Similar studies within the same region determined that higher temperatures have a positive effect on crop yield. For instance, in northern China plain, corn, rice, potato, and winter wheat yields could increases with increasing temperature and precipitation under climate change.

1.2. Statement of the Problem

According to Federal Democratic Republic of Ethiopia Ministry of Agricultural (2011) report on agriculture sector programme plan on adaptation to climate change Ethiopia faced many adverse impacts which are unpleasant appearance of climate variable change. Yet there are

indications by which these impacts will continue to influence the socio-economic activities of the community at larger scale.

Deressa et al. (2008) made an integrated 35 quantitative vulnerability studies for seven regional states of the total eleven regions by using biophysical and social vulnerability indices of Ricardian approach. The study revealed that decline in rainfall and increase in temperature are both damaging to Ethiopian agriculture. Amongst all sectors (energy, agriculture, water, fisheries, livestock etc), agriculture is the most sensitive and vulnerable to climate change (IPCC, 1990). The second (IPCC, 1996) report predicted that tropical and subtropical regions would experience higher losses in crop production, while temperate climates might gain in productivity with climate warming. Issues of hunger and famine in Ethiopia are associated with low cereal crop production like maize as a result of poor rainfall what happens now days in Ethiopia once again. It is apparent therefore; that tropical/subtropical parts of nation are wholly relies on rainfed farming. Ethiopia food production could be greatly impacted by climate changes. Therefore, studying the potential impacts of climate change on rainfed maize production in Ethiopian would be necessary to take timely mitigating actions to minimize the undesirable impacts. Study on climate change impact on cereal crop production like maize is important in Ethiopia due to that Ethiopia is highly affected by climate even today which is related to El`Nino in 2015/2016, so no issue better than climate change impact initiate me to study now days in our country; thus the study would be fruitful because climate change is the current issue of the world as the whole and Ethiopia in particular.

1.3. Objective

The main objective of the study is to evaluate the impacts of climate change on rainfed maize production in rift valley lakes basins of Ethiopia. The study aim to achieve the following specific objectives:

- To predict future changes in temperature and rainfall (2020s,2055s and 2090s);
- To apply AquaCrop model in prediction of maize yield in Hawassa Zuria district, and
- To quantify impact of climate change on maize production in Hawassa *zuria* district.

CHAPTER TWO

2. LITERATURE REVIEW

2.1. Climate Change Impacts on Crop Production

There is no doubt that the earth's planet is warming as a result of greenhouse gasses (IPCC, 2007). If nothing is done to control for the burning of fossil fuels and changes in land concentrations of greenhouse gasses in the atmosphere will increase to great extent by the next century (IPCC, 2007; Mendelsohn, 2008). Climate change is expected to cause various effects on different sectors; however, the largest impact of global climate change was on agriculture (Nordhaus, 1991; Cline, 2007).

The USGCRP (2009) report indicates that despite an increase in crop yields as a result of technological improvements, extreme weather changes have negatively affected production in some years. The report argues that warmer temperatures not only shorten growth periods, they also lead to lower crop yields. Shorter growth periods may be appropriate in areas with soils of low moisture content; however this leads to accelerated growth in some varieties of crops like maize by shortening period of seed germination, crop growth and maturity. Ultimately, accelerated growth of crops results to a significant decrease in crop yields for a given amount of land which contradicts with my study result in which weather changes have positively affect maize yield because of rainfall increase with temperatures. Tubiello et al. (2002) agrees with the idea that climate change greatly affects agricultural crop production, even though the magnitude vary from one place to another and from one crop to another due to different natural and anthropogenic factors that contribute to climate change.

Based on result from Robert (2003) the research conducted on the effect of climate change on global Potato Production using historical data supplied by the Intergovernmental Panel on Climate Change Data Distribution Center (1999) for 25 different countries indicate that when no adaptation is allowed, overall simulated global potato yields decrease between 10% and 19% in 2010-2039, and between 18% and 32% in the 2050s. With adaptation, yields still go down but the decrease is about 40% less: between 5% and 11% in 2010-2039 and between 9% and 18% in 2040-2069. Adaptation typically consists of a shift of one or two months of the planting time and the use of cultivars that have later foliage senescence in terms of thermal time. Several studies indicate that increase in temperature negatively affects crop growth and

hence crop yields, however, the impact varies between crops and across regions since different crops respond differently to climate variability reviewed by (Thornton et al.2006; Mendelshon 2008) different studies that measure the magnitude of the impact of warming on farms in developing countries.

According to study conducted in U.S.A Kimball (1983) ascertained that increased amounts of carbon dioxide (CO2) can increase crop yields. However, this can be counteracted by a rise in temperature, leading to a reduction in crop yield overall. Cai et al. (2009) assessed climate change impacts on rainfed maize production in central Illinois, U.S. Study results indicate that under rainfed conditions, maize yields will decline by 23 to 34% in 2055 in central Illinois. In addition, if no adaptation measures are implemented, the study estimated a probability of 32 to 70% of not meeting 50% of the potential yield by the year 2055. Ringler et al. (2010) assessed Climate Change Impacts on food security in Sub-Saharan Africa using a comprehensive scenario which is based on ensembles of 17 GCMs. The study results depicted high temperatures and mixed changes in rainfall by the year 2050. The study also found that climate change would result in a decrease in crop yields excepting for millet and sorghum; with wheat exhibiting the largest decrease of 22% by year 2050.

You et al. (2009) carried out research in China and found out that an increase in temperature of 1°C during the growing period may lead to wheat production reduction of 3–10% and a decrease in winter wheat production of about 5%-35% Ozdogan (2011). Tao and Zhang (2010) determined that with higher temperatures, corn yields are likely to decrease by 2.4-45.6% in northern China plain. An average decrease in crop production of 15% may be incurred with higher temperatures and evapotranspiration rates despite constant precipitation, as a result of shorter crop growth periods which negatively affects time to crop maturity.

A recent study evaluated the agricultural responses to climate change in Iran's Zayandeh-Rud River Basin for a period of 2015-2035. The study considered four crops; wheat, barley, rice and corn, and determined that for an average monthly temperature increase of 1.1^0C to 1.5^0C and precipitation decrease of 11% to 31% within the basin, crop production would decrease as follows: 2.5% to 20.7% for wheat, 1.4% to 17.2% for barley, 2.1% to 9.5% for rice, and 5.7% to 19.1% for corn (Gohari et al., 2013).

Gebreegziabher et al. (2014) Study on environment for development point out that Climate change has significant negative impacts on Ethiopia's agriculture. From the crop production point of view, the study suggests that it is essential to introduce new crops/varieties that are more appropriate to hot and dry conditions and that will give farmers a hand in adapting to harsh climatic conditions. At the same time, profitable micro-irrigation systems, improved water and soil management, and appropriate meteorological information should be fostered.

2.2. Climate Change Prediction using Global Climate Models (GCMs)

General Circulation Models (GCMs) are "computer based version of earth's system that mathematically simulates the climate system and the interaction between the system components" (Hassan, 2012). They simulate historical, present and future climate scenarios taking into account the level of greenhouse gases and aerosols under different future projections. The process is achieved by dividing the oceans and atmosphere into a horizontal grid with a horizontal resolution of 2^0- 48^0 with 10-20 layers aligned vertically. This enables predictions of climate change for the next 100 years using a coarse grid scale (IPCC, 2001). In general, most GCMs are capable of simulating global and continental scale processes in detail and provide a reliable representation of the average planetary climate (Hassan, 2012).

Global climate models "are the only credible tools currently available for simulating the response of the global climate system to increasing greenhouse gas concentrations" (IPCC-TGCIA 2007.GCMs are fully coupled mathematical representations of the complex physical laws and interactions between ocean/atmosphere/sea-ice/land-surface (Smith and Hulme 1998). They simulate the behavior of the climate system on a variety of temporal and spatial scales using a three-dimensional grid over the globe**.**

A high level of confidence can be placed in climate models based on the fact that they are (Randall et al., 2007): First, fundamentally based on established physical laws, such as conservation of mass, energy and momentum, along with numerous observations; Second, able to simulate important aspects of the current climate; and, Third, able to reproduce features of past climates and climate changes. Climate models have accurately simulated ancient climates, such as the warm mid-Holocene of 6000 years ago and trends over the past century combining both human and natural factors that influence climate.

GCM experiments simulate future climate conditions based on estimated warming effects of carbon dioxide (CO2) and other GHGs and the regional cooling effects of increasing sulphate aerosols, beginning in the late 19th century or early 20th century using scenarios of future radiative forcing.

2.3. Climate Change Emission Scenarios

The Intergovernmental Panel on Climate Change Third Assessment Report (IPCC-TAR) (IPCC 2001b) published forty different emission scenarios provide a range of future possible GHG emissions and atmospheric concentrations from socio-economic scenarios labeled SRES (Special Report on Emission Scenarios) (Nakicenovic et al. 2000). The SRES describes 4 narrative storylines (i.e. A1, A2, B1 and B2) which represent different demographic, social, economic, technological, and environmental and policy future, as emission drivers. The SRES emissions scenarios are the quantitative interpretations of these qualitative storylines. Typically of interest are the pre-industrial control experiments, which run for long periods holding the forcing agents at fixed levels of the year 1850. They are used assess the GCMs ability to reproduce historical natural climate variability and also provide reference for the 20th Century and SRES experiments. The 20th Century experiment begins in the middle of the 19th century continuing to the end of the 21st century with the forcing agents representing the historical (or estimated) record.

Climate models project future climate based on different emission scenarios, each based on a specific set of assumptions (Shaka, 2008). These assumptions include future trends in energy demand, emitted greenhouse gases, changes in land use and behavior of climate system over a long period of time (Houghton et al., 2001).

Figure1 below presents a schematic representation of the four major emission scenarios as per the Special Report on Emission Scenarios (SRES) (IPCC, 2007). These scenarios (A1, A2, B1 and B2) make different assumptions about future population increases, economic and technological developments, energy and land use, and the global approaches to sustainability which differently affects emissions of greenhouse gasses. In general, scenario A prioritizes economic development, whereas scenario B is more concerned with environmental sustainability. Numbers “1” and “2” represent different technological advancements within storylines, with “1” representing a much faster and diverse development and “2” representing a

slower and regional development (IPCC, 2007). To put it another away, a future that is more concerned with addressing global problems and sustainable environment is represented by scenario B1. On the other hand, a future in which nations prioritize their regional development, leading to unsustainable and unequal economic growth is represented by scenario A2 (Anderson et al., 2008). This study focused on "1" which faster economic development and faster and diversified environmental sustainability.

Table 1 shows a summary of the driving forces for the 2020, 2055 and 2100 timelines leading to the development of A1, A2, B1 and B2 scenarios. Table 2 gives a brief description of the major characteristics of each scenario.

Table 1: Driving forces for emission scenarios for 2020, 2050 and 2100 timelines (Reproduced from SRES)

scenario	A1	A2	B1	B2
Population (billion)(1990;5.3)				
2020	7.6	8.2	7.6	7.6
2050	8.7	11.3	8.7	9.3
2100	7	15.1	7	10.4
World GDP(10^{12} USD/year(1990;1)				
2020	57	41	53	51
2050	187	82	136	110
2100	555	243	326	235
Per capita income ratio: developed countries and economies in transition (Kyoto Treaty Annex 1) to developed countries (Kyoto Treaty non-Annex 1) (1990;6.1)				
2020	6.2	9.4	8.4	7.7
2050	2.8	6.6	3.6	4
2100	1.6	4.2	1.8	3

Table 2: Characteristics of the major emission scenarios (IPCC SRES, 2000)

Scenario Group	A1B	A2	B1	B2
Population growth	low	low	low	medium
GDP growth	Very high	Very high	high	medium
Energy use	Very high	high	low	medium
Land use change	low	low	high	medium
Oil/Gas resource Availability	medium	medium	low	medium
Technological change	rapid	rapid	medium	medium
Change favoring	balanced	Non-fossil fuel	Efficiency and Dematerialization	"dynamics as usual"

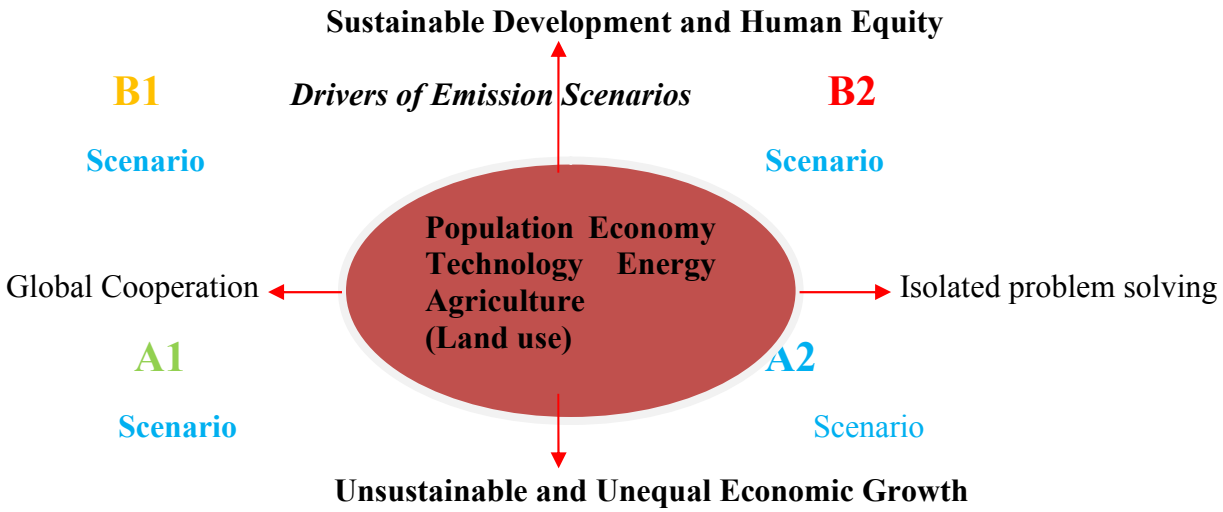

Figure 1: Major emission scenarios (source, Anderson et al., 2008)

Two commonly used emission scenarios used in my studySRA1B and SRB1, are considered here in the analysis of the impacts of future climate change on maize yield. Table 3 below provides a description of these two scenarios.

Table 3: Description of the two emission scenarios used in this study (IPCC- 4th Assessment Report)

Scenario	Description
SRA1B	Characterized by very rapid economic growth (3%/yr), low population growth (0.27%/yr) and rapid introduction of new and more efficient technology. Globally there is economic and cultural convergence and capacity building, with a substantial reduction in regional differences in per capita income.
SRB1	Rapid change in economic structures, 'dematerialization' including improved equity and environmental concern. There is a global concern regarding environmental and social sustainability and more effort in introducing clean technologies. The global population reaches 7 billion by twenty first century.

2.4. Downscaling GCMs Outputs

Global Circulation Models (GCMs) have been developed to predict average large-scale phenomenon of atmospheric weather (Holton, 1992). GCMs are quite capable of simulating global climatic data at continental and hemispherical scales, but have limited capacity in simulating local weather features and dynamics at sub-grid scale (Carter et al., 1994). Outputs from climate models cannot be used directly in climate studies at local level due to the existence of a mismatch in spatial resolution between GCM outputs and regional hydrological/statistical models, in addition to the large coarse resolution of GCMs, compared to hydrologic/statistical models that use very fine spatial resolutions. Despite future GCMs runs on high resolution, there will still be a need to downscale the outputs so that they match the local sites before being further used in climate change studies. Downscaling therefore converts the coarse spatial resolution of any GCM outputs to a fine spatial resolution by generating local data from GCM outputs. This is done by linking global scale predictions to regional dynamics in order to generate climate variables specific to a particular site. Downscaling can be done using different approaches, including: (i) nesting a regional climate model into an existing GCM, (ii) statistical regressions and (iii) Using stochastic weather generators (which was used in this study due to the following reasons).

The first method of downscaling entails identifying a specific area and applying some driving factors from a GCM to the regional climate models. This method is also referred to as dynamic downscaling because regional climate models are dynamic models like GCMs, even though they exist in three layers. The first layer operates through a GCM; the second layer uses the local data for the specified area; and the third layer mathematically generates results based on the previous two layers. The output is moderately local data driven by both global models and regional specifics. The complexity of the models used makes the process challenging and less attractive. The main advantage of this technique is that it better simulates extreme climate events like floods and droughts and climate anomalies at regional scale (Fowler et al., 2007).

Statistical regression involves using different regression methods to link local climate data to specific drivers in GCMs. First, a relationship between large scale variables (driving factors of GCMs) and climate variables at local scale is established. The established relationship is then used to predict future climate variables under various situations as stipulated by GCMs. In other words, regression models entail establishing "linear or nonlinear relationships between sub grid scale (e.g. single-site) parameters and coarse-resolution (grid-scale) predictor variables" (Hassan, 2012).

Stochastic weather generators (WGs, which is used in my study) are statistically driven. WGs generate statistical linkages within climate variables in order to simulate present and future weather conditions of a specified station or area, using the historical observed climate variables of that station/area. Some of the models used in statistical methods include: USCLIMATE WGEN, LARS–WG, CLIMGEN, GEM and SDSM. In recent years, several studies have been done on the impacts of climate change and the prediction of climate variables using down-scaling statistical models in the world. Mavromatis and Hansen (2001) comparing WM, WM2 and LARS-WG models showed that LARS-WG model has produced data in a more acceptable level of confidence (95%). Semenov (2008a) using LARS- WG model studied temperature and precipitation at 20 stations in the UK, which were located in different climates. The results showed the high ability and accuracy of the LARS WG model. Rajabi et al (2010) compared the results of two exponential down-scaling models SDSM and LARS-WG, (this is the reason that make me to choose LARSWG model rather than the others) in Kermanshah. The results showed the better performance of LARS-WG model in the study region. Chen et al (2013)

used the LARS-WG model and the A2 scenario to predict precipitation, minimum temperature and maximum temperature in Sudan and South Sudan. The results showed the good performance of the model in predicting daily data.

2.5. Uncertainty analysis

Uncertainties affect the trustworthy of the outputs, and the subsequent climate impact assessment studies. Outputs from GCMs are often an extreme range of low and high values of climate variables, causing the results infeasible for further assessment studies (Cai et al., 2009). Three major factors contribute to uncertainty of GCMs are first differences in emissions scenarios derived from projections of economic activity, population growth, and technological development; second sensitivity of global climate to greenhouse gas forcing; third regional variability, which occurs between models of different regional responses (RRs) and within models of chaotic behaviors and modes of climate variability (Hunting ford et al., 2005; Cai et al., 2009).

Numerous methods for dealing with uncertainties of GCMs have been proposed, some of which include (i) using a central prediction with error bars, (ii) expressing the results as a central prediction, (iii) using a bounded range with known probability distribution and (iv) by using a bounded range with larger range of unknown probabilities (OECD, 2003). In this study, a bounded range with known probability distribution was used (Gohari et al., 2013) to deal with the uncertainties of fifteen (15) GCMs because it is the most used technique in climate change impact studies in different countries. This technique requires the execution of three steps which are listed below.

2.6. Baseline Period Data Selection

The baseline period is the reference period on which calculation of future climate changes is based. Definition of the baseline period is important in order to select the observed climate dataset that combines with climate change information to generate climate change projections (Houghton et al., 2001). Carter et al. (1994), Mohammed (2009) and Hassan (2012) outline four criteria that are commonly used in selection of the baseline period.

1. The baseline period must truly represent the current or recent averages of climate conditions within the area.

2. The baseline period must be sufficiently long and cover a wide range of climate variations, including extreme weather conditions.
3. The suitable baseline period is the one for which the major climatic data like rainfall (precipitation), temperature, sunshine and relative humidity are readily available, easily accessible and adequately distributed over space.
4. The baseline period should have high quality climate data (with few missing data, if any).

Based on these four selection criteria mentioned a baseline period of 30 years meteorological data from (1985-2014) was used to generate synthetic weather data.

2.7. Crop Model

Several studies have been conducted to evaluate the impacts of climate change on crop production using crop simulation models. Examples of crop models that have been frequently applied thus far include: CERES-Wheat (Crop Environment Resource Synthesis) (Godwin et al., 1989; Jones et al., 2003), DSSAT (Hoogenboom et al., 1994) SWAP (soil–water–atmosphere–plant model) (van Dam et al., 1997), CERES-Maize (corn) (Jones & Kiniry, 1986), Crop Syst (Stöckle et al., 2003), CropWat (Allen et al., (1998), and Info Crop (Singh et al., 2005a). Of these models, three are said to have a strong emphasis on interactions between crop, water and climate change, namely (i) CropWat, (ii) AquaCrop and (iii) SWAP (Aerts and Droogers, 2004). These three models have been widely used and tested in different climate change impact studies worldwide, have a user-friendly interface, and are openly accessible. In this study the FAO (Food and Agriculture Organization) AquaCrop Version 4 was used (Steduto et al., 2009) to estimate maize production in the study area under different climate scenarios. AquaCrop provides an improved and powerful approach for assessing crop yield response to water deficit. This model has been developed and recommended by the FAO for several reasons: requires less climate data than most crop models, has a user-friendly interface, has a strong focus on relationships amongst climate change, carbon dioxide, water and crop yields, and it has a large number of users globally (Steduto et al., 2009). Numerous validation tests for AquaCrop have been carried out in different parts of the world.

2.7.1. Model selection

Potential impacts of climate change on world food supply have been estimated in several studies (Parry et al., 1999). Results show that some regions may improve production, while others suffer yield losses. This could lead to shifts of agricultural production zones around the world. Furthermore, different crops are affected differently, leading to the need for adaptation of supporting industries and markets. Climate change may alter the competitive position of countries with respect, for example, to exports of agricultural products. Some of the frequently applied agricultural models are: CropWat, AquaCrop, CropSyst, SWAP/WOFOST, CERES, DSSAT, and EPIC

Each of these models is able to simulate crop growth for a range of crops. The main differences between these models are the representation of physical processes and the main focus of the model. Some of the models mentioned are strong in analyzing the impact of fertilizer use, the ability to simulate different crop varieties, farmer practices, etc. However, for this study I want to use models with a strong emphasis on **crop-water-climate** interactions. The three models that are specifically strong on the relationship between water availability, crop growth and climate change are CropWat, AquaCrop and SWAP/WOFOST. Moreover, these three models are in the public domain, have been applied world-wide frequently, and have a user friendly interface, but Aquacrop model was selected because of limited data requirements, a user-friendly interface enabling non-specialist to develop scenarios, focus on climate change, CO2, water and crop yields, developed and supported by FAO, fast growing group of users' world-wide and flexibility in expanding level of detail.

2.8. Calculation Procedure of AquaCrop model

The algorithm and calculation procedures of AquaCrop place more emphasis on the soil water balance (Steduto et al., 2009). The model uses a set of equations to simulate soil water movement and root water uptake. The equations describe the dependent variable θ (soil water content), using dimensionless drainage coefficient τ, which is obtained from Ksat (hydraulic conductivity at saturation) for vertical flow of water in the soil profile (Raes et al., 2006). The soil profiles in AquaCrop are grouped into smaller fractions and this is done in order to nearly accurately describe the movement, retention and water uptake of the soil during the growing season. In total, the model comprises 12 soil compartments each of which measure 0.1m thick (Az). Depending on the crop and soil type, the size of each compartment is adjusted to cover

the entire root zone. Each of these soil compartments has different hydraulic characteristics depending on the type of soil associated with a particular compartment (Steduto et al., 2009). Soil drainage, surface runoff and infiltration, soil evaporation, crop transpiration and biomass production are discussed as follow in context of AquaCrop model.

2.8.1. Drainage

Drainage of water in each soil compartment occurs when water content θ, is above field capacity, FC. The amount of water that drains from compartment *i,* at time step Δt, is expressed by exponential drainage function, which considers water content θi and the drainage properties of the soil (Raes, 1982; Raes et al., 1988; 2006)

$$\frac{\Delta\theta_i}{\Delta_t} = \tau(\theta_{sat} - \theta_{FC}) \frac{e^{\theta_i - \theta_{FC-1}}}{e^{\theta sat - \theta_{FC-1}}} \text{ ----------1}$$

Where $\frac{\Delta\theta_i}{\Delta_t}$ is the decrease in soil water content θ during Δt ($m^3m^{-3}d^{-1}$), τ is the drainage coefficient, θsat is volumetric water content at saturation, and θFC is the field capacity. As the value of τ becomes close to 1, a fully saturated soil will drain the fastest (approximately between 1 to 2 days); conversely, smaller values of τ (τ <1) decreases water drainage capabilities of the soil. Numerous studies indicate that AquaCrop perfectly mimics the infiltration and drainage patterns that occur in *in situ* field observations (Descheemaeker, 2006; Raes et al., 2006; Geerts et al., 2008). To simulate drainage in a soil profile containing many and different compartments, the drainage ability $\frac{\Delta\theta_i}{\Delta_t}$ of each compartment is considered. An assumption is made that the total drainage occurring in soil compartments at the top, will pass through lower compartments so long the compartments at the bottom have greater or equal drainage characteristics with compartments at the top. If a compartment at the bottom has less drainage capabilities than the one at the top, excess water is store within the compartment thereby increasing its water content and subsequently its drainage ability.

2.8.2. Surface Runoff and Infiltration

To simulate surface run off, AquaCrop employs the Curve Number Method proposed by USDA (1964), Rallison (1980) and Steenhuis et al. (1995). The Curve Number, abbreviated as CNII, is adjusted according to the wetness of the top layer of the soil. Smedema and Rycroft (1983) uses some derived relationships for curve number values for "antecedent moisture class" (AMC) I (dry), II and III (wet), in which a soil depth of about 0.3m is considered for

determining AMC. For simplicity, surface runoff resulting from crop irrigation is considered to be zero. If the surface runoff through irrigation is significant, the model requires that the user inputs the net water application.

On the other hand, water infiltration (through irrigation or rainfall) into the soil compartments is limited by the saturated hydraulic conductivity (Ksat) of the soil in the top layer. Depending on the drainage characteristics of the soil compartments, storage of water occurs simultaneously with drainage, from top to bottom compartments (Steduto et al., 2009).

2.8.3. Soil Evaporation

In AquaCrop, soil evaporation occurs in two stages: an energy limiting stage (Stage I) and a falling rate stage (Stage II) (Philip, 1957; Ritchie, 1972). In stage I, the readily evaporable water (REW) is estimated using Equation 2.

$$REW = 1000(\theta_{FC} - \theta_{air\ dry}) * z_{c,surf} \text{ ----------2}$$

Where θFC is water content at field capacity, $\theta_{air\ dry}$ is the soil water content (m^3m^{-3}) when air dried, and $Z_{C,surf}$ is the thickness (m) of the evaporating surface. The U value of Ritchie (1972) that binds the relationship between REW and cumulative evaporation for Stage it was determined by assuming that the value of $\theta_{air\ dry}$ equal half the value of permanent wilting point θ_{PWP}, and $Z_{C,surf}$ equals 40mm. Thus evaporation is limited to the energy limiting stage, so long REW remains in surface layer, and the rate of evaporation is the maximum rate. However, when REW is depleted in Stage I, then evaporation occurs in the falling rate stage (Stage II). This results in flow of water from bottom to surface layer of the soil (Ritche, 1972, Raes, 2009). Soil evaporation for both energy limiting and falling rate stages is determined using the equation 3.

$$E = K_r\ x\ E_x = K_r\ x\ K_{C_{e,Wet}}\ X\ ET_0 \text{ ----------3}$$

Where, Ex is the maximum rate of evaporation, $K_{C_{e,Wet}}$ is evaporation coefficient for fully wet and bare soil surface, ETO is reference evapotranspiration, and Kr is the dimensionless evaporation reduction coefficient. For stage I, Kr is set at 1, but decreases to values lower than 1 as evaporation switches from stage I to stage II. As soil water content diminishes, so does its hydraulic conductivity. To account for the decline in hydraulic conductivity, the model uses an exponential function as shown in Equation 4 (Allen et al., 1998).

$$0 = K_r = \frac{e^{f_k x W_{rel}} - 1}{e^{f_k - 1}} \leq 1 \text{ ----------4}$$

Where f_K is the decline factor, and W_{rel} is the relative water content of the soil layer. Ritchie (1972) discovered that when $f_k = 4$, there exists a "good fit between the square root of time approach and the soil water content approach used by AquaCrop in the simulation of stage II evaporation". Kr varies sturdily with W_{rel} and is estimated using Equation 4 above.

Canopy cover impacts on the magnitude of evaporation. For a soil that is covered by crop canopy, the rate of evaporation (Ex) in the energy limiting stage (stage I) is estimated using Equation 5.

$$E_x = (1 - CC^*) x\ K_{Ce,wet}\ x\ ET_0 \text{ ----------5}$$

Where CC* is the portion of soil surface covered and adjusted for micro-advective effects, and is estimated using Equation 6 (Adams et al., 1976; Villalobos and Fereres (1990).

$$CC^* = 172\ x\ CC - CC^2 + 0.3\ x\ CC^3 \text{ ----------6}$$

As canopy cover (CC) senesces (grows old) due to phenology or water stress as a result of Ex, Ex is estimated using Equation 7.

$$E_x = (1 - CC^*) x \left(1 - f_{CC}\ x\ CC_{top}\right) x K_{Ce,wet}\ x\ ET_0 \text{ ----------7}$$

Where fcc is the adjustment factor expressing the sheltering effect of the dead canopy cover, and CCtop is the canopy cover before the senescence. At maximum canopy cover, CCtop = CCx, the maximum canopy cover.

2.8.4. Crop Transpiration

For a well-watered field, crop transpiration is proportional to the canopy cover and is estimated using Equation 8.

$$Tr_x = CC^*\ x\ K_{Ctr,x}\ x\ ET_0 \text{ ----------8}$$

where CC* is the adjusted canopy cover as in Equation 16, and Kctr,x is the coefficient for maximum crop transpiration. After maximum canopy cover (CCx) has been attained, the crop begins to age slowly, consequently transpiration declines. To account for this phenomenon, an adjustment factor fage is multiplied to $K_{Ctr,x}$, leading to the adjusted coefficient of transpiration $K_{Ctr,adj}$. As senescence continues, crop photosynthesis and transpiration remarkably drops, and another adjustment factor that accounts for senescence fsen, is applied

to $K_{Ctr,adj}$ (fsen =1 at start of scenescence (when CC=CCx) and 0 where no canopy exists). These relationships are shown in Equations 9 to 11.

$$Kc_{tr,sen} = f_{sen}\ x\ Kc_{tr,adj} \text{ ----------9}$$

Where

$$f_{sen} = \left[\frac{CC}{CC_X}\right]^{\alpha} \text{ ---------- 10}$$

and

$$Tr_x = CC^*\ x\ Kc_{tr,sen}\ x\ ET_0 \text{ ----------11}$$

where α is a program parameter and is used to decrease (α<1) or increase (α>1) the reduction efficiency of transpiration and photosynthesis of the aging canopy (Raes et al., 2009).

2.8.5. Biomass Production

According to Steduto et al. (2009), biomass (B) above the ground is derived from transpiration through crop water productivity (WP) normalized for reference evapotranspiration (ETo) and carbon dioxide (CO2). Considering effects of low temperatures, chemical properties of harvestable parts of the plant, and modifications of dimensionless factors, the daily above ground biomass (m) is estimated using Equation 12.

$$m = Ks_b\ x\ f_{WP}\ x\ \left|\frac{T_r}{ET_0}\right| \text{ ----------12}$$

where Ksb is the stress coefficient accounting for effects of low temperature on biomass production, fWP is the adjustment factor (fWP ≤1) accounting for differences in chemical composition of biomass and harvestable parts, Tr and ETo are crop transpiration and reference evapotranspiration respectively.

2.8.6. Response of Harvest Index (HI) to Water Stress

As discussed above, final crop yield (Y) is the product of final biomass (B) and harvest index (HI). Steduto et al. (2009) outlines the effects of water stress on HI. As flowering or formation of tuber commences, HI is programmed to increase until plant maturity. The value of HI at plant maturity under no stress conditions is referred to as reference harvest index (HIo) for a specific crop type. The impact of water stress on HI depends on its severity and time of occurrence, with the reproductive stage being the most crucial phase. However, if crop growth continues, water stress may lead to a reduction in leaf growth thereby increasing the HI.

Equation 13 indicates that the rate of increase $\left[\frac{dHI}{dt}\right]$ of harvest index (HI) is expedited when the maximum canopy cover is reached and the value of Ks_{exp} is less than 1.

$$\frac{dHI}{dt} = \left[1 + \frac{1-KS_{exp,t}}{\alpha}\right] x \left[\frac{dHI}{dt}\right]_0 \text{----------13}$$

where, ($\frac{dHI}{dt}$) is the rate of increase of HI for non stress conditions, α is the adjustable crop parameter, and Ksexp,t is the adjustment factor for the competition between vegetative and reproductive growth after flowering begins at time t. Even though growth of canopy cover is complete, Equation 13 is still applicable so long as crop growth continues.

Crop response to water stress includes reduction in leaf growth and closure of stomata. This slows down the increase in HI whose rate of increase is described in Equation 14.

$$\frac{dHI}{dt} = \sqrt[10]{Ks_{sto}}\left[1 - \frac{1-Ks_{exp,t}}{b}\right] x \left[\frac{dHI}{dt}\right]_0 \text{----------14}$$

where *b* is the adjustable crop parameter, and is the adjustment factor for stress that leads to stomata closure and reduction in photosynthesis.

When water stress is so severe to allow pollination to occur, harvest index is represented by the relationship shown in Equation 15 below.

$$HI_{o,adj} = \left[\sum\left(Ks_{pol}\, x\, \alpha\, xF\right)\right] xHI_o \;\leq\; HI_o \text{----------15}$$

where, $HI_{o,adj}$ is the HI_o adjusted for the reduction in pollination caused by stress, Kspol is the water stress coefficient for pollination on a given day, F is the fraction of the total number of potentially successful flowers going through anthesis on that day, and α is a factor allowing for the effects of excessive sinks (Raes et al., 2009).

CHAPTER THREE

3. MATERIALS AND METHODS

3.1. Description of Study Area

3.1.1. Location of Study Area

This study was conducted in Hawassa *zuria* district which surrounds Hawassa town the capital of SNNPR that constitutes different land forms, which can be broadly divided into highlands and low lands. The East African Rift valley bisects the highland plateaus in to two physiographic regions i.e. east and west. In the east, there are highland plateaus of Sidama, Burji and Amaro lying between 2300 to 3338 meters above sea level (masl). To the west of the rift valley, there are also major highland plateaus of Gurage, Kaffa, Dawro and Gamogofa that rise from 2500 to 4200 meters above sea level (m.a.s.l) (SNNPRS–RSA 2006). The study site is located in east of the rift valley in sidama zone; Hawassa *zuria* district as case study site. Hawassa *zuria* district is located in the Great Rift Valley of Ethiopia and at 273km distance from Addis Abeba capital city of Ethiopia. It covers latitudinal area from 6.95^0N to 7.13^0N and longitudinal area 38.5^0E to 38.73^0E. Total urban and rural population of Hawassa district is 123,494 and 375,041, totxaling 498,534 (SNNPRS–RSA 2006). The selection of the study area depends on the area where maize production is high in Hawassa *Zuria* district which is nearest to Hawassa town since daily 30 years meteorological data are collected from Hawassa station that represents Hawassa zuria district weather conditions. Figure 2 below indicates map of study area; from Ethiopia map to sidama zone; from sidama zone to Hawassa *zuria district* where the study was conducted.

3.1.2. Soils Type

There are many types of soils in Hawassa *zuria* district but the soil type prevailing in the study area is Andosols (a black or dark brown soil formed from volcanic material, with an A horizon rich in organic material). Soil property of the area is characterized by wilting point of 18.5% and field capacity of 34.8% with no restrictive soil layer and soil salinity stress. The depth to the static groundwater level varies from a few meters in the low-lying areas to up to 40m deep in elevated areas (Ayenew and Tilahun, 2008). Soil electrical conductivity and bulk density of the area are 0.113 ds/m and 0.96 g/cc respectively.

3.1.3. Crop and Climate

Hawassa *zuria* has an annual average rainfall of 955mm with mean annual temperature of 20^0C (SNNPRS–RSA 2006). The main rainy season generally extends from June to October. Unlike most *woredas* of the Sidama Zone, major crops grown in the area are not cash crops but rather food crops like cereals (maize) and enset.

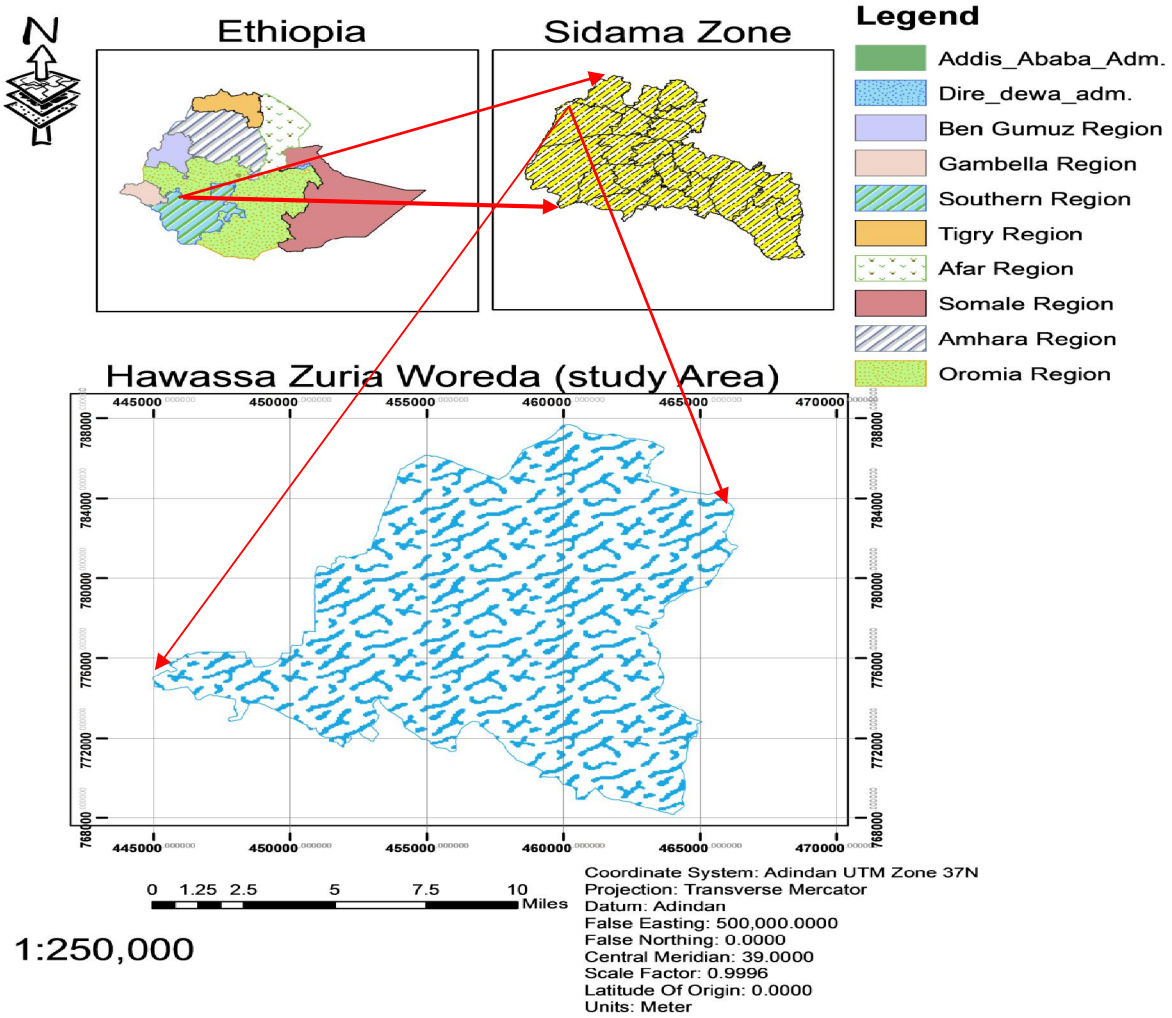

Figure 2: Map of the study area

3.2. Description of Long Ashton Research Station Weather Generator (LARS-WG)

Long Ashton Research Station Weather Generator (LARS-WG Version 5.5, to date version) was used for this study to simulate future weather data for Ethiopia and the model used data of southern region of Ethiopia specifically Hawassa zuria district as a case study. LARS-WG is implemented in C++ with full Windows interface and is freely accessible at **http://www.rothamsted.ac.uk/mas-models/larswg.php** (by providing LARS-WG specific site derivatives e.g. site parameter and diagnostics files, with the research community). The model simulates weather data at a single site under current and future conditions (Racsko et al., 1991). LARS-WG Version 5.5 also includes fifteen (15) General Climate Models (GCMs) which have been used in the IPCC 4th Assessment Report (2007). Each of the models comprises at least three of the following scenarios: SRA1B, SRA2 and SRB1, for three time periods (2020s, 2055s and 2090s) of which this study used two emission scenarios; SRA1B and SRB1 for faster technological and environmental extreme respectively. The simulated data from the model are in form of daily time-series for the following climate variables (Semenov and Barrow, 2002).

- maximum and minimum temperature (°C),
- precipitation (mm) and
- Solar radiation in Mega joule per square meter per day (MJ/m2/day)

Table 4 presents General Climate Models (GCMs) incorporated in LARS WG 5.5 with their respective grid resolution, emission scenarios and time periods based on baseline.

Table 4: Global climate models from IPCC AR4 incorporated into the LARS-WG stochastic weather generator version 5.5 used in this study. B: baseline; T1: 2011–2030; T2: 2046–2065; T3: 2080–2099 (Mikhail A. Semenov, and Pierre Stratonovitch, 2010)

Research Centre	Country	Global Climate Model	Model Acronym	Grid Resolution	Emission Scenarios	Time Periods
Commonwealth Scientific and Industrial Research Organization	Australia	CSIRO-MK3.0	CSMK3	1.9 × 1.9°	SRA1B, SRB1	B, T1,T2,T3
Canadian Centre for Climate Modelling and Analysis	Canada	CGCM33.1 (T47)	CGMR	2.8 × 2.8°	SRA1B	B, T1,T2,T3
Institute of Atmospheric Physics	China	FGOALS-g1.0	FGOALS	2.8 × 2.8°	SRA1B, SRB1	B, T1,T2,T3
Centre National de Recherches Meteorologiques	France	CNRM-CM3	CNCM3	1.9 × 1.9°	SRA1B, SRA2	B, T1,T2,T3
Institute Pierre Simon Laplace	France	PSL-CM4	IPCM4	2.5 × 3.75°	SRA1B, SRA2, SRB1	B, T1,T2,T3
Max-Planck Institute for Meteorology	Germany	ECHAM5-OM	MPEH5	1.9 × 1.9°	SRA1B, SRA2, SRB1	B, T1,T2,T3
National Institute for Environmental Studies	Japan	MRI-CGCM2.3.2	MIHR	2.8 × 2.8°	SRA1B, SRB1	B, T1,T2,T3
Bjerknes Centre for Climate Research	Norway	BCM2.0	BCM2	1.9 × 1.9°	SRA1B, SRB1	B, T1,T2,T3
Institute for Numerical Mathematics	Russia	INM-CM3.0	INCM3	4 × 5°	SRA1B, SRA2, SRB1	B, T1,T2,T3
UK Meteorological Office	UK	HadCM3	HADCM3	2.5 × 3.75°	SRA1B, SRA2, SRB1	B, T1,T2,T3
		HadGEM1	HADGEM	1.3 × 1.9°	SRA1B, SRA2	B, T1,T2,
Geophysical Fluid Dynamics Lab	USA	GFDL-CM2.1	GFCM21	2.0 × 2.5°	SRA1B, SRA2, SRB1	B, T1,T2,T3
Goddard Institute for Space Studies	USA	GISS-AOM	GIAOM	3 × 4°	SRA1B, SRB1	B, T1,T2,T3
National Centre for Atmospheric Research	USA	PCM	NCPCM	2.8 × 2.8°	SRA1B, SRB1	B, T1,T2,
	USA	CCSM3	NCCCS	1.4 × 1.4°	SRA1B, SRA2, SRB1	B, T1,T2,T3

3.2.1. Input Data for LARS-WG

The following weather data (in time series) are required as inputs to the model;

- Minimum temperature (°C)
- Maximum temperature (°C)
- Precipitation (rainfall) (mm)
- Solar radiation (MJ/m2/day)

In the absence of solar radiation, the model accommodates the use of sunshine hours. LARS-WG automatically converts the sunshine hours to solar radiation using an algorithm which was described by Rietveld (1978). The Model would either work with precipitation (rainfall) only, or precipitation and any combination of the aforementioned climate variables. Other important input information to be specified are the name of the station from which historical observed data was obtained and the location of the weather station in form of latitude, longitude and altitude. The ability of LARS-WG to simulate reliable data depends on the availability of observed data. The model simulates future weather data based on as little as a single year of observed weather data. However, the more observed daily weather data used, the closer to a true value are the simulated results. Semenov and Barrow (2002) recommend the use of daily weather data of at least between 20-30 years for better results. Weather data for long periods are significant in a way that they capture some of the less frequent events like droughts and floods. This study used daily historical observed weather data of 30 years from (1985-2014) time periods as baseline data which is maximum period that the model required to obtain best nearest true value outcome for climate variables in future three time periods under each scenarios.

3.2.2. Model Calibration and Validation

According to Semenov and Barrow (2002), the process of generating synthetic weather data can be grouped into three distinct steps: (a**)** model calibration, (b**)** model validation and (c) generation of synthetic weather data.

3.2.2.1. Calibration of the Model

Calibration is the first step that is executed by the model in order to generate synthetic weather data. Calibration of LARS-WG is carried out by a function on the main menu called **"Site**

Analysis". The process is done so as to determine statistical characteristics and site parameters of the observed weather data. In this study, site analysis was performed on observed data for a period of 30 years (1985-2014). Once the program encounters "illegal data" during execution, an "error" is displayed. "Illegal" data includes the value of minimum temperature being greater than maximum temperature and being precipitation values less than zero (negative precipitation).

Examples of statistical characteristics of weather data in the output file include the following;

- Empirical distribution characteristics for the length of wet and dry series of days in the observed data,
- The mean and standard deviation, by month, of wet and dry series length,
- Rainfall distribution, maximum, minimum, number of observed years (months or days), mean and standard deviation.
- Maximum, minimum, number of observed years (months or days), mean and standard deviation of temperature.
- Periods of cool and warm weather
- Maximum, minimum, number of observed years (months or days), mean and standard deviation of solar radiation.

Examples of weather generated site parameters in the output file include the following;

- Histogram intervals and frequency of events in the intervals for precipitation amount by month from January to December.
- Fourier coefficients for means and standard deviations of minimum and maximum temperature on wet and dry days
- Average autocorrelation value for minimum and maximum temperature and solar radiation.
- Solar radiation amount ($MJ/m^2/day$) on wet and dry days by month from January to December.

During calibration period the model calculates the mean and standard deviation for generated and observed data based on 30 years input data and t, K-S and f-statistics with their respective *p*-value for the three climate variables (rainfall, maximum and minimum temperature).

3.2.2.2. Model Validation

Once LARS-WG has been calibrated, its ability to simulate future weather data in the representative study site is assessed. Validation is a process that is used to determine how well a model can simulate potential future climate variables. The process involves comparing and analyzing the statistical characteristics of the observed and synthetic weather data in order to determine the existence of any statistically-significant differences between them. Validation of the model can be conducted in two different ways: (i) using the GENERATOR option to synthesize daily weather data based on the information in the site parameter files and then undertake comparisons between the observed and synthetic data 'off-line', or (ii) using the Q-test option that executes statistical comparisons between climate parameters derived from observed weather data and synthetic weather data generated using LARS-WG. The Q test function was used to determine the ability of LARS-WG to rationally estimate future climate variables. This was achieved using three statistical tests; chi-square test (X^2), t-test and K-S (Kolmogorov-Smirnov) which is output Q test function to test the performance of LARS-WG. The chi-square test was used to determine the existence of any significant difference between the simulated and observed frequencies in the meteorological data. A t-test was used to check the existence of any reliable difference between the means of the generated and observed data sets. Additionally; a K-S test was used to decide if a sample comes from population with a specific distribution. The Kolmogorov-Smirnov (K-S) statistic Δ is the absolute maximum differences between observed cumulative probability P (X_m) and the theoretical cumulative probability F(X_m).

$$\Delta = max|F(x_m) - P(x_m)|$$

Observed cumulative probability is computed using Weibul's formula $P(X_m)=\left\lfloor\frac{(n+1-m)}{(n+1)}\right\rfloor$ and theoretical cumulative probability is obtained for each ordered observation using the selected distribution.

Where n is sample size and m is ordered sequence or rank.

By using two statistical tests X^2(chi-square) and t-test we calibrate and validate LARS-WG model. In addition to these two tests *K-S* test is used to cross check whether observed and

generated distribution is from the same population or not. Large X^2 and t values indicates the existence of real difference between observed and estimated/generated climate variables. Conversely, smaller X^2 and t values indicate that there is less difference between observed and estimated data sets. *K-S* value also should be less than critical value to accept the null hypothesis H_o that says the generated data distribution has the same population distribution as observed data sets. Each X^2, t and *K-S* value has a corresponding *p*-value output from the model Q-test button, which is the probability that the pattern of data in the sample could be produced by random variables. A *p*-value of 0.05 simply means there is a probability of 5% that there is no difference between observed and simulated data. *P*-values below the set significance level indicate that the simulated climate variables are far from the true climate values. For the purpose of this study, a *p*-value was set at 0.05 which is commonly used in statistical tests and climate change studies (Gohari.et al, 2013).

3.2.2.3. Generation of Synthetic Weather Data

Once LARS-WG has been calibrated (Site Analysis) and the performance of the weather generator has been verified (Q-test), the "Generator" option then generates synthetic weather data. Synthetic weather data generated from this option have the same characteristics as observed weather data. This option also enables one to generate synthetic weather data analogous to a scenario of climate change. The following output data is obtained from this function;

- Relative change in monthly mean rainfall
- Relative change in duration of wet and dry spell
- Absolute change in monthly mean minimum temperature
- Absolute change in monthly mean maximum temperature
- Relative changes in daily temperature variability
- Absolute change in monthly mean radiation

LARS-WG is based on the series weather generator described in Racsko et al. (1991). It utilizes semi-empirical distributions (SED) for the lengths of wet and dry day series, daily precipitation, minimum and maximum temperature and daily solar radiation. The semi-empirical distribution Emp= $\{a_0, a_i; h_i, i=1\ldots 23\}$, is a histogram with 23 intervals, (a_{i-1}, a_i), where $a_{i-1} < a_i$, and hi denotes the number of events from the observed data in the i^{th} interval.

Random values from the semi-empirical distributions are chosen by first selecting one of the intervals (using the proportion of events in each interval as the selection probability), and then selecting a value within that interval from the uniform distribution. Such a distribution is flexible and can approximate a wide variety of shapes by adjusting the intervals [a_{i-1}, a_i). The cost of this flexibility, however, is that the distribution requires many parameters (24 parameters for the edges and 23 parameters for the number of events in each interval) to be specified compared with, for example, 3 parameters for the mixed-exponential distribution used in an earlier version of the model to define the dry and wet day series (Racsko et al., 1991).

3.3. GCM's Emission Scenarios

In this study the outputs from 15 GCMs under two emission scenarios: SRA1B and SRB1, as recommended by IPCC Special Report on Emission Scenarios (SRES) (Houghton et al., 2001) was used. Table 5 presents the key assumption the two emission scenarios used to predict future climate variables in three time periods (2020s, 2055s, and 2090s) with their respective $C0_2$ concentrations.

Table 5: CO2 concentrations (ppm) for selected climate scenarios specified in the Special Report on Emissions Scenarios (SRES) (Nakicenovic & Swart 2000)

Scenario	**Key assumptions**	**CO2 concentration, ppm**		
		2011-2030	2046-2065	2081-2100
SRA1B "the rich word"	A world characterized by very rapid economic growth (3%/yr), low population growth (0.27%/yr) and rapid introduction of new and efficient technologies. There is global economic and cultural convergence and capacity building.	418	541	674
SRB1 "The sustainable world"	Rapid change in economic structure, dematerialization, improved equity more global concern regarding environmental and social sustainability, with introduction of clean technologies. Global population reaches 7 billion.	410	494	538

3.4. Uncertainty Analysis of GCMs

3.4.1. Weighting of GCMs

The first step of this technique involves weighting each of the 15 GCMs used in the study based on the Mean Observed Temperature-Precipitation (MOTP) method (Massah-Bavani and Morid, 2005; Gohari et al., 2013). In order to weight each GCM, the ability of the model to project weather data is considered. In other words, the method considers the monthly average difference between observed and simulated climate variables (precipitation and minimum and maximum temperature).

$$w_{ij} = \frac{\frac{1}{|\Delta d_{ij}|}}{\sum_{j=1}^{15}\left[\frac{1}{|\Delta d_{ij}|}\right]} \text{ ----------16}$$

where W_{ij} is the weight of GCM j in month i; and $|\Delta d_{ij}|$ is the absolute difference between the average precipitation (rainfall) or temperature between observed value and the value simulated by GCM j in month i**.**

3.4.2. Generation of Probability Distribution Functions (PDFs)

This step implies generation of PDFs of changes in climate variables based on the calculated weights. The PDFs outline the relationship between the weight of each GCM and the average changes in monthly precipitation, minimum temperature and maximum temperature. With 15 GCMs and 2 emission scenarios used in this work, 30 PDFs are thus constructed for each month. The generated discrete PDFs of the main variables are ultimately converted to cumulative probability functions (CDFs). Several studies have identified the use of Gamma distribution function as an important tool for analysis of climate data (Ines and Hansen, 2006; Block et al., 2009; Piani et al., 2010; Gohari e al., 2013). Based on similar studies that were carried by Pindyck (2012), Teutschbein and Seibert (2012) and Gohari et al. (2013), the Gamma function has been selected for generation of cumulative distribution functions as follows;

$$f(x) = \frac{1}{\beta^{\alpha}\Gamma(\alpha)} X^{\alpha-1} e^{-x/\beta}; x \geq 0 \text{ ----------17}$$

Where α and β are shape and scale parameters of the Gamma distribution function respectively, -x is the climate variable (temperature or precipitation), and is the incomplete Gamma function as given in Equation below.

$$\Gamma(\alpha) = \int_0^\infty x^{\alpha-1}\, e^{-x} dx$$ ----------18

By changing values of α and β, we obtain the best fit based on maximum likelihood model. The summation of squared error (Equation 19) has been used to show how best the Gamma function fits the data.

$$SSE = \sum_{I=1}^{n} (y_i - \bar{y}_i)$$ ----------19

Where yi is the data point; $\bar{y}_i$ is the estimation of Gamma function and n is the number of data points. For this study, n = 15.

3.4.3. Generation of Cumulative Distribution Functions (CDFs)

In this step, the PDFs generated in the second step are converted to CDFs for each of the 12 months (January-December). Next, values of climate change variables at three probability percentiles are extracted from the generated CDFs at the following risk levels: 25th, 50th, and 75th probability percentiles. The calculated climate variables at three different percentiles are then used as input data for modeling of potential maize production with AquaCrop. The 25th probability percentile indicates a scenario of high changes in precipitation and low temperature changes. The 75th probability percentile represents a scenario with low changes in precipitation but high temperature changes. The 50th probability percentile is the median probability percentile for both precipitation and temperature. The generated PDFs were converted to CDFs using the gamma distribution function whose shape and scale parameters alpha (α) and beta (β) were as coded in MATLAB programming language which was resulted in high strength correlation coefficient (r=0.999).

3.5. Crop Yield Estimation with AquaCrop

3.5.1. Model Descrition

AquaCrop is the FAO crop-model to simulate yield response to water. It is designed to balance simplicity, accuracy and robustness, and is particularly suited to address conditions where water is a key limiting factor in crop production. AquaCrop is a companion tool for a wide range of users and applications including yield prediction under climate change scenarios. AquaCrop is a completely revised version of the successful CropWat model. The main

difference between CropWat and AquaCrop is that AquaCrop includes more advanced crop growth routines. AquaCrop includes the following sub-model components: the soil, with its water balance; the crop, with its development, growth and yield; the atmosphere, with its thermal regime, rainfall, evaporative demand and CO2 concentration; and the management, with its major agronomic practice such as irrigation and fertilization (Steduto et al., 2009). The particular features that distinguishes AquaCrop from other crop models is its focus on water, the use of ground canopy cover instead of leaf area index, and the use of water productivity values normalized for atmospheric evaporative demand and of carbon dioxide concentration. This enables the model with the extrapolation capacity to diverse locations and seasons, including future climate scenarios. Moreover, although the model is simple, it gives particular attention to the fundamental processes involved in crop productivity and in the responses to water, from a physiological and agronomic background perspective. Figure 3 shows chart of AquaCrop indicating the main components of the **soil–plant–atmosphere continuum** and the parameters driving phenology, canopy cover, transpiration, biomass production and final yield.

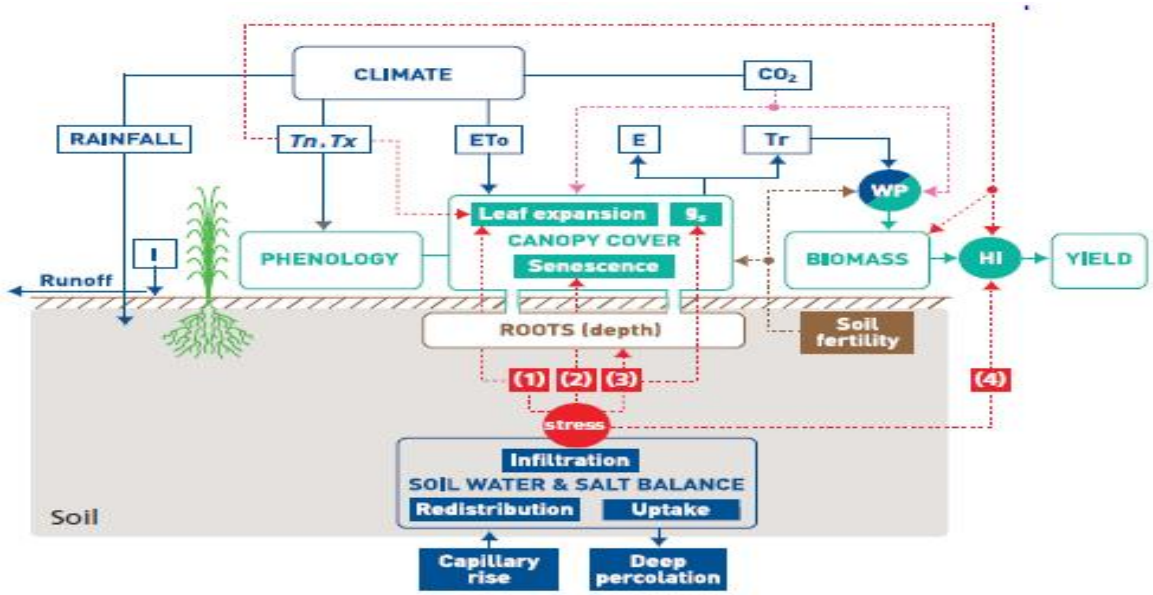

Figure 3: AquaCrop model structure indicating the main components of the soil–plant–atmosphere continuum and the parameters driving phenology, canopy cover, transpiration, biomass production and final yield.

Theoretical assumptions of Aquacrop

The complexity of crop responses to water deficits led to the use of empirical production functions as the most practical option to assess crop yield response to water. Among the empirical function approaches, FAO Irrigation & Drainage Paper 33 (Doorenbos and Kassam, 1979) represented an important source to determine the yield response to water of field, vegetable and tree crops, through the following equation:

$$\left(\frac{Yx-Ya}{Yx}\right) = Ky\left(\frac{ETx-ETa}{ETx}\right)$$ ----------20

Where Yx and Ya are the maximum and actual yield, ETx and ETa are the maximum and actual evapotranspiration, and ky is the proportionality factor between relative yield loss and relative reduction in evapotranspiration.

AquaCrop evolves from the previous Doorenbos and Kassam (1979) approach by separating (i) the ET into soil evaporation (E) and crop transpiration (Tr) and (ii) the final yield (Y) into biomass (B) and harvest index (HI). The separation of ET into E and Tr avoids the confounding effect of the non-productive consumptive use of water (E). This is important especially during incomplete ground cover. The separation of Y into B and HI allows the distinction of the basic functional relations between environment and B from those between environment and HI. These relations are in fact fundamentally different and their use avoids the confounding effects of water stress on B and on HI. The changes described led to the following equation at the core of the AquaCrop growth engine:

$$B = WP \cdot \Sigma Tr$$ ----------21

Where Tr is the crop transpiration (mm) and WP is the water productivity parameter (kg of biomass per m^2 and per mm of cumulated water transpired over the time period in which the biomass is produced). This step from Eq.20 to Eq.21 has a fundamental implication for the robustness of the model due to the conservative behavior of WP (Steduto et al., 2007). It is worth noticing though that both equations are different expressions of a water-driven growth engine in terms of crop modeling design (Steduto, 2003). The other main change from Eq.20 to AquaCrop is in the time scale used for each one. In the case of Eq.20, the relationship is used seasonally or for long periods (of the order of months), while in the case of Eq.21 the relationship is used for daily time steps, a period that is closer to the time scale of crop

responses to water deficits. The main components included in AquaCrop to calculate crop growth are :(i) Atmosphere (ii)Crop (iii)Soil (iv) Field Management (v) Irrigation management

I) Atmosphere

The minimum weather data requirements of AquaCrop include the following five parameters are daily minimum air temperatures, daily maximum air temperatures, daily rainfall, daily evaporative demand of the atmosphere expressed as reference evapotranspiration (ETo) and mean annual carbon dioxide concentration in the bulk atmosphere. The reference evapotranspiration (ETo) is in contrast to CropWat, not calculated by AquaCrop itself, but is a required input parameter. This enables the user to apply whatever ETo method based on common practice in a certain region and/or availability of data. From the various options to calculate ETo reference is made to the Penman-Monteith method as described by FAO (Allen et al., 1998). The same publication makes also reference to the Hargreaves method in case of data shortage.

A companion software program (ETo calculator) based on the FAO.56 publication used on preference of Penman-Monteith method. A few additional parameters were used for a more reliable estimate of the reference evapotranspiration. Besides the minimum and maximum temperature, measured dew point temperature and wind speed were used for the calculation. The procedure followed for ETo calculation is identical to that outlined in the FAO Irrigation and Drainage Paper 56, using the FAO Penman-Monteith equation (Allen et al., 1998) which is given by:

$$ET_o = \frac{0.408\Delta(R_n - G) + \gamma \frac{900}{T+273} U_2 (e_s - e_a)}{\Delta + \gamma(1 + 0.34u_2)} \quad \text{----------22}$$

Where

ETo	reference evapotranspiration (mm/ day)
Rn	net radiation at the crop surface (MJ/m^2 /day)
G	soil heat flux density (MJ/ m^2 /day)
T	mean daily air temperature at 2 m height (^{0}C)
U_2	wind speed at 2 m height (m/s)
es	saturation vapor pressure (kPa)
ea	actual vapor pressure (kPa)
es-ea	saturation vapor pressure deficit (kPa)

Δ slope vapor pressure curve (kPa/ ^{o}C)

γ psychometric constant (kPa/ ^{o}C)

AquaCrop calculations are performed always at a daily time-step. However, input is not required at a daily time-step, but can also be provided at 10-daily or monthly intervals. The model itself interpolates these data to daily time steps. The only exception is the CO2 levels which should be provided at annual time-step and are considered to be constant during the year.

II) Crop

AquaCrop considers five major components and associated dynamic responses which are used to simulate crop growth and yield development are phenology, aerial canopy, rooting depth, biomass production, and harvestable yield. As the crop grows, its canopy expands and its roots are simultaneously deepened, thereby establishing main development stages. The canopy represents the source of actual transpiration which is used to determine the amount of biomass produced from the water productivity (WP). Using the harvest index (HI), the actual harvestable part of biomass, the yield, is calculated using Equation below (Steduto et al., 2009)

Y = B X HI----------23

where, Y is the yield, B is biomass and HI is harvest index. The harvest index is essentially a percentage of biomass that is translated into yield.

Steduto et al. (2009) states that canopy is the most significant component of AquaCrop, because the amount of water transpired from the crop determines biomass production and hence the yield. Its expansion is expressed as a percentage of green canopy ground-cover (CC), such that where there is no water stress for the crop, canopy expansion from emergency to full development follows exponential growth and exponential decay during the first and second halves of full development respectively as shown in Equations 24 and 25.

$$CC = CCoe^{CGC.t}$$ ----------24

$$CC = CC_X - (CC_X - CC_0).e^{-CGC.t}$$ ----------25

Where CC is canopy cover at time t, CCo is the canopy cover at t=0, CGC is the canopy growth coefficient in fraction per day or per degree day, CCx is the maximum canopy cover and t is the time in days or degree days. The growing degree days (GDD) which is the number of temperature degrees that determine a proportional crop growth and development are calculated using Equation 26:

$$GDD = \frac{T_{max} + T_{min}}{2} - T_{base}$$ ----------26

Where Tmax and Tmin are maximum and minimum temperatures and Tbase is the temperature at which crop growth stops.

III) Soil

AquaCrop is flexible in terms of description of the soil system. Special features are Hydraulic characteristics which include hydraulic conductivity at saturation, volumetric water content at saturation, field capacity, wilting point. Soil fertility can be defined as additional stress on crop growth influenced by; water productivity parameter, the canopy growth development, maximum canopy cover, Rate of decline in green canopy during senescence. AquaCrop separates soil evaporation (E) from crop transpiration (Tr). The simulation of Tr is based on Reference evapotranspiration, Soil moisture content and Rooting depth whereas Simulation of soil evaporation depends on Reference evapotranspiration, Soil moisture content, Mulching, Canopy cover, Partial wetting by localized irrigation, Shading of the ground by the canopy.

IV) Field management

Characteristics of general field management can be specified and are reflecting two groups of field management aspects: soil fertility levels and practices that affect the soil water balance. In terms of fertility levels one can select from pre-defined levels (none limiting, near optimal, moderate and poor) or specify parameters obtained from calibration. Field management options influencing the soil water balance that can be specified in AquaCrop are mulching, runoff reduction and soil bunds.

V) Irrigation management

Simulation of irrigation management is one of the strengths of AquaCrop with the following options:

- rainfed-agriculture (no irrigation) used in this study
- sprinkler irrigation
- drip irrigation
- surface irrigation by basin
- surface irrigation by border
- surface irrigation by furrow

Scheduling of irrigation can be simulated as fixed timing/Depletion of soil water

Irrigation application amount can be defined as fixed depth/Back to field capacity

Climate change

The impact of climate change can be included in AquaCrop by three factors: adjusting the precipitation data file, adjusting the temperature data file and Impact of enhanced CO2 levels. The first two options are quite straightforward and require the standard procedure of creating climate input files in AquaCrop. Impact of enhanced CO2 levels is calculated by AquaCrop itself. AquaCrop uses for this the so-called normalized water productivity (WP*) for the simulation of aboveground biomass. The WP is normalized for the atmospheric CO2 concentration and for the climate, taking into consideration the type of crop (e.g. C3 or C4). The C4 crops assimilate carbon at twice the rate of C3 crops. A C4 plant is a plant that cycle's carbon dioxide into four-carbon sugar compounds to enter into the Calvin cycle (maize, pineapple, and sugar cane).

3.5.2. Calibration of AquaCrop

Calibration of AquaCrop has been achieved by comparing the actual maize production (as provided by the Department of Agriculture of southern nations, nationality and peoples of Ethiopia regional state, sidama zone) with the maize yield of simulated by the model. Input data for various crop and soil parameters used in the model are obtained from South Region Agricultural Research Institute and Wondo Genet Agricultural Research Center Hawassa Maize Research Sub Center of Ethiopia. By comparing the actual and simulated maize yields crop parameters(*CC_O, canopy development, root deepening, flowering and yield formation, canopy expansion relative to water stress, stomata closure relative to water stress etc..)*, field management(*soil fertility stress percentage for biomass production in respective to canopy, biomass, water productivity and percentage soil surface covered) and* soil characteristics *(characteristics of soil horizon, soil surface, restrictive soil layer and capillary rise*) are adjusted through trial and error, until a closest match between recorded and simulated maize yield was achieved. Data (recorded maize yields, rainfall, minimum and maximum temperature) from Hawassa station for year 2014 has been used to calibrate the model. Table 6 shows some important final calibrated values of crop parameters (Gebreselassie et al.,2014, Abedinpour et al., 2012) which were used in determining the final Biomass, Harvest Index and hence Yield of maize using AquaCrop.

Table 6: Input crop parameters used in calibration of AquaCrop

Description of parameter	Value used	Unit of parameter
Base temperature	10	^{o}c
Cut-off temperature	40	^{o}c
Canopy growth coefficient (CGC)	20.9	%/day
Canopy decline coefficient (CDC) at senescence	0.98	%/day
Leaf growth threshold (Pupper)	0.2	% of TAW (fraction of total available water (TAW)
Leaf growth threshold (Plower)	0.55	% of TAW
Leaf growth stress coefficient curve shape	3.1	Unit less (moderately convex curve)
Expansion stress coefficient (Pupper)	0.18	% of TAW
Expansion stress coefficient (PLower)	0.55	% of TAW
Expansion stress coefficient curve shape	3.1	% of TAW
Stomatal conductance threshold (Pupper)	0.55	Unit less
Stomatal stress coefficient curve shape	1.9	Unit less (high convex curve)
Senescence stress coefficient curve shape	1.6	Unit less (moderately convex curve)
Senescence stress coefficient (Pupper)	0.46	Unit less (Initiation of canopy senescence)
Coefficient, inhibition of leaf growth on HI	12	Unit less (HI increased by inhibition of leaf growth at anthesis
Coefficient, inhabitation of stomata on HI	5	Unit less (HI increased by inhibition of stomata at anthesis
Maximum basal crop coefficient (Kcb)	1.25	Unit less
Time from sowing to emergence	8	Days
Time to maximum canopy cover	52	Days
Time from sowing to start flowering	66	Days
Time from sowing to start senescence	110	Days
Time from sowing to maturity	148	Days
Length of the flowering stage	10	Days
Length of building up HI	66	Days

3.5.3. Validation of AquaCrop

Having calibrated AquaCrop, it was significant that the model be validated in order to evaluate its performance in simulating crop yields. Model validation is important in order to determine if the model has the ability to replicate the data, to analyze the effectiveness of model calibration and compare synthetic data with those done in previous studies. Loague and Green (1991) indicates that there are numerous statistical indicators for evaluating performance of AquaCrop, nonetheless, Willmott (1984) argues that each of the statistical indicators have their own weaknesses and strengths. To effectively evaluate the performance of the model, the use of ensemble statistical indicators is appropriate (Willmott, 1984). In analysis of performance of AquaCrop, the following lists of statistical indicators were used: prediction error (Pe), coefficient of determination (R^2), mean absolute error (MAE), root mean square error (RMSE) and Nash and Sutcliffe (Ns). Ns and R^2 indicate the predictive power of the model whilst Pe, MAE and RMSE are used to signify the amount of error associated with the model prediction (Abedinpour et al., 2012).

Calibrated crop parameters, management practices and soil types and conditions remained constant. Maize yields for years 2008 to 2013 were used to compare with those simulated by the model within the same time period. Equations 27-31 below show the statistical relationships that were used to evaluate the performance of the model based on its predictive prowess and amount of error associated with it (Nash and Sutcliffe, 1970). Equation 27 is a relationship used to estimate, R^2, which is the squared values of Pearson correlation coefficient that illustrates squared ratio between covariance and the multiplied standard deviations of the observed and estimated maize yields.

$$R^2 = \left[\frac{\sum(O_i-\overline{0})(S_i-\bar{s})}{\sqrt{\sum(O_i-\overline{0})^2\sum(S_i-\overline{0})^2}}\right]^2 \text{----------27}$$

$$Ns = 1 - \frac{\sum_{i=1}^{i=N}(0_i-S_i)^2}{\sum_{i=1}^{i=N}(0_i-\overline{0})^2} \text{----------28}$$

$$Pe=\frac{(S_i-o_i)}{O_i}\times 100\text{----------29}$$

Where, S_i and Oi are synthetic and actual (observed) production $\overline{0\iota}$ is the mean value of O_i and N is the number of observations.

$$RMSE= \sqrt{\sum_{i=1}^{N} \frac{(S_{i-} O_i)^2}{N}} \text{ ----------30}$$

$$MAE=\frac{1}{n}\sum_{i=1}^{n}|S_i - O_i| \text{ ----------31}$$

The model is said to perform better when values of E and R^2 approaches one and when values of Pe, MAE and RMSE approaches zero (Moriasi et al., 2007).

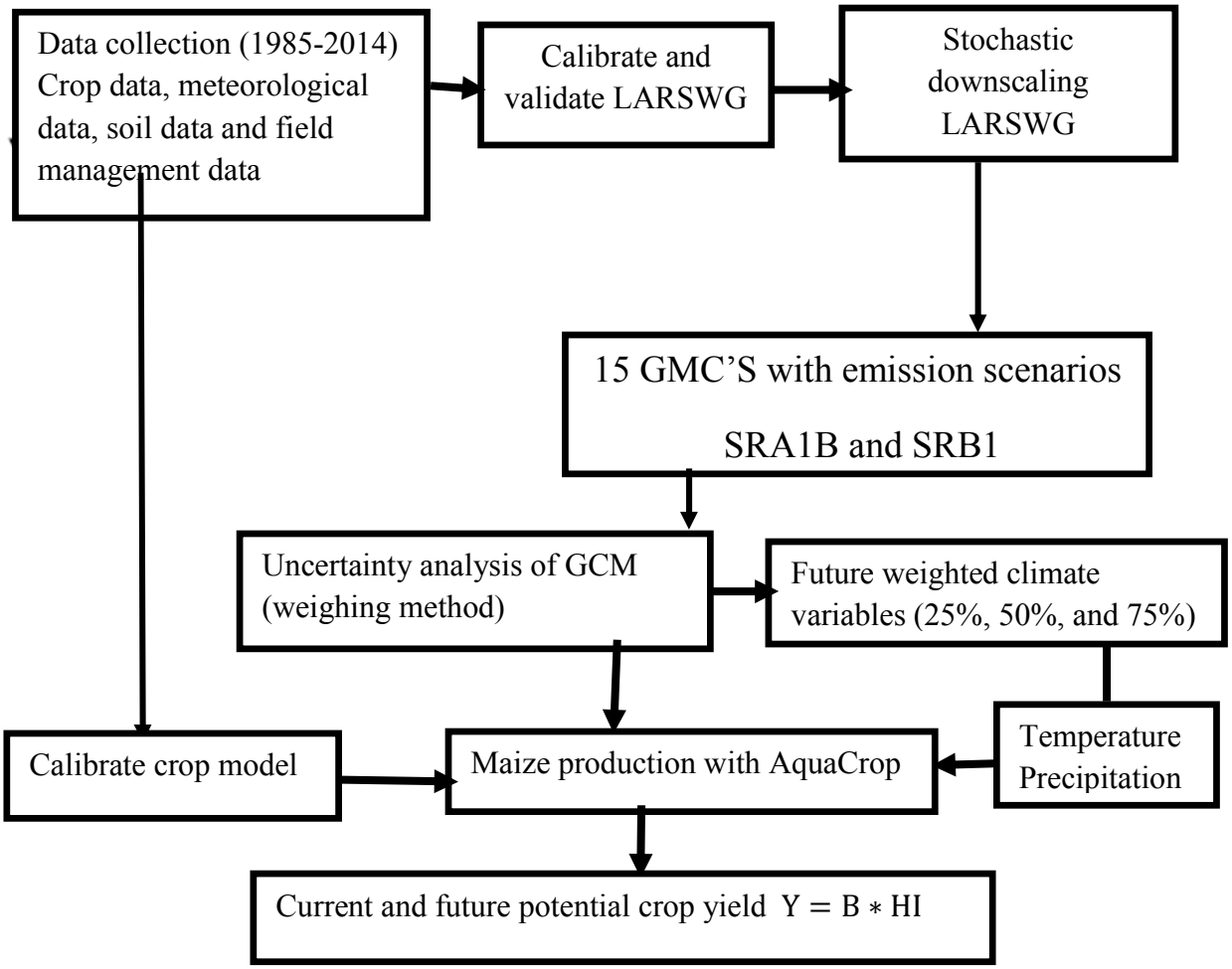

Figure 4: Schematic overview of the general methodology adopted in this study.

CHAPTER FOUR

4. RESULTS AND DISCUSSIONS

4.1. Calibration and validation of LARS-WG

Table 7 shows the results of the *p*-values for all chi-square (X^2), Kolmogorov-Smirnov (*K-S*) and *t*-tests for rainfall, minimum and maximum temperature from January to December. Figure 5 presents the monthly *p*-values of X^2, *K-S* and *t*-tests for rainfall; *K-S* and *t*-tests plot for minimum and maximum temperatures as shown in table. The figure indicates *p*-value for chi-square and t-test varies among months whereas *p*-value for k-S test approaches to unity for all months which shows generated and observed climate variables are from the same population. Chi-square test is not important for temperatures since chi-square is used to determine the existence of any significant difference between simulated and observed frequencies in meteorological weather data whereby frequency test is necessary only for rainfall. The results indicate that *p*-values in all months for both rainfall and temperatures are higher than the selected significance level of 0.05 for the three tests. Thus the model is satisfactorily to simulate future climate data.

Table 7: Statistical comparison of generated and observed weather data using Q test button of LARSWG5.5 (Significant *p*-value = 0.05)

Month	Rainfall						Min temperature				Max temperature			
	k-s	*p*-value	t	*p*-value	x2	*p*-value	k-s	*p*-value	t	*p*-value	k-s	p-value	t	p-value
Jan	0.1	1	1.64	0.11	1.85	0.057	0.053	1	-0.66	0.511	0.053	1	-0.66	0.512
Feb	0.05	1	-0.6	0.58	1.78	0.074	0.053	1	-0.878	0.383	0.106	0.99	0.324	0.747
Mar	0.05	1	0.77	0.45	1.01	0.952	0.106	0.99	0.098	0.923	0.105	0.99	-0.2	0.84
Apr	0.05	1	1.16	0.25	1.02	0.975	0.106	0.99	1.29	0.201	0.053	1	-0.78	0.435
May	0.06	1	0.27	0.79	1.1	0.805	0.053	1	-1.185	0.24	0.053	1	0.81	0.421
Jun	0.12	0.99	0.19	0.85	1.12	0.708	0.053	1	-1.249	0.216	0.053	1	-0.29	0.776
July	0.02	1	0.29	0.77	1.48	0.26	0.053	1	-0.983	0.329	0.053	1	-0.69	0.492
Aug	0.05	1	-0.2	0.85	1.11	0.776	0.053	1	0.143	0.887	0.053	1	-1.87	0.066
Sep	0.11	0.99	-0.1	0.93	1.16	0.627	0.106	0.99	1.636	0.106	0.106	0.99	0.588	0.558
Oct	0.07	1	0.83	0.41	1.41	0.28	0.053	1	0.028	0.977	0.106	0.99	0.47	0.64
Nov	0.05	1	0.16	0.87	1.8	0.067	0.053	1	-1.611	0.111	0.053	1	0.72	0.473
Dec	0.05	1	-0.8	0.44	2.01	0.051	0.053	1	0.194	0.847	0.053	1	-1	0.321

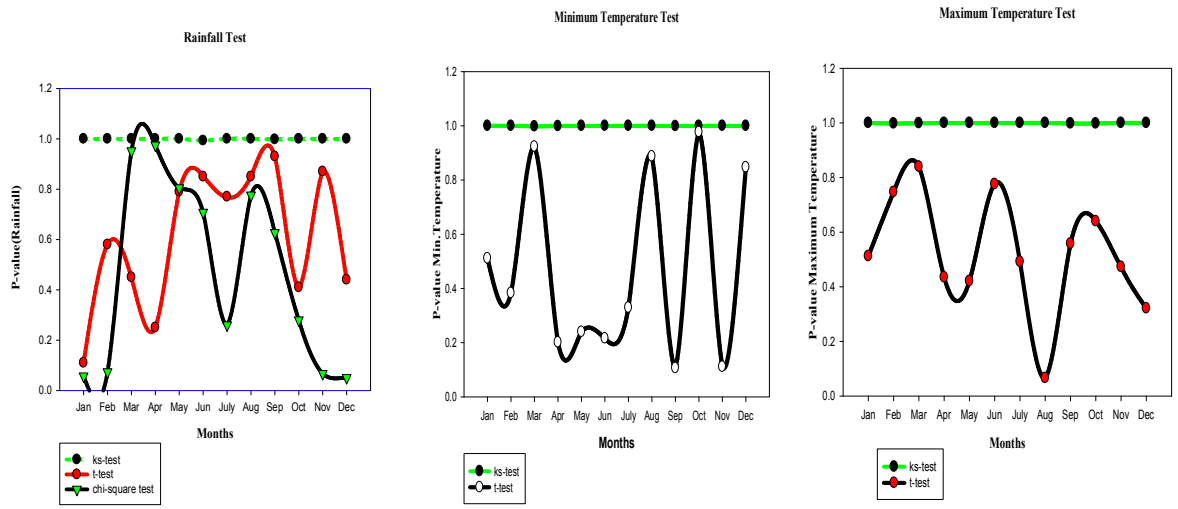

Figure 5: Plot of *P*-values for X^2, *K-S* and *t*- tests for rainfall and temperatures.

Table 8: Series seasonal distributions statistics for WET and DRY

	Wet Series Statistics				Dry Series Statistics			
Month	Max	Mean	Sd	Number Of Observation	Max	Mean	Sd	Number Of Observation
Jan	6	1.73	1.14	88	57	7.41	9.11	90
Feb	7	2.03	1.39	102	32	4.74	6.05	100
Mar	16	2.88	2.42	161	21	2.83	3.54	150
Apr	14	3.35	2.67	163	13	2.3	2.29	162
May	17	2.81	2.43	175	16	2.22	1.98	176
Jun	12	2.06	1.63	227	7	1.85	1.21	228
July	15	2.94	2.45	194	10	1.95	1.35	191
Aug	19	3.03	2.59	200	7	1.73	1.18	199
Sep	21	4.08	3.4	155	40	1.81	3.24	158
Oct	14	2.84	2.52	134	31	4.28	5.47	140
Nov	7	2.14	1.48	79	58	10.41	11.38	86
Dec	7	1.68	1.29	79	79	10.56	15.21	79

In addition to these three tests to be more confident on the model we can see the output of wet and dry series statistical length of the meteorological data from LARS-WG. Table 8 shows the maximum, mean, standard deviation and number of observation of wet and dry statistical series of each month from January to December. As we can observe from simulated weather data in Table 8 the maximum wet day (rainfall $> 0\ mm$) length is recorded in month from September

to August (19-21) and the minimum wet day length is in month from November to January (6-7). Similarly the maximum dry day (rainfall= 0 mm) length is recorded in the month from November to December (10.41-1056) and the minimum dry day length is in month from June to August (7-10) for this particular area which is similar to raw data used as input for this specific site of study.

Beside all tests above figure 6 below show that the mean and standard deviation of monthly observed data resemble with generated/estimated data for three climate variables rainfall, maximum and minimum temperatures. This ensures our confidence to use LARSWG5.5 for future synthetic meteorological weather data simulation.

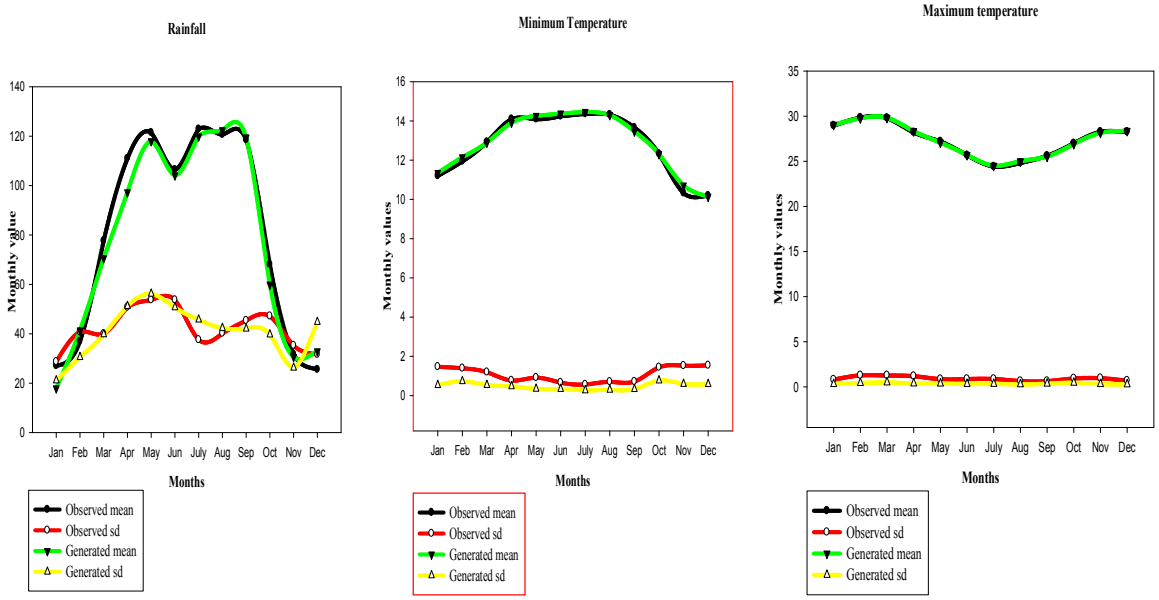

Figure 6: Comparison of generated and observed monthly weather data using mean and standard deviation.

The model also generated bias, paired t-test with its respective *p*-value as shown in table 9.The three climate variables (rainfall, maximum temperature, and minimum temperature) paired t-test *p*-value is higher than significance probability level 5% which increase our confidence on the model to simulate future climate variables.

Table 9: Paired t-test, bias and *p*-value for climate variables

Climate variable	Bias	Paired t-test	*p*-value
Rainfall	2.758	1.658	0.123
Minimum temperature	-0.057	-1.248	0.236
Maximum temperature	-0.023	-0.82	0.428

4.2. Future Climate Variables Generation

Future mean climate variables (rainfall and temperatures) for fifteen (15) GCMs are generated using Generator key function of LARS-WG 5.5 with perspective to two emission scenario (SRA1B and SRB1) in the model. Figures 7 to 9 show the simulated mean monthly values of rainfall, minimum and maximum temperature in each time horizon in each emission scenarios at different probability percentiles. The figures presents that historical observed rainfall mean remain in the range of synthetic rainfall mean for three time horizons (2020s, 2055s and 2090s) under both emission scenarios; whereas historical observed maximum and minimum temperatures mean coming out of the ranges of synthetic temperatures mean generated gradually increases in coming three time periods (2020s, 2055s, 2090) respectively which indicate that temperatures increase gradually in coming time periods under both scenarios whilst synthetic rainfall increase or decrease is uncertain in coming three time periods in each scenario. Figures 7 to 9 also presents the 15 GCMs predictions that indicate a wide range in synthetic climate variables. For instance, consider the estimated rainfall amount in the month of March estimated under emission scenario A in 2055s (SRA1B-2055s). Simulated rainfall amount by all GCMs for this month ranges approximately between 58mm (BCM2) GCM model to 136mm (NCPCM) GCM model where the difference is about 70mm. The box plots in figure 7 to 9 indicate the lower (25%) and upper (75%) quartiles whereby the line between them is the median (50%), and the lower and upper whiskers represent the mean ± standard deviation. The straight line shows the historical observed mean monthly rainfall.

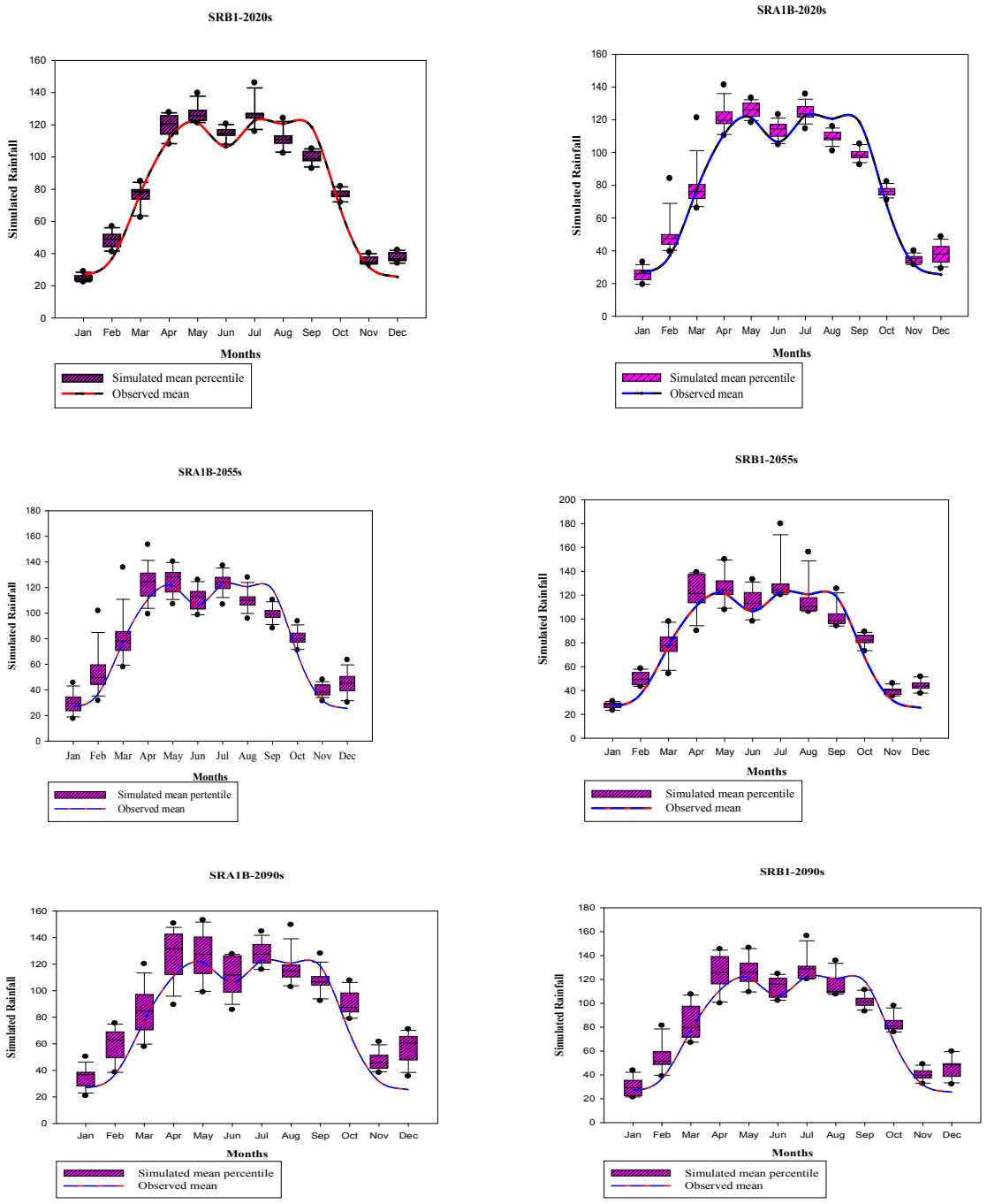

Figure 7: Box plots showing the simulated mean monthly rainfall for 15 GCMs under scenarios A and B for three different time steps.

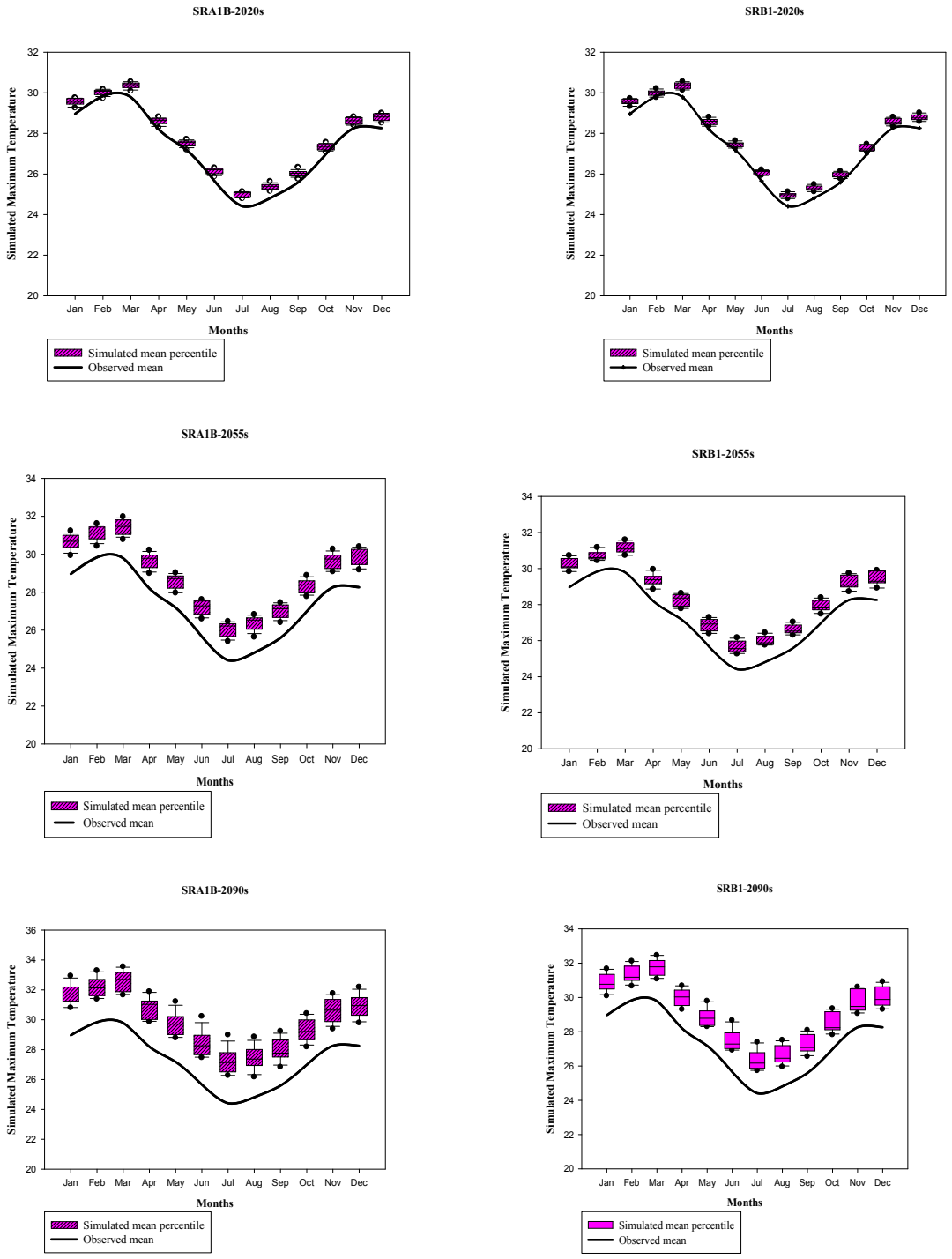

Figure 8: Box plots showing the simulated mean monthly maximum temperature for 15 GCMs under scenarios A and B for three different time steps.

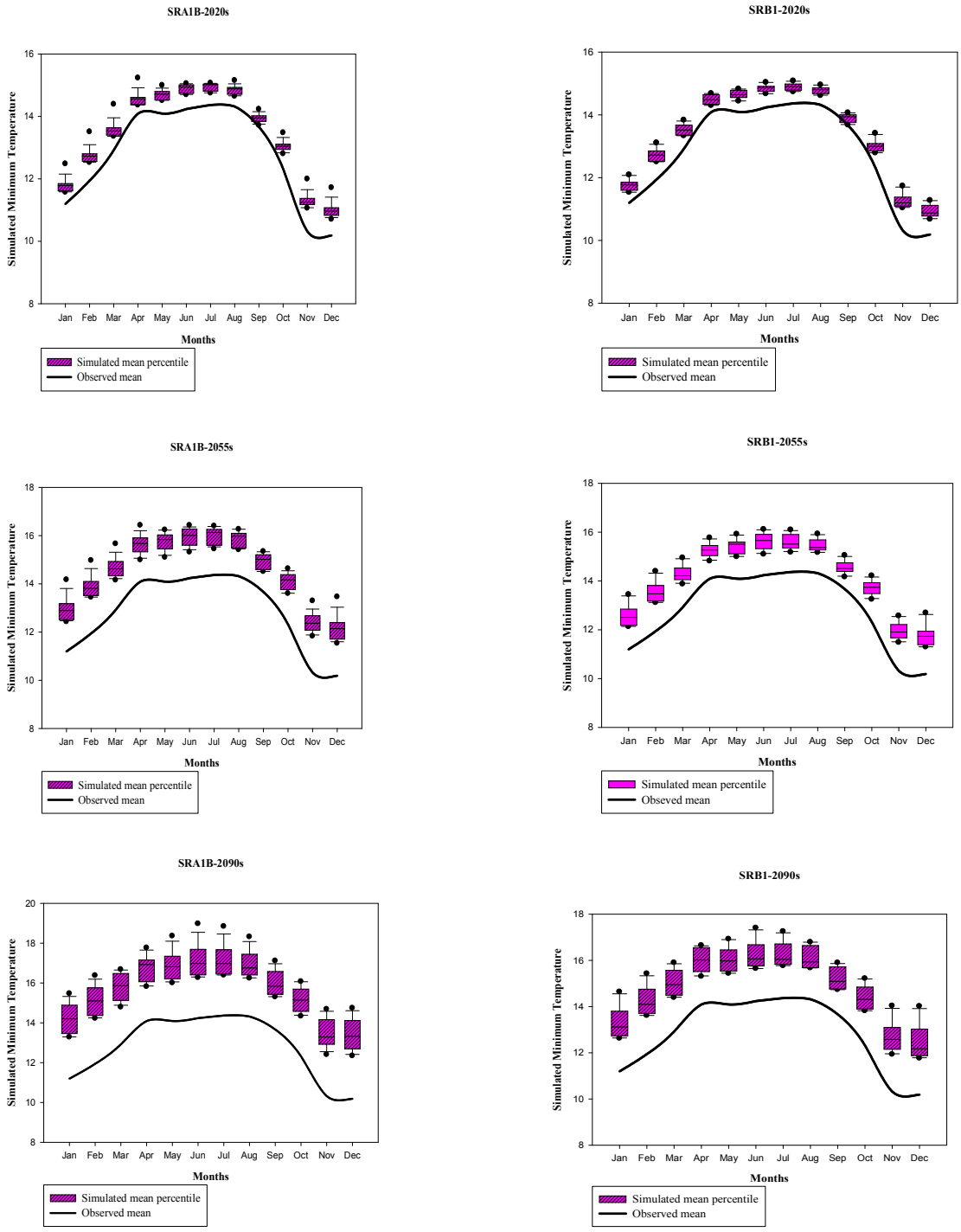

Figure 9: Box plots showing the simulated mean monthly minimum temperature for 15 GCMs under scenarios A and B for three different time periods**.**

Figures 7 to 9 clearly presents those 15 GCMs predictions variations among each model for the three climate variables (maximum, minimum temperature and rainfall) but the variation is high in rainfall than temperatures. Consider the estimated maximum temperature amount in the month of June estimated under emission scenario A in 2090s (SRA1B-2090s); The simulated maximum temperature amount by all GCMs for this month ranges approximately between 27.46 ^{0}c (GIAOM) GCM model to 30.23 ^{0}c (MPEH5) GCM model where the difference is about 2.768 ^{0}c. Similarly simulated minimum temperature in the month of December under emission scenario B in 2090s (SRB1-2090s) by all GCMs ranges between 11.76 ^{0}c (NCCCSM) GCM model to 14.02 ^{0}c (INCM3) GCM model where the difference is about 2.25 ^{0}c. This range in magnitude of output data simply confirms the notion that output weather variables from GCMs are associated with uncertainties. This phenomenon recurs in the rest of the months, scenarios and in all time periods both in simulated rainfall and minimum and maximum temperature data. It is therefore significant that such uncertainties are accounted for before outputs of GCMs are used in climate change assessment studies.

4.3. Uncertainty Analysis of GCMs

It was explained well under section 4.2 how much difference exist among GCMs output peculiarly in rainfall (70mm) which leads to uncertainty on the result. High uncertainties associated with GCMs' output greatly affect the confidence levels of the results of any climate assessment studies. Several methods have been proposed for dealing with uncertainties of GCMs as explained under section 3.4. This study employs the use of probability assessment of bounded range with known probability distribution in order to deal with uncertainties of the 15 GCMs. This process first involves determination of individual weights of each model, generation of probability distribution functions (PDFs) and construction of cumulative distribution functions (CDFs) based on the generated PDFs.

4.3.1. Weighting of GCMs

Each GCM is weighted according to its potential to simulate climate variables using formula explained in aforementioned section. Table 10 shows the weight of each GCM in simulating future changes in rainfall; Table 11 shows the weight of each GCM in simulating future changes in minimum temperature and Table 12 shows the weight of each GCM in simulating future changes in maximum temperature in each month. Generally, the expected relative

precipitation changes are more uncertain about 0.83 weight differences among GCMs models than the relative expected temperatures change which only is about 0.09 weight differences among GCM models. This result shows that LARS WG 5.5 model is more certain to predict monthly mean temperatures than to predict monthly mean rainfall.

4.3.2. Probability Distribution Functions (PDFs)

This is the second process of uncertainty analysis of GCMs. It involves generating monthly PDFs of rainfall and minimum and maximum temperature. Table 1-7 under Appendix A shows sample example of relative change of precipitation, minimum temperature and maximum temperature under scenario of SRA1B and SRB1 for the three time periods (2020s, 2055s, and 2090s). Figures 10-12 show sample monthly discrete PDFs for the 15 GMs under scenarios A (SRA1B) and B (SRB1) against weight of each model to simulate climate variables in coming three time horizons. For instance, first figure under figure 10 shows relative rainfall change against GCMs weight for the month of March for the period of 2020s under scenario SRA1B. The figure show that massive rainfall changes from 0.8 to 1.2 ranges in GCM weight of 0 to 0.1.

Table 10: Calculated weight of each GCM in simulating future rainfall

	Jan	Feb	Mar	Apr	May	Jun	Jul	Aug	Sep	Oct	Nov	Dec
BCM2	0.05	0.15	0.01	0.08	0.06	0.33	0.26	0.06	0.06	0.05	0.01	0.06
CGMR	0.02	0.04	0.26	0.05	0.03	0.02	0.02	0.04	0.05	0.05	0.01	0.04
CNCM3	0.02	0.06	0.02	0.17	0.08	0.03	0.05	0.05	0.06	0.03	0.01	0.03
CNCM3	0.04	0.11	0.02	0.12	0.06	0.17	0.07	0.05	0.05	0.09	0.02	0.09
FGOALS	0.03	0.04	0.02	0.03	0.06	0.04	0.09	0.05	0.06	0.03	0.01	0.04
GFCM21	0.03	0.1	0.03	0.15	0.12	0.02	0	0.04	0.16	0.05	0.01	0.1
GIAOM	0.07	0.07	0.04	0.04	0.04	0.04	0.19	0.06	0.06	0.05	0.01	0.07
HADCM3	0.05	0.04	0.01	0.03	0.16	0.07	0.11	0.06	0.06	0.06	0.01	0.05
HADGEM	0.02	0.16	0.23	0.06	0.1	0.07	0.01	0.03	0.04	0.22	0.83	0.2
INCM3	0.01	0.03	0.02	0.04	0.05	0.03	0.01	0.16	0.07	0.03	0.01	0.04
IPCM4	0.44	0.06	0.04	0.03	0.02	0.02	0.02	0.07	0.08	0.05	0.01	0.05
MIHR	0.02	0.04	0.09	0.03	0.02	0.02	0.07	0.05	0.06	0.05	0.01	0.04
MPEH5	0.13	0.05	0.09	0.11	0.1	0.08	0.04	0.18	0.09	0.05	0.01	0.06
NCCCSM	0.06	0.05	0.13	0.05	0.05	0.02	0.01	0.06	0.05	0.06	0.01	0.05
NCPCM	0.01	0.01	0	0.02	0.05	0.05	0.04	0.04	0.05	0.13	0.04	0.08

Table 11: Calculated weight of each GCM in simulating future minimum temperature

	Jan	Feb	Mar	Apr	May	June	July	Aug	Sept	Oct	Nov	Dec
BCM2	0.06	0.06	0.06	0.06	0.07	0.07	0.07	0.07	0.07	0.07	0.07	0.07
CGMR	0.05	0.06	0.06	0.05	0.05	0.05	0.05	0.04	0.04	0.05	0.06	0.06
CNCM3	0.05	0.05	0.05	0.05	0.05	0.05	0.05	0.05	0.04	0.05	0.05	0.05
CSMK3	0.08	0.08	0.08	0.08	0.08	0.08	0.08	0.09	0.10	0.09	0.08	0.08
FGOALS	0.09	0.08	0.08	0.09	0.09	0.08	0.08	0.08	0.08	0.08	0.09	0.09
GFCM21	0.06	0.06	0.06	0.05	0.06	0.06	0.06	0.07	0.06	0.06	0.07	0.06
GIAOM	0.08	0.08	0.08	0.08	0.08	0.08	0.08	0.08	0.09	0.08	0.07	0.08
HADCM3	0.06	0.06	0.06	0.06	0.05	0.05	0.05	0.06	0.05	0.06	0.06	0.06
HADGEM	0.09	0.09	0.09	0.09	0.08	0.08	0.07	0.07	0.08	0.08	0.09	0.08
INCM3	0.04	0.04	0.04	0.04	0.05	0.05	0.06	0.06	0.06	0.05	0.04	0.04
IPCM4	0.05	0.05	0.05	0.05	0.05	0.05	0.05	0.05	0.05	0.05	0.05	0.06
MIHR	0.04	0.05	0.05	0.04	0.05	0.05	0.05	0.05	0.04	0.05	0.05	0.05
MPEH5	0.05	0.06	0.05	0.05	0.05	0.04	0.04	0.05	0.05	0.05	0.06	0.06
NCCCSM	0.08	0.08	0.08	0.07	0.07	0.08	0.07	0.07	0.07	0.07	0.07	0.08
NCPCM	0.11	0.10	0.11	0.13	0.12	0.12	0.12	0.11	0.13	0.10	0.09	0.10

Table 12: Calculated weight of each GCM in simulating future maximum temperature

	Jan	Feb	Mar	Apr	May	June	July	Aug	Sept	Oct	Nov	Dec
BCM2	0.08	0.06	0.05	0.05	0.05	0.06	0.06	0.07	0.07	0.08	0.09	0.09
CGMR	0.05	0.05	0.06	0.05	0.05	0.05	0.05	0.04	0.04	0.04	0.04	0.05
CNCM3	0.05	0.04	0.05	0.04	0.05	0.05	0.05	0.05	0.04	0.04	0.04	0.04
CSMK3	0.07	0.07	0.07	0.07	0.07	0.07	0.07	0.07	0.07	0.08	0.08	0.07
FGOALS	0.08	0.08	0.08	0.08	0.09	0.08	0.08	0.08	0.08	0.08	0.08	0.08
GFCM21	0.05	0.05	0.05	0.05	0.05	0.06	0.06	0.07	0.06	0.06	0.05	0.05
GIAOM	0.10	0.11	0.09	0.10	0.10	0.09	0.09	0.09	0.09	0.09	0.09	0.10
HADCM3	0.05	0.05	0.06	0.05	0.05	0.05	0.05	0.05	0.05	0.05	0.05	0.05
HADGEM	0.08	0.10	0.09	0.09	0.08	0.08	0.07	0.07	0.07	0.08	0.08	0.08
INCM3	0.08	0.08	0.08	0.08	0.07	0.08	0.09	0.10	0.10	0.10	0.11	0.09
IPCM4	0.05	0.04	0.05	0.05	0.05	0.05	0.05	0.05	0.05	0.04	0.04	0.05
MIHR	0.05	0.04	0.05	0.04	0.04	0.05	0.05	0.05	0.04	0.04	0.04	0.05
MPEH5	0.05	0.05	0.05	0.05	0.04	0.04	0.04	0.05	0.05	0.05	0.04	0.05
NCCCSM	0.07	0.07	0.07	0.07	0.07	0.08	0.07	0.07	0.07	0.07	0.06	0.07
NCPCM	0.10	0.12	0.10	0.13	0.14	0.13	0.11	0.11	0.11	0.10	0.09	0.09

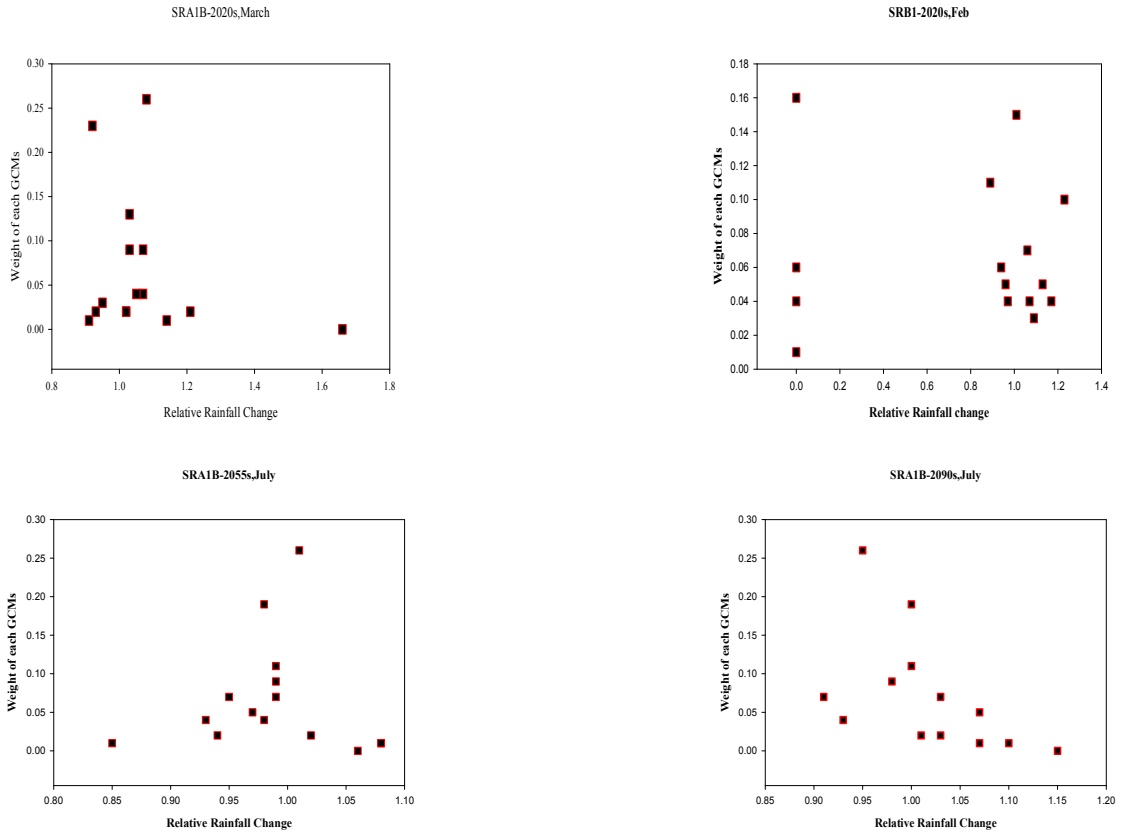

Figure 10: Sample Discrete PDFs outlining the relationship between weights of 15 GCMs and monthly changes in relative rainfall.

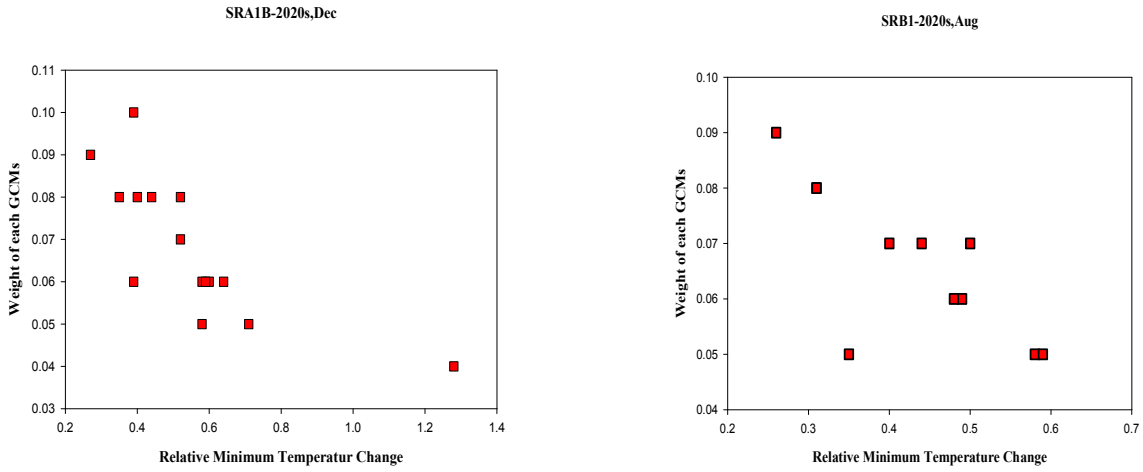

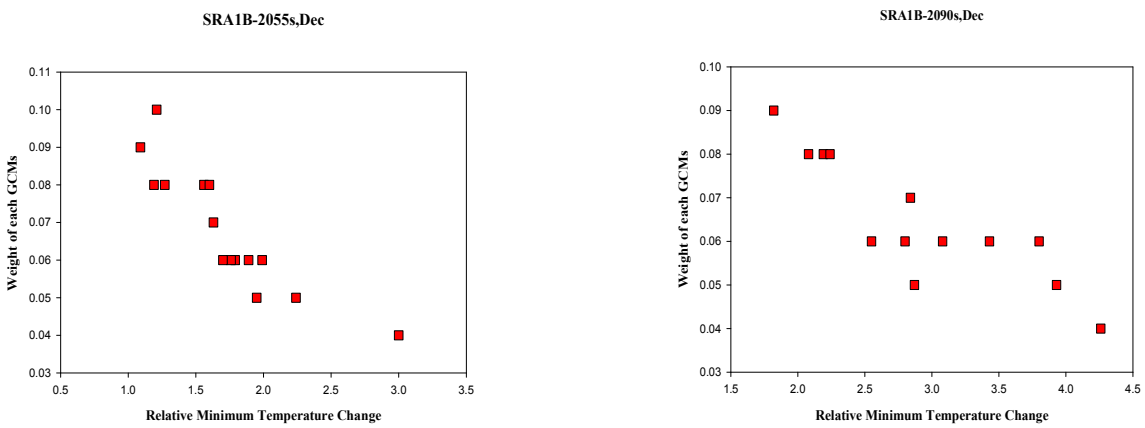

Figure 11: Sample Discrete PDFs outlining the relationship between weights of 15 GCMs and monthly changes in relative minimum temperature**.**

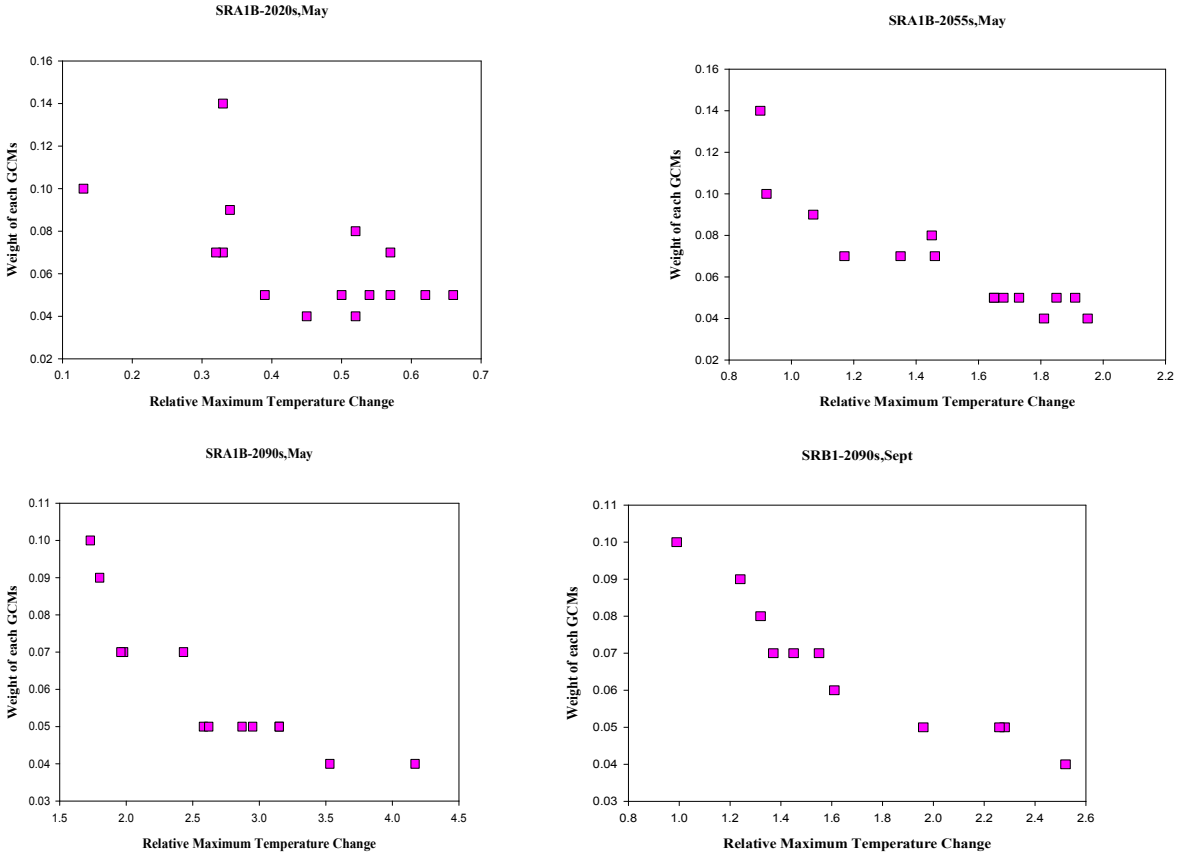

Figure 12: Sample Discrete PDFs outlining the relationship between weights of 15 GCMs and monthly changes in relative maximum temperature.

4.3.3. Cumulative Distribution Functions (CDFs)

The climate variables extracted at 25%, 50% and 75% probability percentiles from the developed CDFs as explained in section 3.4.3. Climate values at these three percentiles were then used as input data for maize yield climate impact assessment using AquaCrop model.

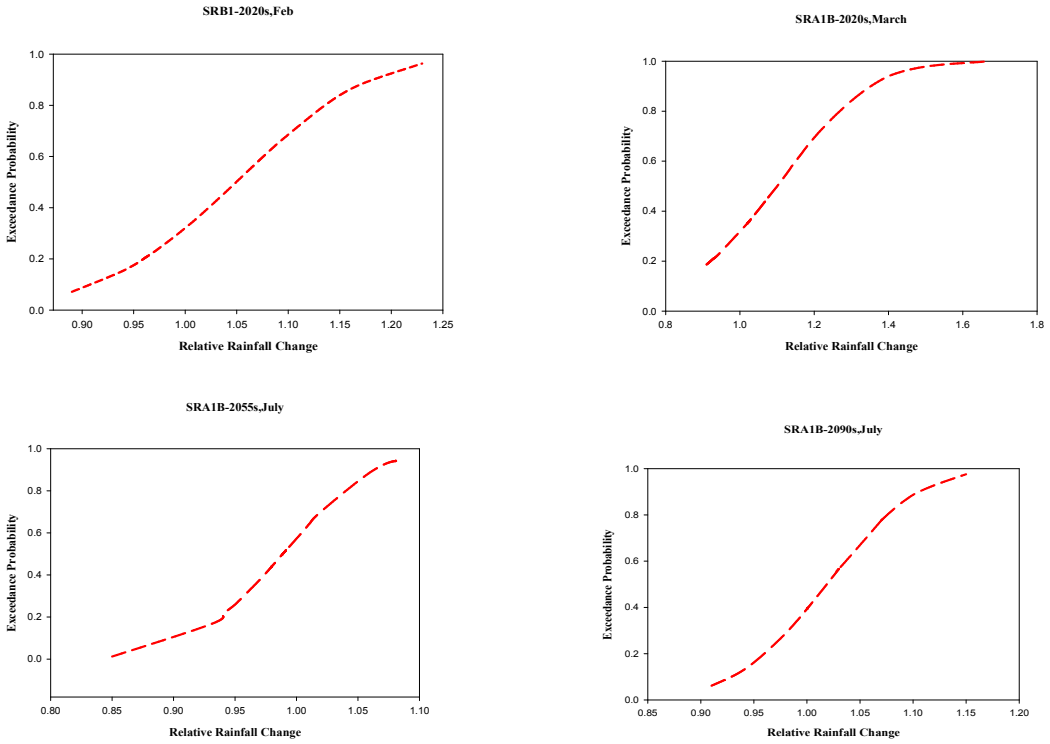

Figure 13: Sample CDFs for rainfall based on sample PDFs shown above under figure 10**.**

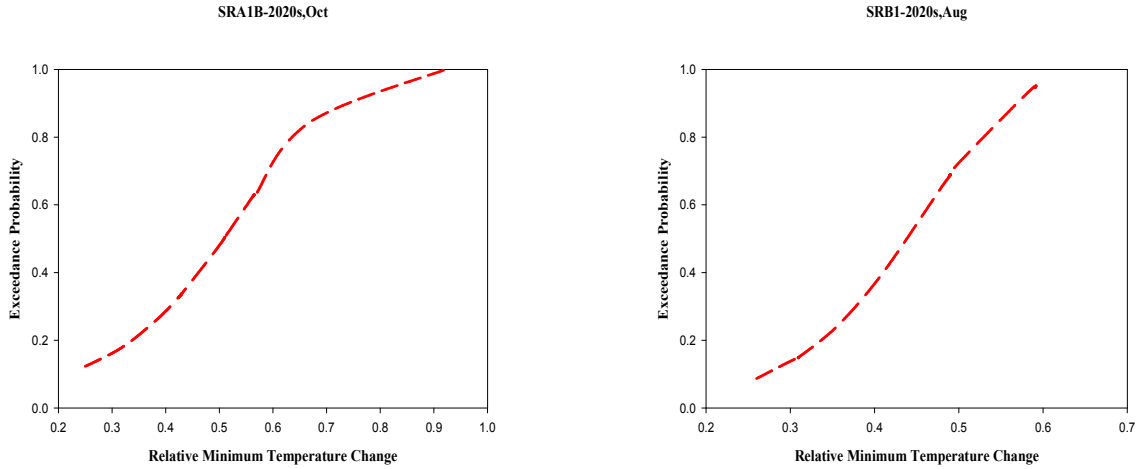

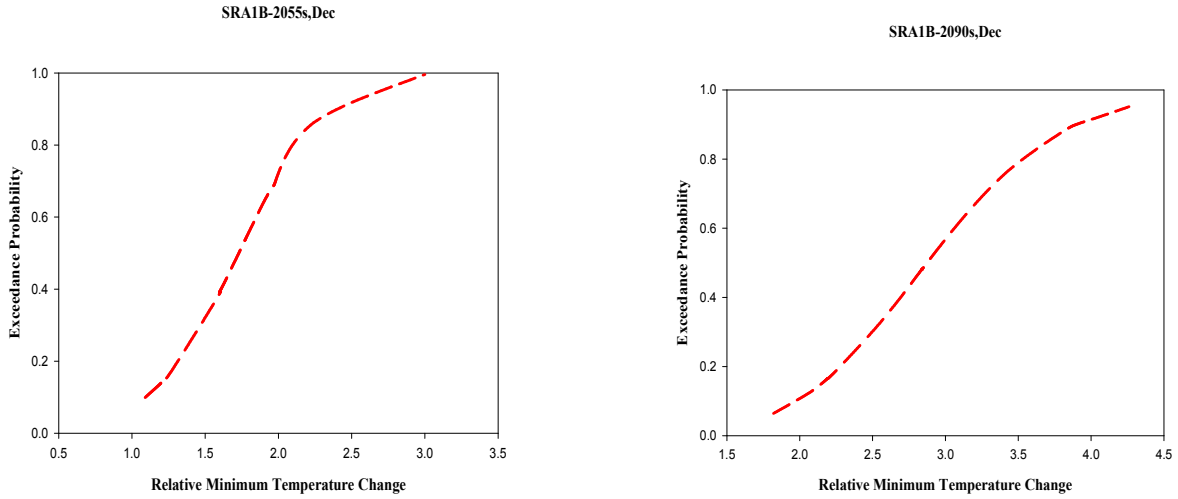

Figure 14: Sample CDFs for minimum temperature based on sample PDFs shown above under figure 11.

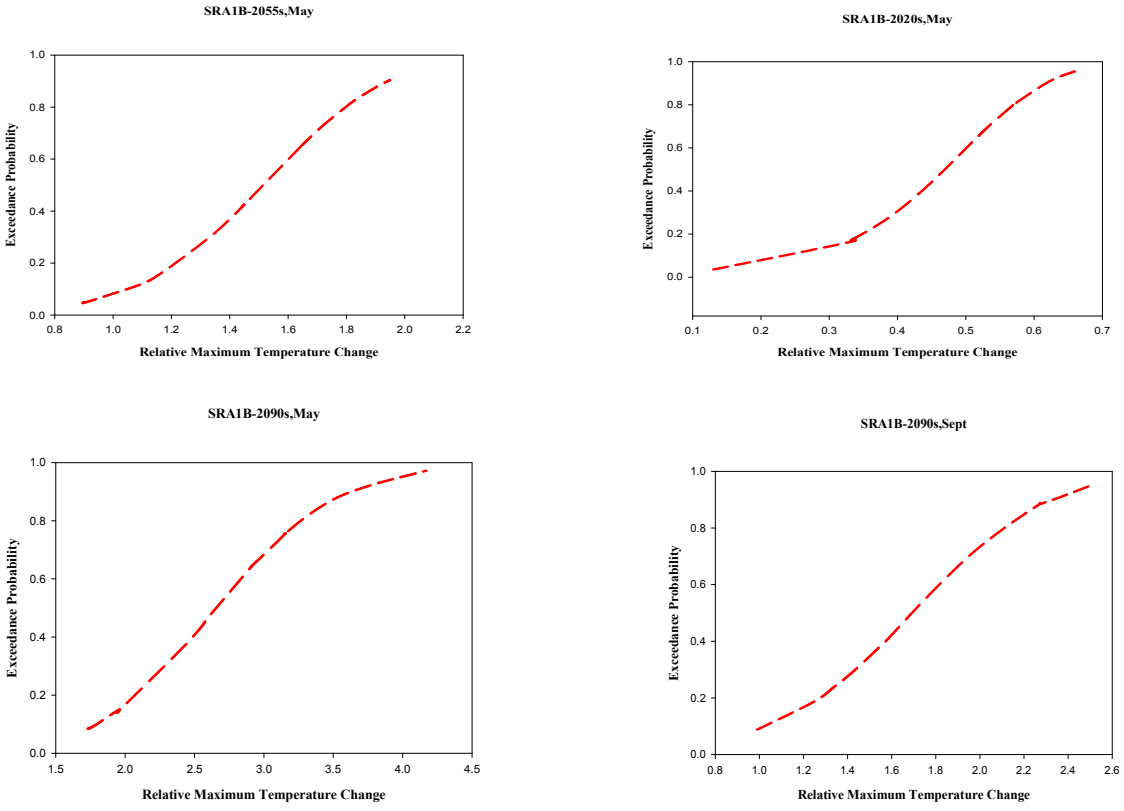

Figure 15: Sample CDFs for max temperature based on sample PDFs shown above under figure 12

4.4. Generation of Probability Percentiles

The magnitude of the expected changes in rainfall, minimum and maximum temperature at three different probability percentiles (25%, 50% and 75%), were determined from the synthetic CDFs for both scenarios (SRA1B and SRB1) and in three time steps (2020s, 2055s and 2090s). Figure 16 shows the expected changes in future rainfall amounts under two scenarios. The simulated results describe that higher rainfall changes are expected under scenario A than scenario B in all three time periods excepting in period 2055s at 25% probability percentile. The expected changes in monthly rainfall for each time period varies between risk levels. Results indicate high increase in rainfall in some months like December, January, and February (DJF) which is winter ('bega') season of the country. However, some months of year like May to August indicate low increase in rainfall under both scenarios for three time periods at each risk level and very low rainfall increase is generated in summer ('kiremt') season of the country from June to August (JJA). Table 8 under appendix A shows the general seasonal rainfall variability at each time periods under both emission scenarios at three probability percentile. The result shows the seasonal increase of rainfall in descending order as winter ('bega', DJF), autumn ('tseday', SON), spring ('belg', MAM), summer ('kiremt', JJA). Therefore as we observe from this result planting date schedule should be taken into account based on the result to overcome plant water scarcity for this particular study area. On average, summer rainfall amounts are expected to increase and/or decrease with the ranges of -2.34% to 2.67%, -5.5% to 4.67% and -4% to 8.34% in 2020s, 2050s and 2090s respectively and winter rainfall amounts are expected to increase and/or decrease with ranges -3.67% to 15%, 6.34 to 37.5% and 7.84% to 66.34% in 2020s, 2050s and 2090s respectively. However, overall mean monthly rainfall prediction indicate rainfall increase in the study area which ranges -2.3 to 7%, 0.375 to 15.83% and 2.625 to 31.0% in three time periods 2020s,2055s and 2090s respectively, whereas the same study using 10 GCMs models (Gohari A.et al, 2013) conducted in Iran show that precipitation decrease from 11%-31% in mid period(2046-2065).

Ethiopia national meteorological agency (NMA) released climate projections for Ethiopia that has been generated using the software MAGICC/SCENGEN (Model for the Assessment of Greenhouse-gas Induced Climate Change)/ (Regional and global Climate SCENario GENerator) coupled model (Version 4.1) for three periods centered on the years 2030, 2050

and 2080. Rainfall prediction for coming three time periods based on 19 GCMs models for different parts of the country under scenario A1B and B1 with relative to baseline period of 1961-1990 normal. The study result outlined that rainfall projections from different models in the ensemble are broadly consistent in indicating increases in annual rainfall in Ethiopia. However these increases are likely to occur in the October, November and December rainfall season (OND) in southern Ethiopia and in an increasing amount of rainfall occurring in "heavy events." Annual changes in heavy events range from -1 to +18%. The largest increases are seen in JAS and OND rainfall (F.D.R.E, MoWR-NMA, 2011). Projections of change in the rainy seasons April, May, June (AMJ) and July, August, September (JAS) rainfall seasons which affect the larger portions of Ethiopia are more mixed, but tend towards slight increases in the south west and deceases in the north east (F.D.R.E, MoWR-NMA, 2011). Figure 16 to 18 present estimated future changes in rainfall, maximum temperature and minimum temperature at three probability percentiles**.** The top two plots indicate changes for the near future (2020s), the middle plots indicate changes for the middle period (2055s) and the bottom plots indicate the changes in the long term period (2090s), for each climate variables all under SRA1B and SRB1

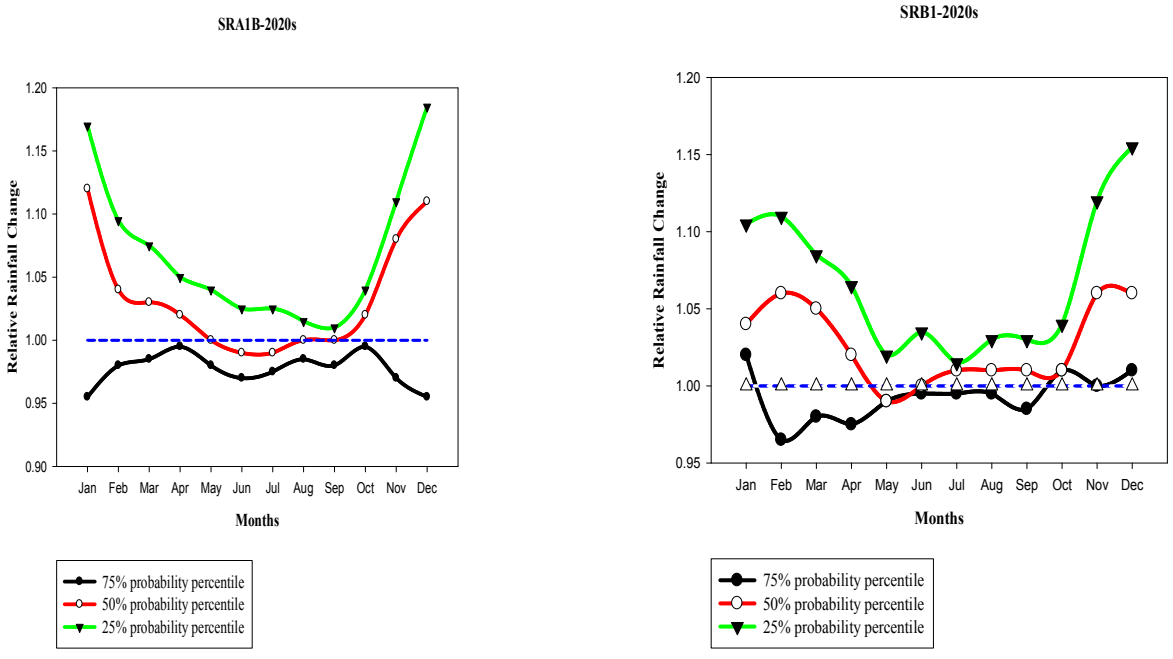

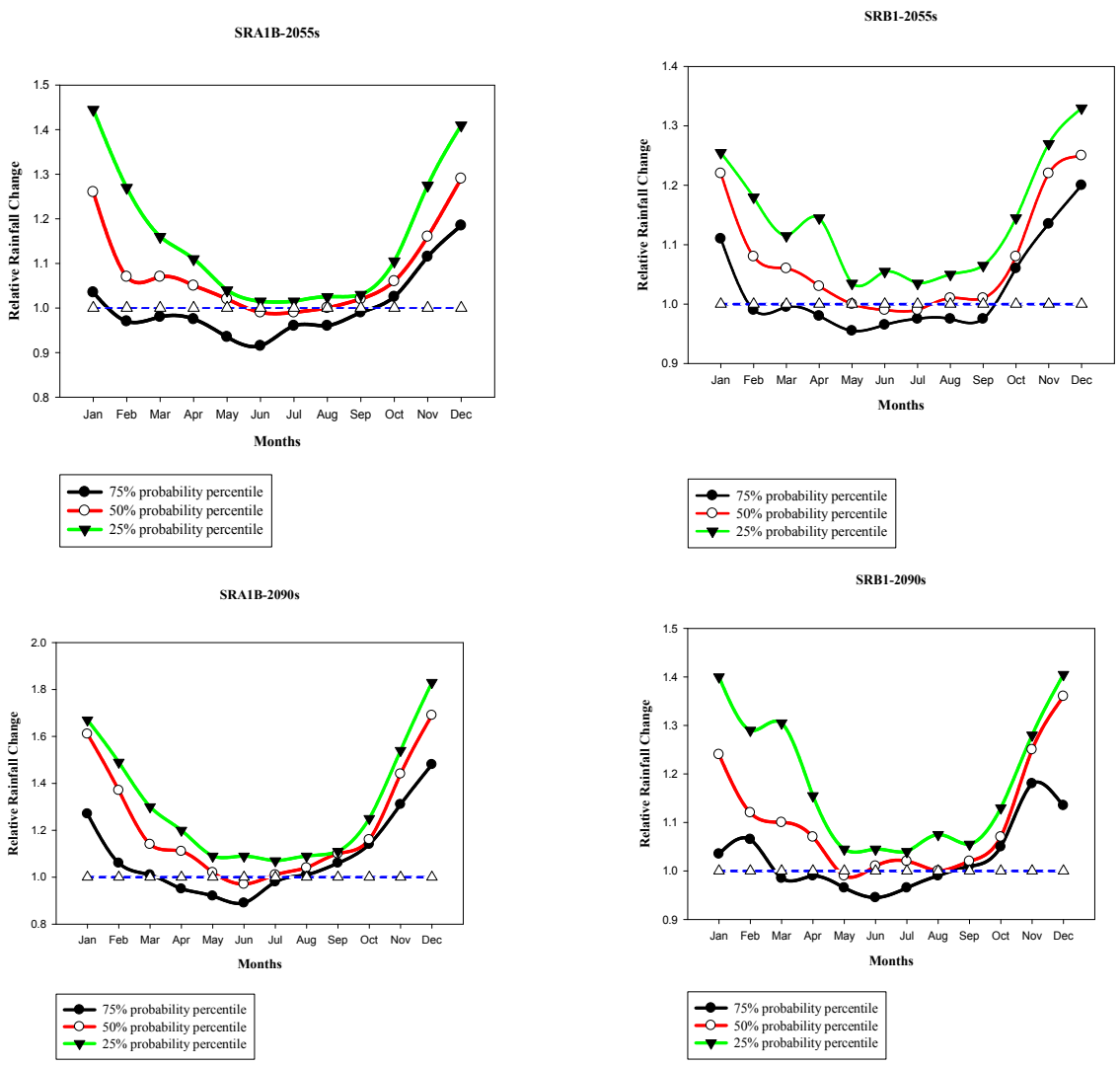

Figure 16: The estimated future changes in relative rainfall at three probability percentiles.

Figures 17 and 18 are plots of minimum and maximum temperatures for scenarios A and B under three percentiles at three time periods. Overall, temperature is expected to increase in all cases, with higher temperature changes expected under scenario A than in scenario B. Absolute values for changes in minimum temperature for 2020s, 2055s and 2090s are 0.34ºC to 0.58ºC, 0.94ºC to 1.8ºC and 1.42ºC to 3.2ºC respectively. Similarly, changes in maximum temperature for the same time periods were estimated as follows; 0.32ºC to 0.56ºC, 0.91ºC to 1.8ºC and 1.34ºC to 3.035ºC respectively.

The same study released by national meteorological agency (NMA) of Ethiopia as explained above for rainfall using the IPCC mid-range (A1B) emission scenario, the mean annual temperature will increase in the range of 0.9 -1.1 °C by 2030, in the range of 1.7 - 2.1 °C by 2050 and in the range of 2.7-3.4 °C by 2080 over Ethiopia compared to the baseline 1961-1990 normal. Other sources of data have also substantiated the variability of climate and its trends in a somewhat similar ways. Historical climate analysis for Ethiopia indicates that mean annual temperature has increased by 1.3°C between 1960 and 2006, an average rate of 0.28°C per decade. The result of the study also declared that an increase in temperature in Ethiopia has been most rapid in June, August and September at a rate of 0.32°C per decade (F.D.R.E, MoWR-NMA, 2011) whereas the result of this study indicates rapid temperature increase is simulated in December, January and March. Therefore the result of the study confirms this study result even though that study result didn't downscale the climate variables to specific site and only outlined direct GCMs outputs for all the country whereas this study is for some specific area in southern region by using LARS WG weather generator downscaling tool; Hawassa as center of grid resolution which depends on the model spatial resolution. Even though the study uses 19 GMCs models with baseline 1961-1990 which is normal whereas this study depends on 15 GCM model with baseline 1985-2014, three climate change variables are in the same range. A summary of average changes in precipitation, minimum and maximum temperature for each scenario and time period is shown in Table 13.

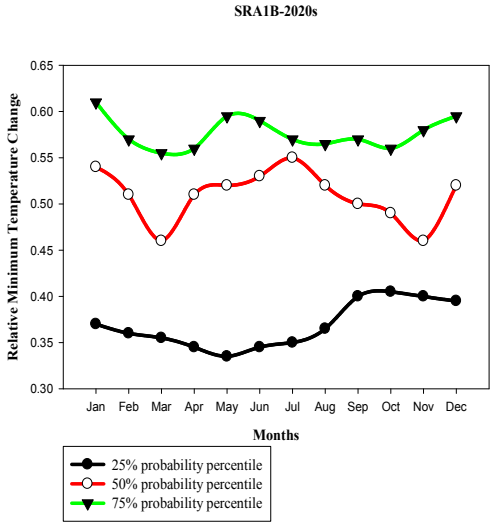

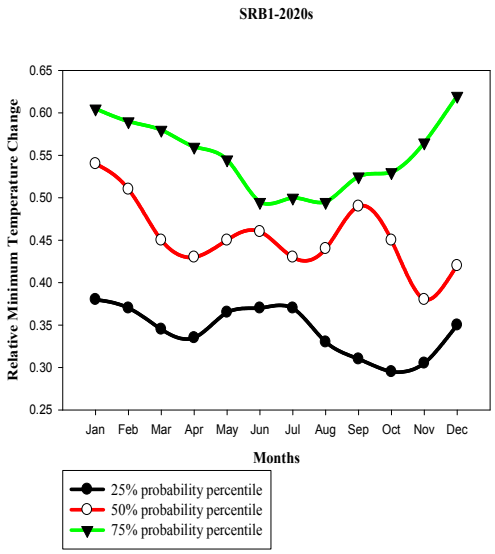

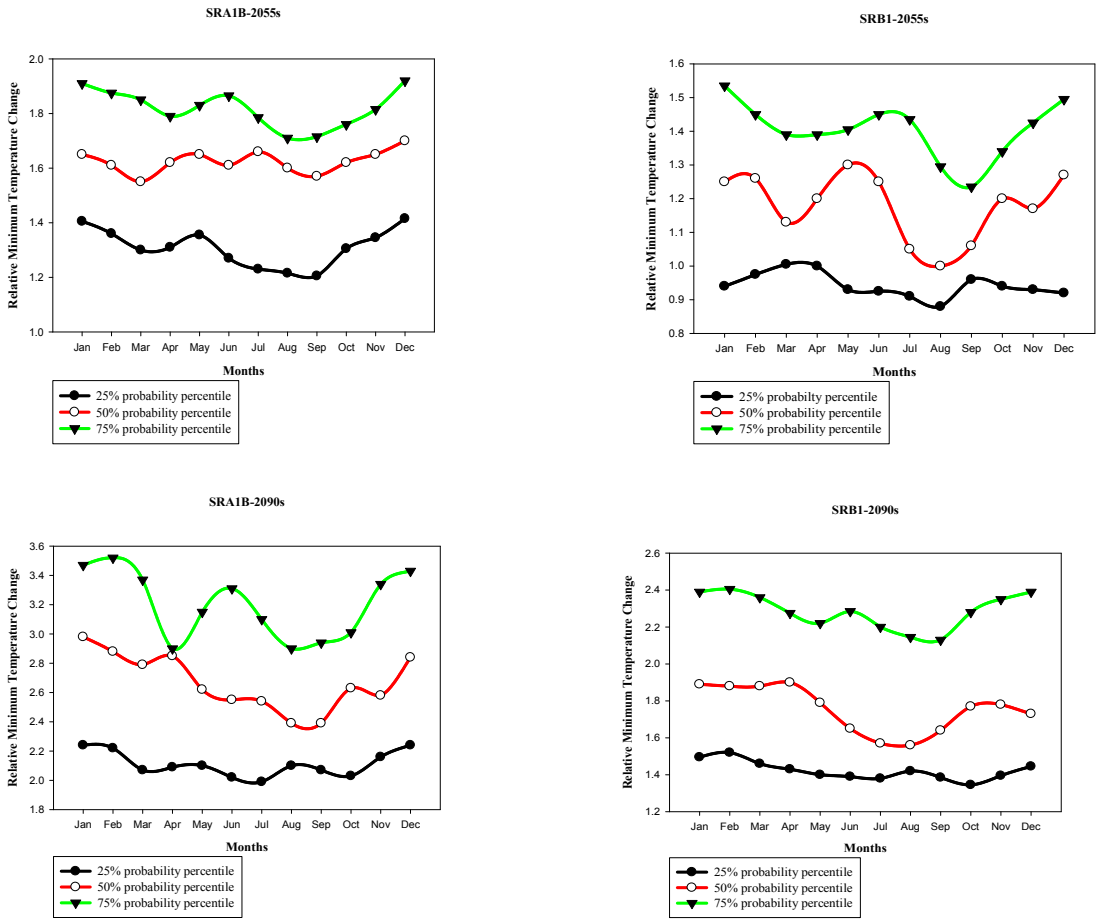

Figure 17: Estimated future changes in minimum temperature at three probability percentiles.

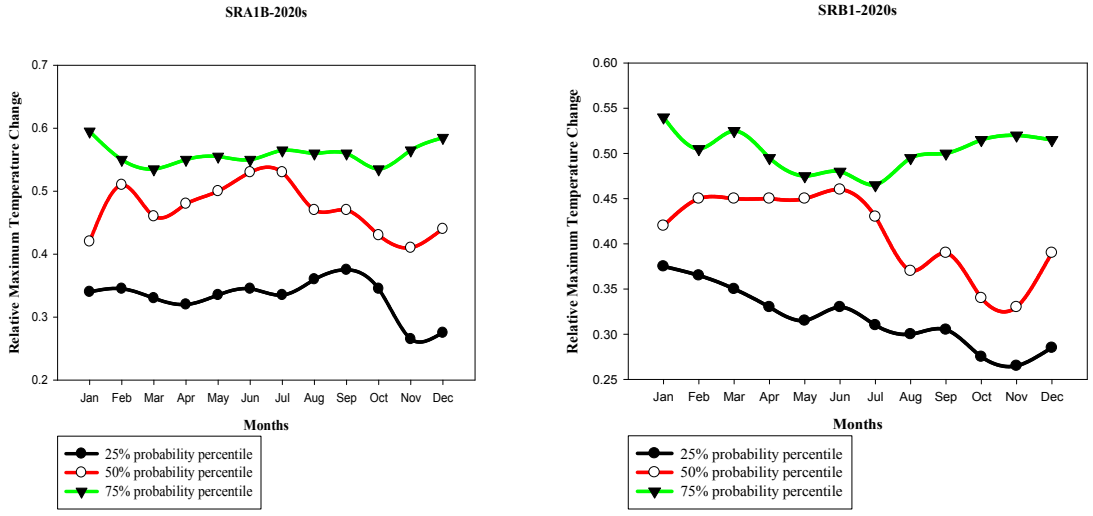

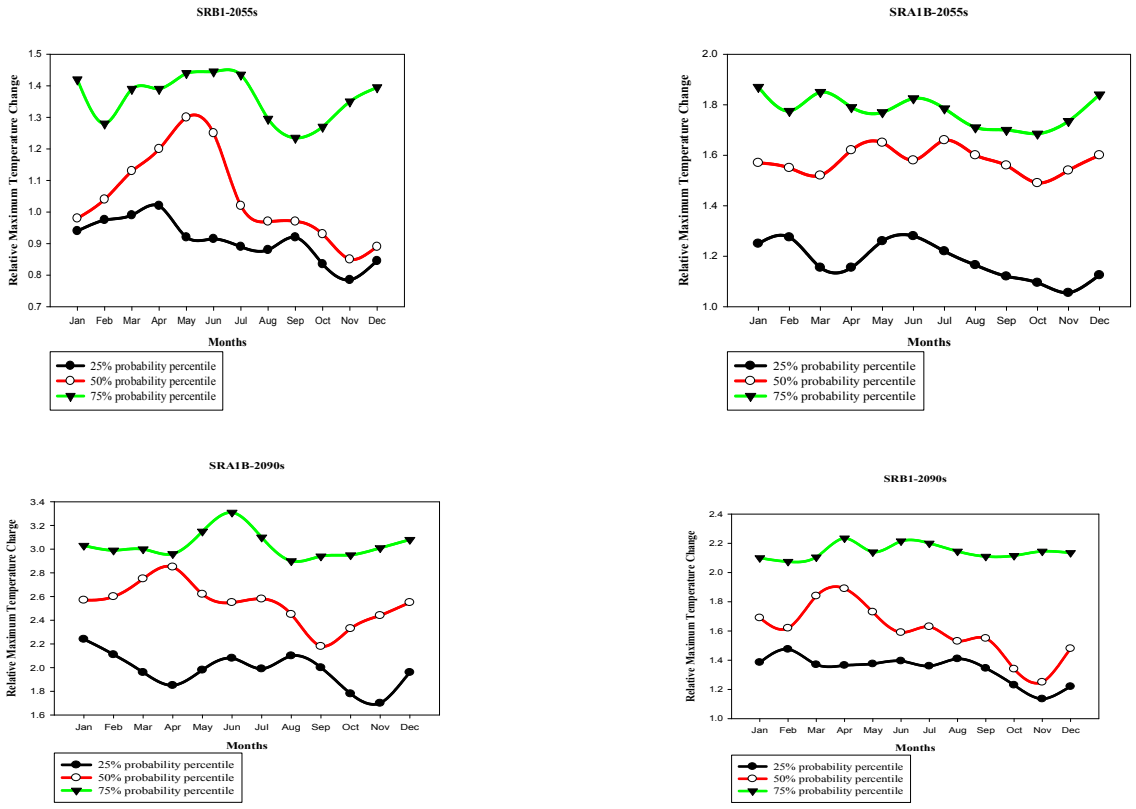

Figure 18: Estimated future changes in maximum temperature at three probability percentiles**.**

Table 13: Summary of mean annual and overall ranges of estimated climate variables in each time period, at different scenarios and probability percentiles

Climate Variable	Scenario percentile	A			B			Range	
		25A	50A	75A	25B	50B	75B		
Rainfall Change (%)	2020	7	3.33	-2.3	6.75	2.67	0.67	-2.3	7
	2055	15.83	8.17	0.375	14	7.83	2.625	0.375	15.83
	2090	31.1	22.17	9	18.54	10.42	2.625	2.625	31.1
Minimum Temperature Change(^{0}C)	2020	0.37	0.51	0.58	0.34	0.45	0.55	0.34	0.58
	2055	1.3	1.6	1.8	0.94	1.18	1.4	0.94	1.8
	2090	2.11	2.67	3.2	1.42	1.75	2.29	1.42	3.2
Maximum Temperature Change(^{0}C)	2020	0.33	0.47	0.56	0.32	0.41	0.5	0.32	0.56
	2055	1.18	1.58	1.8	0.91	1.04	1.36	0.91	1.8
	2090	1.98	2.54	3.035	1.34	1.6	2.14	1.34	3.035

Even though no similar study conducted in this area using GCMs models on climate change impacts on crop production to compare the result of this study with it, the result of this study indicate that precipitation change is increasing in all time period and all probability percentiles except it decreases in 2020s at 75 probability percentile under scenario A. In general as summarized in table 13 rainfall increases with ranges from -2.3 to 7%,0.375 to 15.83% and 2.625 to 31.0% in three time periods 2020s,2055s and 2090s respectively relative to baseline 1985-2014. Like precipitation temperature increase in all months in the coming three time periods gradually as explained above.

According Manfred K. and Netsanet Z., (2013) research conducted in Upper Blue Nile River Basins using mono and multi-modal statistical downscaling of GCMs Climate Predictors based on A2 and A1B SRES suggests that increase of the seasonal temperatures for both downscaling tools and both SRES scenarios. Thus, for the 2050s time period the seasonal maximum temperatures T_{max} rise between 0.6 ^{0}C to 2.7 ^{0}C and the minimum ones T_{min} by 2.44 ^{0}C. Similarly, during the 2090s the seasonal T_{max} increase by 0.9 ^{0}C to 4.63 ^{0}C and T_{min} by 1 ^{0}C to 4.5 ^{0}C relative to baseline (1970-2000), whereby these increases are generally higher for the A2 than for the A1B scenario. For both SRES scenarios and both simulated future time periods, the T_{max} and T_{min} for spring and summer seasons are warmer than for the autumn and winter seasons.

Study done in Malawi Saka et al. (2003) used four GCMs (CSIRO, ECHAM, CGCMI and HadCM2) to estimate future changes in weather data for years 2020, 2075 and 2100 using baseline weather data of 1961-1990 also indicate that mean temperature will increase by 1^{o}c by the year 2020, 2^{0}C by the year 2075 and 4^{0}C by the year 2100. In terms of rainfall, they also discovered that its pattern was not so certain with increase and decrease in different months in a year. However, they predicted a decrease in annual rainfall amounts ranging from 2% to 8% relative to the baseline. Study in Iran using 10 GCMs (Gohari et al.2013) based on base line 1961-1990 also indicate that expected monthly precipitation changes under climate change with respect to the baseline are very different for different probability percentiles. Results suggest negative changes for some months of the year and positive changes in other months at different probability percentiles. In most cases winter precipitations are expected to decrease with climate change in contrast to this study where a precipitation in winter is expected to increase. The projected annual and seasonal changes of 30-year mean temperature and total

precipitation were calculated under different probability percentiles of climate change indicate that 11–31% decrease in precipitation and 1.1–1.5 °C increase in temperature by 2050s.

4.5. Maize Yield Estimation with AquaCrop

4.5.1. Model Calibration

By inputting the 2014 weather data into the model benchmark for future simulation is set at three probability percentiles and three time periods. The model grossly overestimated maize yields when compared with recorded data in the study area for year 2014. It was therefore essential that adjustment of important and sensitive parameters in the model be carried out. By adjusting crop, management and soil properties in the main menu of AquaCrop, an output yield close in value to the recorded yield in 2014 was derived. Before calibrating the model, first the potential evapotranspiration (ETo) was estimated using the FAO ETo Calculator which uses the Penman-Monteith equation. Recorded data for maize production in year 2014 for Hawassa district was averagely 7.5 tons per hectare. After varying the model parameters, the closest simulated production was 7.496 tons per hectare. Once model calibration was complete, the model was then validated to determine its potential to simulate maize yields.

4.5.2. Model Validation

Historical recorded maize yields for the area from 2008-2013 were used to compare with those simulated by AquaCrop in order to determine its potential to simulate future maize yields at three probability percentiles and time periods. Table 14 presents observed versus estimated maize yield production with their respective statistical indicators used for the validation of AquaCrop model.

Table 14: AquaCrop validation statistical analysis results for maize yields.

Year	Yields(ton/ha)		Pe(±%)	Ns	R2	RMSE	MAE(ton/ha)
	observed	simulated					
2008	6.5	6.39	1.69				
2009	6.4	6.56	2.50				
2010	6.7	6.746	0.69				
2011	6.8	6.852	0.76				
2012	7.25	7.245	0.07	0.906	0.908	0.11	0.12
2013	7.2	7.06	1.67				

The minimum and maximum prediction error (Pe) for maize yields for four growing season (2008-2013) ranges 0.07 to 2.5% whereas RMSE and MAE are 0.11 and 0.12 respectively. The three statistical parameters are close to zero, which indicates the suitability of the model to simulate future maize yields for three time periods and three percentiles. Estimated values of Nash and Sutcliffe (Ns) and coefficient of determination (R^2) of 0.906 and 0.908 respectively are both close to 1, which further increases confidence in the model's potential to simulate future maize yields. The validation results indicate that the model can be used to simulate future maize yields within acceptable deviations from the true values.

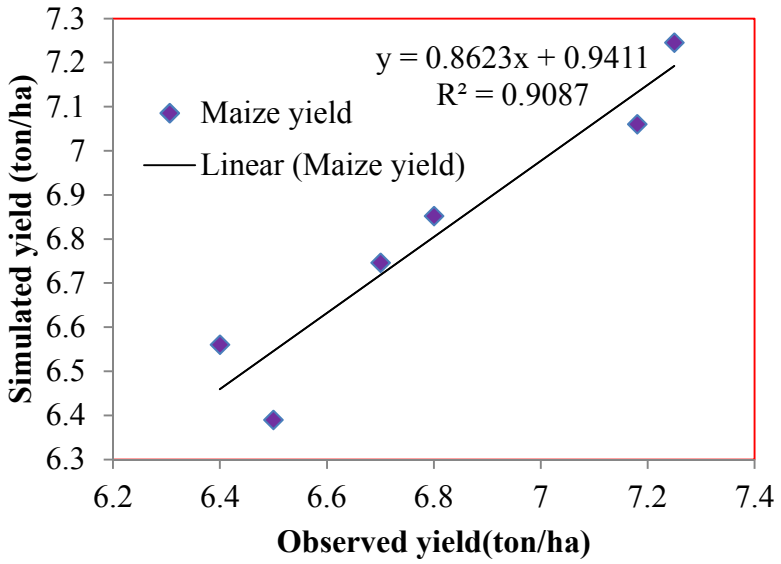

Figure 19: AquaCrop validation results using the 2008-2013 simulated and recorded maize yields.

4.5.3. Simulating Future Maize Yields with Climate Change

Simulating future potential rainfed maize yields with climate change is the main objective of this study. To achieve this objective calibrated and validated crop model (AquaCrop) was used to estimate both average historical maize yields for the baseline period (1985-2014) and future potential maize production at three probability percentiles and time periods. Climate data (rainfall, minimum and maximum temperature, sunshine hours, relative humidity) for the 30 years baseline period (1985-2014) were broken down into monthly averages in each of the 12 months. By keeping all parameters the same and changing only climate parameters which used

during model calibration and validation the results from the model run indicated an average baseline period maize production of 7.2 ton/ha. This value is considered as maize production without climate change. Average values of future potential maize yields at various probability percentiles were calculated in a similar manner. Table 15 summarizes the simulated maize yields as a percentage, relative to the baseline period.

Table 15: Maize production (tons/hectare) at different probability percentiles and time periods

Period	Percentile	Production Change (%)		Range (%)	
		Scenario A	Scenario B		
2011-2030 (2020s)	25	3.89	3.63	3.63	7
	50	7	4.13		
	75	5.43	4.53		
2046-2065 (2055s)	25	6.79	5.39	5.39	14.08
	50	9.32	6.36		
	75	14.08	10.03		
2080-2099 (2090s)	25	9.33	6.83	6.83	15.61
	50	12.04	9.26		
	75	15.61	12.58		

In general, the results suggest an increase in maize yields for all the three time periods, scenarios and percentiles. The expected percentage changes in maize yields for 2011-2030, 2046-2065, and 2080-2099 are 3.63% to 7%, 5.39% to 14.08%, and 6.83% to 15.61% respectively. This result indicates that in coming three time periods maize production increases with climate change, whereby all crop parameters, soil fertility and field management were kept the same or improved relative to baseline of (1985-2014).

CHAPTER FIVE

5. CONCLUSIONS AND RECOMMENDATIONS

The main focus of this study was to evaluate climate change impacts on rainfed maize production in Ethiopia. 15 GCMs were used to estimate future climate variables in three different time periods (2020s, 2055s and 2090s) using two scenarios (SRA1B and SRB1). Historical weather data (1985-2014) for Hawassa Meteorological Station in Hawassa town was utilized for future climate projections under climate change. Hawassa district was selected as a case study site.

Due to low resolution of GCMs that result in a mismatch between simulated global and local data, it was significant to downscale the outputs of GCMs (rainfall and temperature data). Downscaling of GCMs simulated weather data was achieved using latest version LARS-WG 5.5 model, a stochastic weather generator that has been extensively used in climate change studies. The model was calibrated and validated in order to determine its potential to estimate significant and reliable future climate variables. High *p*-values of chi-square, *K-S* and *t*-tests signified high similarity and reliability between observed and simulated climate data. GCMs are also associated with high uncertainty levels which negatively impact on the credibility of the output data. This study employed the use of probability analysis in which a bounded range with known probability distribution was used to account for the uncertainties of fifteen (15) GCMs. The procedure involved

- weighting of GCMs,
- generating monthly probability distribution functions (PDFs)
- Constructing monthly cumulative probability functions (CDFs) from which weather data at three risk levels (25%, 50% and 75%) in three time periods and two scenarios, were extracted and used as input data for the crop model.

AquaCrop Version 4, a new model developed by FAO that simulates the yield response to water deficit conditions, was used to assess potential maize production under rainfed farming with and without climate change. The model was first calibrated and validated using historical data to determine its reliability to simulate maize yields and statistical indicators like R^2, Ns, RMSE, MAE and Pe were used to assess the suitability of the model to simulate potential maize yields. AquaCrop does not include an algorithm for calculating ETo, therefore, the FAO

ETo Calculator was used to estimate evapotranspiration for potential crop production in AquaCrop.

5.1. Conclusions

The study result indicates that LARS-WG 5.5 model is more uncertain to simulate future mean rainfall than generating maximum and minimum temperature whereby GCMs weight difference for rainfall is about 0.83 and 0.09 for temperatures. The results of this study also indicate that mean annual rainfall changes of the area ranges -2.3 to 7%, 0.375 to 15.83% and 2.625 to 31.1% in 2020s, 2055s and 2090s respectively. However, mean monthly rainfall patterns depicted both increase and decrease behavior in different months and time period; indicating relatively rainfall decrease in summer and rainfall increase in winter for all three time periods and three probability percentiles. An overall increase in mean monthly temperature in all three time periods was observed. Average minimum temperature changes range for 2020s, 2055s and 2090s are 0.34^0C to 0.58^0C, 0.94^0C to 1.8^0C and 1.42^0C to 3.2^0C respectively. Similarly, changes in maximum temperature for the same time periods are 0.32^0C to 0.56^0C, 0.91^0C to 1.8^0C and 1.34^0C to 3.035^0C respectively. An overall temperature change for three time periods ranges 0.32^0C to 0.58^0C, 0.91^0C to 1.8^0C and 1.34^0C to 3.2^0C in 2020s, 2055s and 2090s respectively. Simulated temperature results compare well with the 2007 report of the Intergovernmental Panel on Climate Change (IPCC) which indicates that in sub-Saharan Africa, temperatures will rise by over 3°C in 21st century. The results from the crop model show an overall increase in maize production yields in all three time periods for this particular district with climate change by keeping all crop parameters, soil fertility and field management constant or improved under both emission scenarios (SRA1B and SRB1). The expected range of changes in maize production for changed climate for three time periods 2020s, 2055s, and 2090s are 3.63% to 7%, 5.39% to 14.08%, and 6.83% to 15.61% respectively.

Many studies discussed above conducted in different countries show that maximum and minimum temperature will increase whereas rainfall decreases in coming three time periods under different emission scenarios; on the other hand climate change study released by Ethiopian National Meteorological Agency indicate that temperature and rainfall change increase in the same range with this study. This study shows that minimum and maximum

temperature will increase with rainfall in coming times periods what makes maize yield to increase for this particular study area.

5.2. Recommendations

Even though maize productions yield responds positively to the climate change impact the following recommendations should be taken in account.

- Since there is seasonal climate change variability (inter seasonal variation) planting date should be considered.
- Well managed field which improve the water retaining of soil through mulching and erecting soil bunds considered during yield simulation. Therefore since crop water requirement depends on rainfall water management should be taken into account.
- Soil fertility should be improved since soil fertility stress free considered during yield simulation.
- Maize variety should be considered since this study uses BH-546 maize variety which is highly resistance water stress during simulation.

5.3. Study Limitations

Like any other work, this study also has some limitations which may to a certain extent affect the overall results. Human error is one of the crucial areas which may affect the results. The AquaCrop model uses annual average yield of different area in the district which grow with different soil type and different planting schedule for calibration and validation. Long term averages do not account for intra-annual weather variability which may be critical in assessing climate change impacts on crop production. Additionally, AquaCrop a crop simulation model used in this study, does not consider the effect of pests and weeds on maize yields. Pests and weeds play a significant role in total biomass production and hence yield. However, the assumption is that proper field management practices are employed which retards the growth of weeds and outbreak of pests.

REFERENCES

Abedinpoura M., Sarangib A., Rajputb T.B.S., Singhb M., Pathakc H., and Ahmad T. 2012. Performance evaluation of AquaCrop model for maize crop in a semi-arid environment. Agricultural Water Management 110 :55– 66.

Adams J.E., Arkin G.F., and Ritchie J.T. 1976. Influence of row spacing and straw mulch on first stage drying. Soil Sci. Soc. Am.J. 40:436-442.

Adams R.M. 1989. Global climate change and agriculture: An economic perspective. American Journal of Agricultural Economics 71(5):1272-1279.

Aerts, J. Droogers, P. 2004. Climate Change in Contrasting River Basins: Adaptation Strategies for Water, Food, and Environment. CABI Books, Londen, p. 288.

Allen R., Pereira L.S., Raes D., and Smith M. 1998. Crop evapotranspiraron-Guidelines for computing crop water requirements. Irrigation and Drainage Paper No. 56. FAO, Rome.

Anderson E.R., Cherrington., E.A., Flores A.I., Perez J.B., Carrillo R., and Sempris E. 2008. Po tential Impacts of Climate Change on Biodiversity in Central America, Mexico, and the Dominican Republic, CATHALAC / USAID. Panama City, Panama. 105 pp.

Arega D. 2003.Improved Production Technology and Efficiency of Small Holder Farmers In Ethiopia: extended parametric and non-parametric approaches to production efficiency analysis PHD thesis university of Pretoria.

Ayenew T. and Tilahun N., 2008, Assessment of lake-groundwater interactions and anthropogenic stresses, using numerical groundwater flow model, for a Rift lake catchment in central Ethiopia, Lakes & Reservoirs; Research and Management 2008 **13**: 325-343

Barron J., Rockcträm, J., Gichuki, F., Hatibu, N. 2003. Dry spell analysis and maize yields for two semi-arid locations in East Africa. Agric. For. Meteorol. 117, 23–37.

Block PJ, Souza Filho FA, Sun L, Kwon HH.2009. A stream flow forecasting framework using multiple climate and hydrological models 1. J Am Water Resour Assoc;45(4): 828–43.

Brown, D.R., Dettmann, P., Rinaudo, T., Tefera, H. and Tofu, A. 2011. Poverty alleviation and environmental restoration using the clean development mechanism: A case study from Hum bo, Ethiopia, Environmental Management, 48:322–333.

Buishand T.A. 1978. Some remarks on the use of daily rainfall models. Journal of Hydrology 36, 295–308.

Cai X., Wang D., Lauren R. 2009. Impact of Climate Change on Crop Yield: A Case Study of Rainfed Corn in Central Illinois, Journal of Applied Meteorology and Climatology. Vol.48:1868-1881.

Carlson R.E., Todey D.P., Taylor S.E. 1996. Midwestern corn yields and weather in relation to extremes of the southern oscillation. J Prod Agric 9:347–352.

Carter T. R., Parry M. L., Harasawa., H., and Nishioka S. 1994. IPCC technical guidelines for assessing climate change impacts and adaptations. London,United Kingdom/Tsukuba, Japan : University College/Centre for Global Environmental Research.

Chamberlin J. and Schmidt E. 2012. Ethiopian agriculture a dynamic geographic perspective in Dorosh, P. & Rashid, S., eds. Food and agriculture in Ethiopia: progress and policy challenges. Philadelphia, PA. University of Pennsylvania Press.

Chen,H., Guo,J., Zhang,C. and Xu C.2013. Prediction of temperature and precipitation in Sudan and South Sudan by using LARS-WG in future, Springer, 113, (2013), 363-375.

Chen J., Zhang X.C., Liu W.Z. and Li Z. 2009. Evaluating and extending CLIGEN precipita tion generation for the Loess Plateau of China. Journal of the American Water Resources Association 45 (2), 378–396.

Cline W. 2007. Global Warming and Agriculture (Washington, DC: Peterson Institute for International Economics.

CSA (Central Statically Agency), federal democratic republic of Ethiopia. 2010. Agricultural Sample Survey (2009/2010) report on area and production of crops volume I Addis Abeba, Ethiopia.

Deressa, T.T., R.M. Hassen and C. Ringler. 2008. Measuring Ethiopian Farmers' Vulnerability to climate Change across Regional States. IFPRI Discussion Paper 00806. Washington, DC:International Food Policy Research Institute.

Descheemaeker, K. 2006. Pedological and hydrological effects of vegetation restoration in enclosures established on degraded hill slopes in the highlands of Northern Ethiopia. Ph.D. diss.,Dissertationes de Agricultura no. 725. K.U. Leuven Univ., Leuven, Belgium.

Doorenbos J. and Kasssam A.H**.** 1979. Yield response to Water. FAO Irrigation and Drainage Paper No. 33. Rome, FAO.

Droogers P., van Dam J., and Hoogeveen J. 2004.Adaptation strategies to climate changes to sustain food security. In: Aerts J, Droogers P, editors. Climate change in contrasting river

basins: adaptation strategies for water, food and environment. The Netherlands: CABI Publishing; p. 49–73.

ECA (Economic Commission for Africa). 2002. Harnessing technologies for sustainable Development. Economic Commission for Africa Policy Research Report, Addis Ababa, 178pp.

EEA/EEPRI,Report on Ethiopian economy. 2005. Transformation of the Ethiopian Agriculture:Potentials, Constraints and Suggested Intervention Measures, Ethiopian Economic Association (EEA) Ethiopian economy association. Volume IV, Addis abeba Ethiopia.

Eitzinger J., Stastna M., and Zalud Z. 2003. A simulation study of the effect of soil water balance and water stress on winter wheat production under different climate change scenarios. Agric Water Manage; 61:195–217.

Ethiopian business community. 2006. A review of SDPRP, recommendation for inclusion in PASDEP, Addis abeba.

FAO. 2002. Compressive Agriculture Development Program.

FAO. 2007. Adaptation to Climate Change in Agriculture, Forestry, and Fisheries Perspective framework and priorities.FAO, Rome.

FAO. 2008. The state of world fisheries and aquaculture. FAO, Rome.

FAO. 2009. ETo Calculator: Land and Water Digital Media Series No. 36.FAO, Rome.

F.D.R.E. 2010. Growth and Transformation Plan (GTP) 2010/11-2014/15 (Draft), Federal Demo cratic Republic of Ethiopia, Addis Ababa.

F.D.R.E. 2011. Ethiopia's climate-resilient green economy: Green economy strategy, Federal Democratic Republic of Ethiopia, Addis Ababa.

F.D.R.E. MoA.2011. Agriculture Sector Programme of Plan on Adaptation to Climate Change Ayana Salehu, Beyene Sebeko, Nebil Shekur,Sertse Sebuh, Tefera Tadese. Addis Abeba 101pp.

F.D.R.E, MoWR-NMA. 2007. Climate Change National Adaptation Programme of Action (NAPA) of Ethiopia. Addis Ababa.

Fraser E.D.G. 2007. Travelling in antique lands: using past famines to develop an adaptabili ty/resilience framework to identify food systems vulnerable to climate change. Climatic Change, 83 (4): 495–514.

Fowler H. J., Blenkinsop S., and Tebaldi C. 2007. Linking climate change modelling to impacts studies: Recent advances in downscaling techniques for hydrological modelling. Int J Climatol, 27, 1547–1578.

Funk, C., Dettinger, M.D., Michaelsen, J.C., Verdin, J.P, Brown, M.E., Barlow, M. and Hoell A.2008. Warming of the Indian Ocean threatens eastern and southern African food security but could be mitigated by agricultural development. PNAS – Proceedings of the National Academy of Science, 105(32): 11081-11086.

Geerts S., D. Racs M. Garcia Cardenas O. Condori J. Mamani R. Miranda J. Cusicanqui C. Ta boada E., Yucra and J. Vacher. 2008. Could deficit irrigation be a sustainable practice for quinoa (Chenopodium quinoa Willd.) in the Southern Bolivian Altiplano? Agric. Water Manage. 95:909-917.

Geerts, S., Raes, D., Gracia, M., Miranda, R., Cusicanqui, J. A., Taboada, C., Mendoza, J., Huanca, R., Mamani, A., Condori, O.,Mamani, J., Morales, B., Osco, V., Steduto, P. 2009. Simulating yield response of Quinoa to water availability with AquaCrop. Agron.J. 101, 499 – 508.

Godwin D.C., Ritchie J.T., Singh U., and Hunt L. 1989. A User's Guide to CERES Wheat-V2.10.International Fertilizer Development Center, Muscle Shoals, AL.

Gohari A., Eslamian S., Abedi-Koupaei J., Bavani A.M., Wang D. and Madani K. 2013. Climate change impacts on crop production in Iran's Zayandeh-Rud River Basin. Science of the To tal Environment, 442: 405–419.

Hassan Z.B. 2012. Climate Change Impact on Precipitation and Stream flow in a Humid Tropi cal Watershed.

Heng, L.K., Hsiao, T.C., Evett, S., Howell, T. and Steduto, P. 2009. Validating the FAO AquaCrop model for irrigated and water deficient field maize. Agron. J. 101: 488–498.

Herrero M., Ringler C., van de Steeg, J., Thornton P., Zhu T., Bryan E., Omolo A., Koo J. and Notenbaert, A. 2010. Climate variability and climate change and their impacts on Kenya's agricultural sector. Nairobi, Kenya. ILRI.

Holton J. R. 1992. An introduction to dynamic meteorology, 3rd Edition. SanDiego, CA: Academic.

Hoogenboom G., Jones J.W., Wilkens P.W., Batchelor, W.D.,Bowen W.T., Hunt L.A., Picker ing N.B., Singh U., Godwin D.C., Bear B., Boote K.J., Ritchie J.T., Whit, J.W. 1994.

Crop Models, DSSAT Version 3.0. International Benchmark Sites Network for Agrotech nology Transfer, University ofHawaii, Honolulu, 692 pp.

Houghton J. T., Ding. 2000. Climate change 2001: the scientific basis: contribution of working group I to the third assessment report of the intergovernmental panel on climate change. Cambridge: Cambridge University Press.

Hua Chen, Jiali Guo, Zengxin Zhang and Chong-Yu Xu.2012. Prediction of temperature and precipitation in Sudan and South Sudan by using LARS-WG in future. State Key Laboratory of Water Resources and Hydropower Engineering Science, Wuhan University, 430072 Wuhan, China.

Hulme, M., E.M. Barrow, N. Arnell, P.A. Harrison, T.E. Downing, and T.C. Johns. 1999. Rel ative Impacts of Human-Induced Climate Change and Natural Climate Variability. Nature, 397: pp. 688-91.

Hulme. 2000. Using a Climate Scenario Generator for Vulnerability and Adaptation.

Hunink J.E. and Droogers P. 2010. Climate Change Impact Assessment on Crop Production in Albania, World Bank Study on Reducing Vulnerability to Climate Change in Europe and Central Asia (ECA) Agricultural Systems.

Huntingford C., C. H. Lambert, J. H. C. Gash, C. M. Taylor, and Challinor A. J. 2005. Aspects of climate change prediction relevant to crop productivity. Philos. Trans. Roy. Soc. London,360B, 1999–2009, doi:10.1098/rstb.2005.1748.

Ines AVM, Hansen JW.2006. Bias correction of daily GCM rainfall for crop simulation studies. Agric For Meteorol;138(1–4):44–53.

IPCC, 1990: IPCC First Assessment Report (1990): Scientific Assessment of Climate Change. Contribution of Working Group I to the Intergovernmental Panel on Climate Change, J.T. Houghton, G.J. Jenkins and J.J. Ephraums, Eds., Cambridge University Press, Cambridge, 365 pp.

IPCC. 1996. Impacts, Adaptation, and Mitigation of Climate Change. Scientific-Technical Analyses. Report of Working Group II. Contribution of Working Group II to the Second Assessment of the Intergovernmental Panel on Climate Change, R.T.Watson,M.C. Zinyowera, R.H.Moss, Eds., Cambridge University Press, Cambridge, 878 pp.

IPCC. 2001a. Impacts, Adaptation and Vulnerability, Contribution of Working Group II to the Third Assessment Report of the Intergovernmental Panel on Climate Change. Cambridge, UK:

Cambridge University Press.

IPCC, 2001b: Climate Change 2001: Impacts, Adaptation, and Vulnerability. Contribution of Working Group II to the Third Assessment Report of the Intergovernmental Panel on Climate Change, J.J. McCarthy, O.F. Canziani, N.A. Leary, D.J.Dokken andK.S.White, Eds., CambridgeUniversity Press, Cambridge, 1032 pp.

IPCC (Intergovernmental Panel on Climate Change). 2007. Climate Change: Impacts, Adaptation and Vulnerability, Contribution of Working Group II to the Fourth Asessment Report of the Intergovernmental Panel on Climate Change (Cambridge Univ Press, Cam bridge, UK), in press.

IPCC-TGCIA. 2007. General Guidelines on the Use of Scenario Data for Climate Impact and Adaptation Assessment. Version 2.Prepared by T.R. Carter on Behalf of the Intergovernmen tal Panel on Climate Change, Task Group on Data and Scenario Support for Impact and Cli mate Assessment.pp. 66.

Johnson G.L., Hanson C.L., Hardegree S.P. and Ballard E.B. 1996. Stochastic weather simulation:overview and analysis of two commonly used models. Journal of Applied Meteorology 35 (10), 1878–1896.

Jones C.A. and Kiniry J.R. 1986. CERES-Maize model: A simulation model of maize growth and development. Texas A & M University Press, 194 pp.

Jones J.W., G. Hoogenboom C.H. Porter, K.J. Boote, W.D. Batchelor, L.A.Hunt, P.W. Wilkens, U. Singh, A.J. Gijsman, and J.T. Ritchie. 2003. The DSSAT cropping system model. Eur. J. Agron. 18:235–265.

Kaiser H.M, Riha S.J, Wilks DS, Rossiter D.G and Sampath R. 1993. A farm-level analysis of economic and agronomic impacts of gradual climate warming. AmJ Agric Econ 75(2):387–398.

Kang, Khan S.and Ma X. 2009. Climate change impacts on crop yield, crop water productivity and food security-A review. Progress in Natural Science, Pp 1665–1674.

Kevin M., Ramesh R., John O., Imran A.and Bahram G. 2005. Evaluation of weather generator ClimGen for southern Ontario, Canadian Water Resources Journal 30(4), 315–330.

Kimball B.A. 1983. Carbon Dioxide and Agricultural Yield: An Assemblage and Analysis of 430 Prior Observations. Agron. J. 75:779-788.

Loague, K.and Green, R.E. 1991. Statistical and graphical methods for evaluating solute

transport models; overview and application. J. Contam. Hydrol. 7, 51–73.

Manfred K. and Netsanet Z. 2013. Mono- and multi-modal statistical Downscaling of GCM-Climate Predictors for the Upper Blue Nile River Basin, Ethiopia. Department of Geohydraulics and Engineering Hydrology, Kassel University.

Massah Bavani AR. and Morid S.2005. The impacts of climate change on water resources and agricultural production. J Water Resour Res.

Mavromatis, Th. and Hansen J. 2001. Inter annual variability characteristics and simulated crop response of four stochastic weather generators. Agricultural and forest meteorology, 109, 283-296.

McCann,J.2001. Maize and grace: history, corn and Africa's new landscapes 1500-1999 society of cooperative study and history.

Mendelsohn R. 2008. The Impact of Climate Change on Agriculture in Developing Countries, Journal of Natural Resources Policy Research, 1:1, 5-19.

Mohammed Y. 2009. Climate change impact assessment on soil water availability and crop yield in Anjeni Watershed Blue Nile Basin. Arba Minch University: Master Thesis.

Moriasi D. N., Arnold, J. G., Liew M. W. V., Bingner R. L., Harmel R. D., and Veith T. L. 2007. Model evaluation guidelines for systematic quantification of accuracy in watershed simula tions. Transactions of The ASABE 50, 885–900.

Nakicenovic, N., J. Alcamo, G. Davis, B. de Vries, J. Fenhann, S. Gaffin, K. Gregory, A. Grübler, T.Y. Jung, T. Kram, E.L. La Rovere, L. Michaelis, S. Mori, T. Morita, W. Pepper, H. Pitcher, L. Price, K.Riahi, A. Roehrl, H.H. Rogner, A. Sankovski, M. Schlesinger, P.Shukla, S. Smith, R. Swart, S. van Rooijen, N. Victor, and Z. Dadi. 2000. " IPCC Special Report on Emissions Scenarios." 599. Cambridge University Press, Cambridge, United Kingdom and New York, NY, USA.

Nakicenovic N, Swart R (eds).2000. Emissions scenarios.Special Report of the Intergovernmental Panel on Climate Change. Cambridge University Press, Cambridge.

Nash J.E.and Sutcliffe J.V. 1970. River flow forecasting through conceptual models. I. A discussion of principles. Journal of Hydrology 10, 282–29.

Nordhaus William D. 1991. To slow or not to slow: The economics of the greenhouse effect, The Economic Journal.

OECD. 2003. Special Issue on Climate Change: Climate Change Policies: Recent development

and long term issues. Paris: Organization for Economic Cooperation and Development (OECD) publications.

Ozdogan M. 2011. Modeling the impacts of climate change on wheat yields in northwestern Turkey. Agr Ecosyst Environ; 141:1-12.

Parry M., Rosenzweig C., Iglesias A. 1999. Climate change and world food security: a new as sessment. Global Environ Change: S51–67.

PASDEP.2006. Ethiopia Building on Progress. A Plan for Accelerated and Sustained Development to End Poverty. (PASDEP) (2005/06-2009/10). Volume I.

Piani C, Haerter JO and Coppola E.2010. Statistical bias correction for daily precipitation in regional climate models over Europe. Theor Appl Climatol ;99(1):187–92.

Pindyck RS.,2012.Uncertain outcomes and climate change policy. J Environ Econ Manag; 63(3):289–303.

Podestá G.P., Messina C.D.,Grondona M.O and Magrin G.O. 1999. Associations between grain crop yields.

Qian, B.D., Gameda, S., Hayhoe, H., De Jong, R. and Bootsma, A. 2004. Comparison of LARS-WG and AAFC-WG stochastic weather generators for diverse Canadian climates. Climate Research, 26, 175-191.

Racsko, P., Szeidl, L. & Semenov M.A. 1991. A serial approach to local stochastic weather models, Ecol Model, 57, 27–41.

Raes D, Steduto P, Hsiao T. C., and Fereres E. 2012. FAO, Reference Manual for AquaCrop Version 4, Land and Water Division Rome, Italy.

Raes D. 1982. A summary simulation model of the water budget of a cropped soil: Ph.D. diss. Dissertationes de Agricultura no. 122. K. U. Leuven Univ., Leuven, Belgium.

Raes D., Geerts S., Kipkorir E., Wellens J., and Sahli A. 2006. Simulation of yield decline as a result of water stress with a robust soil water balance model. Agric. Water Manage. 81:335-357.

Raes, D., H. Lemmens P., Van Aelst M., Vanden Bulcke, and Smith M. 1988. IRSIS-IrrigationScheduling Information System. Volume 1. Software Reference Manual. K.U. Leuven, Dep. Land Management, Reference Manual 3. Leuven, Belgium.

Rajabi A. Sedghi H. Eslamian S. and Musavi H. 2010. Comparison of LARS-WG and SDSM Downscaling Models in Kermanshah (Iran). Ecology, Environment and Conservation,

16:465-474.

Rallison R.E. 1980. Origin and evolution of the SCS runoff equation. p.912924. In Proc. Symp. on Watershed Management. ASCE, New York.

Randall, D.A., R.A. Wood, S. Bony, R. Colman, T. Fichefet, J. Fyfe, V. Kattsov, A. Pitman, J. Shukla, J. Srinivasan, R.J. Stouffer, A. Sumi, and K.E. Taylor. 2007. "Climate Models and Their Evaluation, in Climate Change 2007: The Physical Science Basis." In Contribution of Working Group I to the Fourth Assessment Report of the Intergovernmental Panel on Cli mate Change, edited by S. Solomon, D. Qin, M. Manning, Z. Chen, M. Marquis, K.B. Averyt, M. Tignor and H.L. Miller. Cambridge, UK and New York, NY, USA: Cambridge University Press.

Rietveld, M.R. 1978. A new method for the estimating the regression coefficients in the formu la relating solar radiation to sunshine. Agricultural and Forest Meteorology, 19, 243-252

Riha S.J,et al. 1996. Impact of temperature and precipitation variability on crop model predict tions. Clim Change.

Ringler C., Zhu, T., Cai X., Koo J., and Wang,D. 2010. Climate Change Impacts on Food Security in Sub -Saharan Africa. IPFPRI.

Ritchie, J.T. 1972. Model for predicting evaporation from a row crop with incomplete cover. Water Resources Research 8(5): 1204-1213.

Robert J. 2003.The effect of climate change on global potato production. International Potato Center (CIP), 80:271-280.

Rockström J. 2000. Water resources management in smallholder farms in Eastern and Southern Africa: an overview. Phys. Chem. Earth (B) 25 (3), 275–283.

Rockström J. 2003. Resilience building and water demand management for drought mitigation. Phys. Chem. Earth, 28, 869-877.

Rubas D.J., Hill H.S.J. and Mjelde J.W. 2006. Economics and climate applications: exploring the frontier. ClimRes 33:43–54.

Saka A.R, Phiri I.M.G, Kamdonyo D.R, and Kumwenda J.D.T. 2003. The Potential Impact of Climate Change on the Agiculture Sector in Malawi. Ministry of Natural Resources and Environmental Affairs, Agriculture and Livelihood.

Samuael .G. 2006. Intensification Of Smallholder Agriculture In Ethiopia :Option And Scenarios paper prepared for future agriculture consortium meeting at the institute of

Development studies 20-22 march 2006 Addis Abeba.

Semenov M.A. 2008a. Extreme impacts of climate change on wheat in England and Wales. Aspect of Applied Biology 88, Effects of Climate Change on Plants: Implications for Agriculture, 37-39.

Semenov M.A. 2008b. Predicting crop yields using probabilistic weather ensembles. International Symposium on Crop Modeling and Decision Support, April 19-22, 2008, Nanjing, China, 15-16.

Semenov M. A., and Barrow E. M. 2002. LARS-WG: a stochastic weather generator for use in climate impact studies (Version 3.0). User Manual.

Semenov M. A., and Brooks R. J. 1999. Spatial interpolation of the LARS-WG stochastic weather generator in Great Britain. Climate Research, 11, 137-148.

Semenov MA, Brooks RJ, Barrow EM and Richardson CW.1998. Comparison of the WGEN and LARS-WG stochastic weather generators in diverse climates. Climate Research 10:95-107 (C100 E50 W65).

Semenov, M.A.and Stratonovitch, P. 2010. The use of multi-model ensembles from global climate models for impact assessments of climate change. Climate Researc: 41, 1-14.

Shaka, A. K. 2008. Assessment of climate change impacts on the hydrology of Gilgel Abbay Catchment in Lake Tana Basin, Ethiopia Enschede, Netherlands. The International Institute for Geo-information Science and Earth Observation: Master Thesis.

Singh J.P., Govindakrishnan P.M., Lal SS. and Aggarwal P.K. 2005. Increasing the efficiency of Agronomy.

Slegers, M.F.W. and Stroosnijder, L. 2008. 'Beyond the Desertification Narrative: A Frame work for Agricultural Drought in Semi-arid East Africa', Ambio, 37(5): 372-380.

Smith, J.B. and M. Hulme. 1998. "Climate Change Scenarios." In Hanbook on Methods of Cli mate Change Impacts Assessment and Adaptation Strategies.Version 2.0, edited by J. Feen stra, I. Burton, J.B. Smith and R.S.J. Tol, 3-1 to 3-40. Vrije Universiteit, Amsterdam: United Nations Environment Programme and Institute for Environmental Studies.

Smith, M.2000. The application of climatic data for planning and management of sustainable rainfed and irrigated crop production. Agric. Forest Meteorol. 103, 99 – 108.

SNNPRS–RSA. 2006. Southern Nations, Nationalities and People's Regional State–Regional Statistical Abstract, 2004/5, Bureau of Finance and Economic Development Division of

Statistics and Population. Awassa, Ethiopia.

Smedema, L.K., and D.W. Rycroft. 1983. Land drainage – planning and design of agricultural drainage systems. Batsford Ltd., London, U.K.

Steenhuis T.S., M. Winchell, J., Rossing J.A., Zollweg, and M. F. Walter. 1995. SCS Runoff equation revisited for variable-source runoff areas. J. Irrig. Drain. Eng. 121:234-238.

Stöckle C.O., Donatelli, M.and Nelson R. 2003. CropSyst, a cropping systems simulation model. Eur. J. Agron. 18 (3/4), 289–307 (Second special issue "2nd International Symposium on Modeling Cropping Systems, Florence, Italy").

Steduto, P. 2003. Biomass Water-Productivity. Comparing the Growth-Engines of Crop Models. FAO Expert Consultation on Crop Water Productivity Under Deficient Water Supply, 26 – 28 February 2003, Rome, Italy.

Steduto P., Hsiao, T.C. & Fereres, E. 2007. On the conservative behavior of biomass water productivity. Irrigation Science, 25:189–207.

Steduto, P., Hsiao, T.C., Raes, D. & Fereres, E**.** 2009. Aquacrop - The FAO Crop Model to Simulate Yield Response to Water: I. Concepts and Underlying Principles. Agronomy Journal, 101:426–437.

SZPED.2004. Socioeconomic profile of Sidama Administrative zone. SZPED (Sidama Zone Planning and Economic Development). Hawassa, Ethiopia.

Taffesse, A.S., Dorosh P.and Asrat, S. 2012. Crop production in Ethiopia: regional patterns and trends. ESSP Working Paper 16. Washington, DC, International Food Policy Research Institute (IFPRI) and Addis Ababa, Ethiopia, Ethiopian Development Research Institute (EDRI).

Tao F and Zhang Z. 2010. Adaptation of maize production to climate change in North China Plain:quantify the relative contributions of adaptation options. Eur J Agron; 33:103–16.

Teutschbein C, Seibert J. 2012. Bias correction of regional climate model simulations for hydrological climate-change impact studies: review and evaluation of different methods. J Hydrol; 456–457:12–29.

Thornton P.K., Jones P.G., Owiyo T, Kruska R.L., Herrero M., Kristjanson P., Notenbaert A., Bekele N and Omolo A.2006. with contributions from Orindi V, Otiende B, Ochieng A, Bhadwal S, Anantram K, Nair S, Kumar V and Kulkar U.: Mapping Climate Vulnerability and Poverty in Africa. Report to the Department for International Development, ILRI,

Nairobi. p.171.

Tubiello F.N, Rosenzweig C, Goldberg R. A., Jagtap S. and Jones J. W. 2002. Effects of climate change on US crop production: simulation results using two different GCM scenarios. Part I: Wheat, potato, maize, and citrus.

USDA. 1964. Estimation of direct runoff from storm rainfall. In National Engineering Handbook. Soil Conservation Service, USDA, Washington, DC.

USGCRP. 2009. Global Climate Change Impacts in the United States. Karl, T.R., J.M. Melillo, and T.C. Peterson (eds.). United States Global Change Research Program. Cambridge Uni versity Press, New York, NY, USA.

Van Dam, J.C., Huygen, J., Wesseling, J.G., Feddes, R.A., Kabat,P., van Walsum, P.E.V., Groe nendijk, P.and van Diepen, C.A. 1997. Theory of SWAP Version 2.0, Report 71. Depart ment Water Resources, Wageningen Agricultural University, 167 pp.

Villalobos, F. J. and E. Fereres. 1990. Evaporation measurements beneath corn, cotton, and sunflower canopies. Agron. J. 82:1153-1159.

Walker N.J.and Schulze R.E. 2006. An assessment of sustainable maize production under different management and climate scenarios for smallholder agro-ecosystems in KwaZulu-Natal, South Africa. Phys Chem Earth; 31:995–1002.

Willmott, C. J. 1984. On the evaluation of model performance in physical geography. InSpatial Statistics and Models, Gaile GL, Willmott CJ (eds). D. Reidel: Boston. 443–460.

Yemane Gebresilassie.,Mokonen Ayana.,Kassa Tadele. 2014.Field experimentation based simulation of yield response of maize crop to deficit irrigation using Aquacrop model,Arba minch,Ethiopia,African Journal of Agricultural Research, Volume 10(4),pp.269-280.

You L, Rosegrant MW, Wood S.and Sun D. 2009. Impact of growing season temperature on wheat productivity in China. Agric for Meteorol; 149:1009–14.

Zenebe Gebreegziabher, Alemu Mekonnen, Rahel Deribe, Samuel Abera, And Meseret Molla Kassahun.2014. Climate change can have significant negative impacts on Ethiopia's, Environment for Development, DRB 13-14.

Zenebe Gebreegziabher,Jesper Stage, Alemu Mekonnen, and Atlaw Alemu.2011.climate change and Ethiopian economy. A Computable General Equilibrium Analysis. EfD DP pp. 11-09.

Zhai, F., and Zhuang, J.2009. Agricultural Impact of Climate Change: A General Equilibrium Analysis with Special Reference to South East Asia. Asian Development Bank (ADBI)

APPENDIX A. LIST OF TABLES

Table 1: Sample relative Rainfall change example for scenario SRA1B of period 2020s

Month	BCM2	CGMR	CNCM3	CSMK3	FGOALS	GFCM21	GIAOM	HADCM3	HADGEM	INCM3	IPCM4	MIHR	MPEH5	NCCCSM	NCPCM
Jan	1.09	1.33	1.2	1.14	0.94	0.82	1.03	0.97	0.84	1.4	0.92	1.12	1.12	1.13	1.24
Feb	0.96	1.18	1.09	1.01	0.94	0.9	1.03	1.07	0.86	1.29	1	1.05	1.1	1.04	1.83
Mar	0.91	1.08	1.02	0.93	1.02	0.95	1.07	1.14	0.92	1.21	1.05	1.03	1.07	1.03	1.66
Apr	0.95	0.99	1.01	0.95	1.02	1	1.06	1.04	0.94	1.13	1.04	1.07	1.02	1.01	1.17
May	0.97	0.99	1	0.99	0.99	1.04	1.03	0.95	0.94	1.04	1.06	1.05	0.96	1.01	1.04
Jun	0.95	1.03	0.98	0.98	0.98	1.05	1	0.96	0.93	1.02	1.1	0.99	0.94	1.04	1.02
Jul	0.95	1.02	0.96	0.97	0.99	1.05	0.99	0.98	0.91	1.03	1.09	0.98	0.99	1.03	0.99
Aug	1	0.99	0.96	0.99	1.01	1.02	1.01	0.98	0.92	1.03	1.05	0.99	1.05	1	0.96
Sep	1.01	0.98	0.99	0.98	1.01	1	1.04	0.98	0.93	1.01	1.05	0.99	1.06	1	0.97
Oct	1.02	1.02	1.04	1	1.09	1.01	1.04	0.99	0.95	1.06	1.03	0.98	1.04	1.02	0.99
Nov	1.1	1.18	1.09	1.11	1.19	0.95	1.05	1	0.96	1.17	0.98	0.96	1.08	1.11	0.94
Dec	1.16	1.36	1.18	1.19	1.11	0.83	1.06	0.99	0.91	1.35	0.92	1.04	1.14	1.2	0.86

Table 2: Sample relative Rainfall change example for scenario SRB1 of period 2020s

Month	BCM2	CGMR	CNCM3	CSMK3	FGOALS	GFCM21	GIAOM	HADCM3	HADGEM	INCM3	IPCM4	MIHR	MPEH5	NCCCSM	NCPCM
Jan	0.99	0	0	1.01	1.08	1.16	1.04	1.08	0	1.13	0.96	1.22	1.04	1.03	0
Feb	1.01	0	0	0.89	0.97	1.23	1.06	1.07	0	1.09	0.94	1.17	1.13	0.96	0
Mar	0.92	0	0	0.86	1.04	1.08	1.09	1.13	0	1.05	0.98	1.1	1.08	0.98	0
Apr	0.91	0	0	0.92	1.06	0.98	1.07	1.09	0	1.02	1.08	1.05	1.01	0.97	0
May	0.97	0	0	1	1.02	0.99	1.02	0.99	0	0.99	1.1	1.03	0.99	0.98	0
Jun	0.99	0	0	1.03	1	1.05	1	0.92	0	1	1.04	1	0.98	1.04	0
Jul	1.01	0	0	1.01	1	1.14	1.01	0.92	0	1.02	0.97	0.99	1	1.05	0
Aug	1.05	0	0	1	1.01	1.14	1.03	0.93	0	1.01	0.96	0.99	1.03	1.02	0
Sep	1.04	0	0	0.97	1.02	1.04	1.02	0.93	0	1.01	0.99	0.98	1.06	1.01	0
Oct	1.03	0	0	0.98	1.08	1.01	1.01	0.96	0	1.07	1.01	1.01	1.05	1.03	0
Nov	1	0	0	1.03	1.2	1	1	1.06	0	1.12	1	1.12	1.06	1.15	0
Dec	0.95	0	0	1.06	1.24	1	1.02	1.13	0	1.13	0.98	1.22	1.02	1.18	0

Table 3: Sample example relative minimum temperature change for scenario SRA1B of period 2020s

	BCM2	CGMR	CNCM3	CSMK3	FGOALS	GFCM21	GIAOM	HADCM3	HADGEM	INCM3	IPCM4	MIHR	MPEH5	NCCCSM	NCPCM
Jan	0.54	0.61	0.6	0.35	0.33	0.66	0.38	0.56	0.42	1.22	0.61	0.69	0.35	0.54	0.36
Feb	0.45	0.51	0.54	0.31	0.34	0.58	0.37	0.52	0.37	1.31	0.6	0.6	0.32	0.56	0.35
Mar	0.37	0.46	0.51	0.3	0.32	0.6	0.38	0.53	0.4	1.35	0.57	0.59	0.3	0.54	0.34
Apr	0.36	0.56	0.51	0.33	0.32	0.67	0.37	0.55	0.48	1.11	0.56	0.64	0.3	0.55	0.32
May	0.33	0.62	0.5	0.32	0.34	0.66	0.32	0.57	0.52	0.8	0.54	0.66	0.45	0.57	0.33
Jun	0.29	0.55	0.49	0.29	0.35	0.63	0.31	0.56	0.53	0.64	0.53	0.64	0.62	0.55	0.34
Jul	0.34	0.57	0.53	0.28	0.36	0.56	0.3	0.51	0.55	0.55	0.57	0.59	0.57	0.59	0.31
Aug	0.38	0.74	0.58	0.29	0.35	0.52	0.31	0.47	0.55	0.55	0.57	0.56	0.45	0.62	0.34
Sep	0.4	0.79	0.58	0.27	0.34	0.53	0.33	0.47	0.5	0.64	0.56	0.57	0.41	0.57	0.4
Oct	0.43	0.67	0.56	0.25	0.3	0.49	0.34	0.51	0.43	0.92	0.58	0.56	0.42	0.51	0.39
Nov	0.46	0.61	0.56	0.3	0.24	0.46	0.37	0.57	0.41	1.23	0.59	0.61	0.41	0.49	0.39
Dec	0.52	0.64	0.58	0.35	0.27	0.58	0.4	0.6	0.44	1.28	0.59	0.71	0.39	0.52	0.39

Table 4: Sample example relative minimum temperature change for scenario SRB1 of period 2020s

Month	BCM2	CGMR	CNCM3	CSMK3	FGOALS	GFCM21	GIAOM	HADCM3	HADGEM	INCM3	IPCM4	MIHR	MPEH5	NCCCSM	NCPCM
Jan	0.54	0	0	0.3	0.29	0.61	0.4	0.58	0	0.84	0.6	0.76	0.36	0.47	0
Feb	0.51	0	0	0.29	0.32	0.51	0.42	0.5	0	0.92	0.65	0.66	0.31	0.53	0
Mar	0.43	0	0	0.29	0.28	0.45	0.4	0.45	0	0.77	0.62	0.62	0.27	0.54	0
Apr	0.43	0	0	0.28	0.24	0.42	0.39	0.45	0	0.6	0.52	0.62	0.26	0.6	0
May	0.42	0	0	0.27	0.24	0.45	0.37	0.48	0	0.63	0.47	0.63	0.36	0.61	0
Jun	0.4	0	0	0.27	0.27	0.46	0.34	0.49	0	0.63	0.5	0.63	0.46	0.47	0
Jul	0.42	0	0	0.27	0.31	0.43	0.32	0.49	0	0.51	0.56	0.62	0.44	0.43	0
Aug	0.4	0	0	0.26	0.31	0.44	0.31	0.49	0	0.48	0.58	0.59	0.35	0.5	0
Sep	0.38	0	0	0.23	0.3	0.49	0.31	0.5	0	0.61	0.55	0.59	0.31	0.5	0
Oct	0.39	0	0	0.23	0.26	0.5	0.3	0.53	0	0.88	0.53	0.67	0.29	0.45	0
Nov	0.36	0	0	0.29	0.23	0.51	0.3	0.6	0	0.95	0.53	0.79	0.31	0.38	0
Dec	0.42	0	0	0.31	0.23	0.61	0.33	0.63	0	0.8	0.54	0.83	0.37	0.39	0

Table 5: Sample example relative maximum temperature change for scenario SRA1B of period 2055s

Month	BCM2	CGMR	CNCM3	CSMK 3	FGOAL S	GFCM 21	GIA OM	HADC M3	HAD GEM	INC M3	IPCM4	MIHR	MPE H5	NCCC SM	NCPC M
Jan	1.25	1.86	1.94	1.34	1.19	2.14	0.81	1.72	1.54	1.02	1.88	1.9	1.65	1.57	1.25
Feb	1.61	1.69	1.86	1.3	1.25	2.02	0.87	1.62	1.4	1.09	1.89	1.9	1.55	1.47	1.25
Mar	1.9	1.55	1.83	1.09	1.22	1.93	0.83	1.58	1.33	1.03	1.87	2.03	1.52	1.4	1.09
Apr	1.99	1.63	1.79	1.18	1.13	1.93	0.82	1.69	1.34	1.02	1.79	2.07	1.62	1.44	0.92
May	1.65	1.68	1.65	1.35	1.07	1.91	0.92	1.85	1.45	1.17	1.73	1.95	1.81	1.46	0.9
Jun	1.36	1.58	1.64	1.41	1.07	1.86	1	1.92	1.61	1.2	1.79	1.91	1.93	1.43	0.91
Jul	1.31	1.66	1.72	1.46	1.13	1.77	1.04	1.8	1.7	0.84	1.89	1.91	1.81	1.5	0.98
Aug	1.19	1.86	1.73	1.35	1.14	1.67	1.03	1.66	1.69	0.68	1.91	1.85	1.6	1.54	1.06
Sep	1.14	1.83	1.75	1.19	1.1	1.64	1	1.65	1.57	0.85	1.87	1.86	1.56	1.5	1.06
Oct	1.1	1.69	1.83	1.11	1.06	1.65	1.01	1.68	1.41	0.89	1.88	1.99	1.62	1.49	1.09
Nov	0.87	1.66	1.89	1.08	1.03	1.73	0.92	1.74	1.41	0.87	1.9	2.06	1.65	1.54	1.16
Dec	0.87	1.79	1.95	1.16	1.09	1.99	0.8	1.76	1.56	0.92	1.89	1.99	1.7	1.6	1.21

Table 6: Sample example relative rainfall change for scenario SRA1B of period 2090s

Month	BCM2	CGMR	CNCM3	CSMK3	FGOALS	GFCM21	GIAOM	HADCM3	HADGEM	INCM3	IPCM4	MIHR	MPEH5	NCCCSM	NCPCM
Jan	1.12	1.67	1.63	0.88	1.51	1.27	1.14	1.71	0	1.68	1.61	2.14	1.63	1.58	0
Feb	0.84	1.37	1.06	0.85	1.39	1.23	1.06	1.65	0	1.49	1.22	1.61	1.56	1.47	0
Mar	0.89	1.14	0.86	0.79	1.36	1.01	1.12	1.64	0	1.3	1.13	1.18	1.27	1.42	0
Apr	0.9	1.08	0.94	0.75	1.2	0.95	1.14	1.29	0	1.11	1.22	1.17	0.96	1.2	0
May	0.87	1.13	1.02	0.8	1.04	0.97	1.06	0.92	0	1.01	1.21	1.18	0.81	1.09	0
Jun	0.89	1.13	1.06	0.86	0.97	0.96	1	0.86	0	0.97	1.1	1.09	0.76	1.12	0
Jul	0.95	1.01	1.07	0.91	0.98	1.15	1	1	0	1.07	1.03	1.03	0.93	1.1	0
Aug	1.01	0.94	1.03	0.94	0.99	1.37	1.03	1.1	0	1.13	1.06	1.04	1.09	1.06	0
Sep	1.03	0.99	1.1	0.95	1.09	1.28	1.08	1.1	0	1.14	1.15	1.1	1.11	1.06	0
Oct	1.07	1.14	1.36	1.05	1.42	1.17	1.15	1.16	0	1.31	1.25	1.23	1.15	1.09	0
Nov	1.31	1.41	1.77	1.14	1.83	1.18	1.24	1.45	0	1.7	1.52	1.54	1.44	1.35	0
Dec	1.48	1.69	1.99	1.03	1.83	1.2	1.26	1.76	0	1.87	1.79	2.04	1.66	1.66	0

Table 7: Sample example relative maximum temperature change for scenario SRA1B of period 2090s

month	BCM2	CGMR	CNCM3	CSMK3	FGOALS	GFCM21	GIAOM	HADCM3	HADGEM	INCM3	IPCM4	MIHR	MPEH5	NCCCSM	NCPCM
Jan	2.26	2.57	2.96	2.31	2.06	3	1.67	3.03	0	1.76	3.47	3.11	3.83	2.24	0
Feb	2.6	2.41	2.99	2.35	2.11	2.82	1.83	2.88	0	1.96	3.52	3.26	3.71	2.01	0
Mar	2.75	2.35	3	2.31	1.96	2.79	1.83	2.76	0	1.91	3.45	3.52	3.6	1.69	0
Apr	2.96	2.49	2.88	2.4	1.83	2.9	1.69	2.85	0	1.85	3.22	3.63	3.67	1.76	0
May	2.95	2.58	2.62	2.43	1.8	2.87	1.73	3.15	0	1.98	3.15	3.53	4.17	1.96	0
Jun	2.82	2.49	2.55	2.44	1.87	2.75	1.79	3.31	0	2.08	3.31	3.5	4.63	1.94	0
Jul	2.75	2.58	2.68	2.42	1.94	2.44	1.74	3.1	0	1.66	3.41	3.41	4.4	1.99	0
Aug	2.45	2.9	2.75	2.24	1.95	2.1	1.65	2.86	0	1.22	3.37	3.28	3.94	2.13	0
Sep	2.18	2.94	2.75	2	1.89	2.14	1.59	2.87	0	1.27	3.27	3.33	3.65	2.07	0
Oct	2.1	2.63	2.78	1.74	1.78	2.33	1.6	2.95	0	1.32	3.24	3.43	3.5	2.03	0
Nov	1.99	2.44	2.8	1.67	1.7	2.46	1.61	3.01	0	1.19	3.34	3.35	3.59	2.16	0
Dec	1.97	2.55	2.87	1.96	1.82	2.8	1.6	3.08	0	1.35	3.43	3.16	3.8	2.24	0

Table 8: Seasonal Rainfall variability output under each scenario and in each time horizons at different risk levels.

Periods	Seasons	Scenaro A			Scenario B			Range	
		25A	50A	75A	25B	50B	75B		
2020s	DJF('bega')	-3.67	9	15	-0.17	5.34	12.34	-3.67	15
	MAM('belg')	-1.34	1.67	5.5	-1.84	2	5.67	-1.87	5.67
	JJA('kiremt')	-2.34	-0.67	2.17	-0.5	0.67	2.67	-2.34	2.67
	SON('tseday')	-1.84	3.34	5.34	-0.17	2.67	6.34	-1.84	6.34
2055s	DJF('bega')	6.34	20.67	37.5	10	18.34	25.5	6.34	37.5
	MAM('belg')	-3.67	4.67	10.34	-2.34	3	9.84	-3.67	10.34
	JJA('kiremt')	-5.5	-0.67	1.84	-2.84	0.34	4.67	-5.5	4.67
	SON('tseday')	4.34	8	13.67	5.67	10.34	16	4.34	16
2090s	DJF('bega')	27	55.67	66.34	7.84	24	36.5	7.84	66.34
	MAM('belg')	-4	9	19.67	-2	5.34	16.84	-4	19.67
	JJA('kiremt')	-4	0.67	8.34	-3.34	1	5.34	-4	8.34
	SON('tseday')	17	20.34	30	8	11.34	15.5	8	30

APPENDIX B. LIST OF FIGURES

SRA1B-2020s

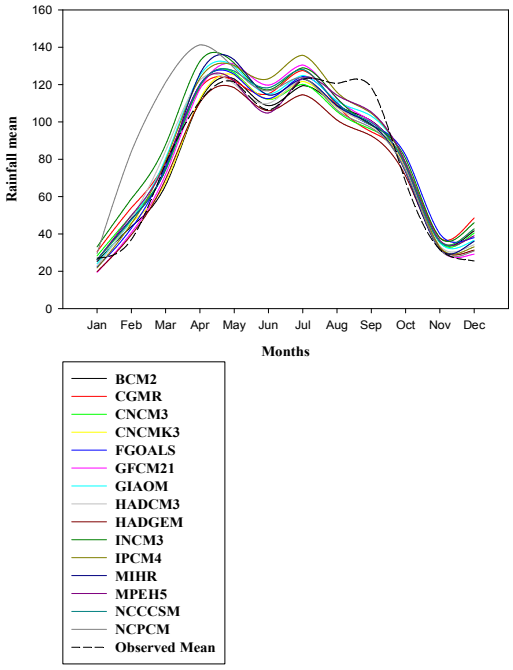

SRB1-2020s

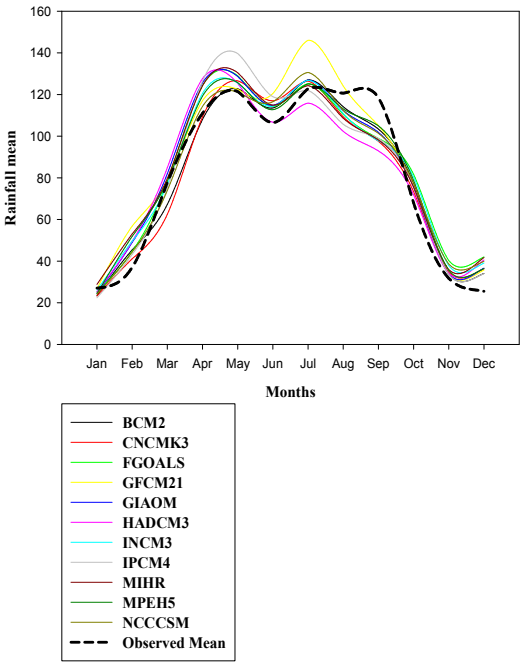

SRA1B-2055s

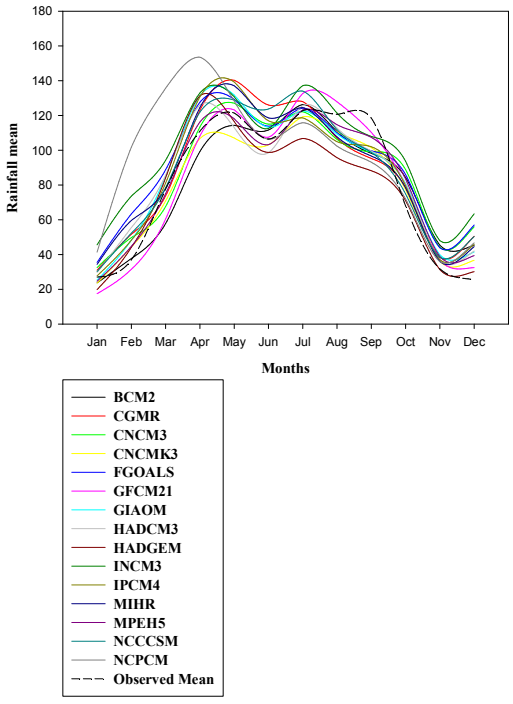

SRB1-2055s

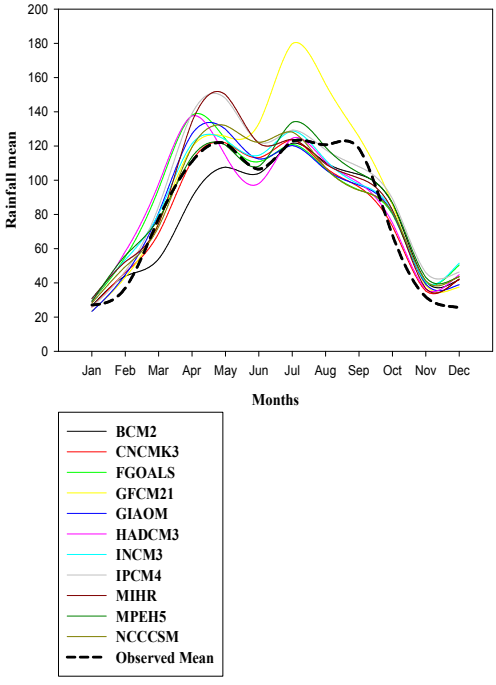

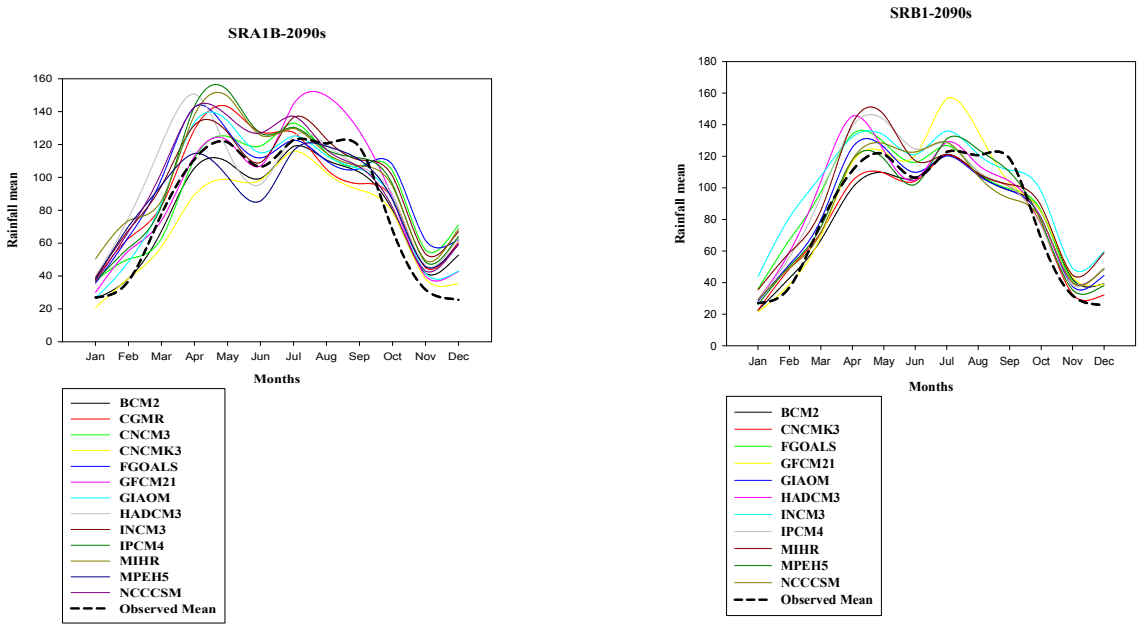

Figure 1: Monthly 15 GCMs model output of Simulated Versus Observed Rainfall mean under two emission scenarios and three time periods. The solid lines show mean of each 15GCMs output and short dash black line is observed historical mean.

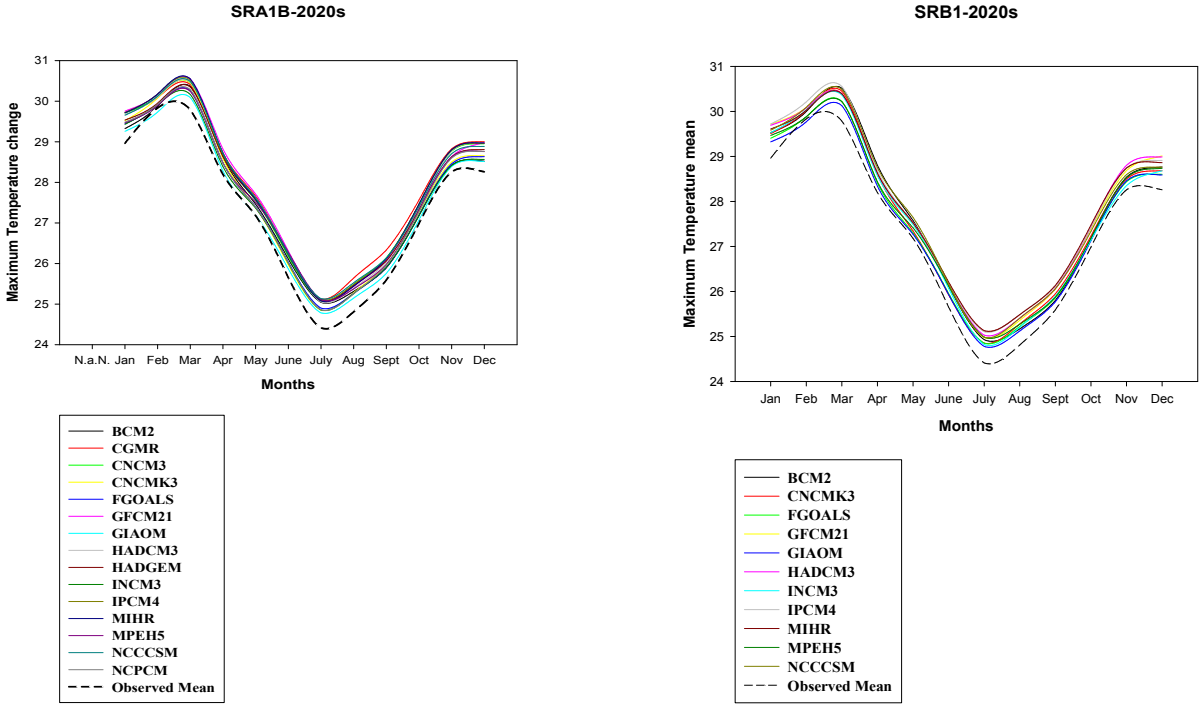

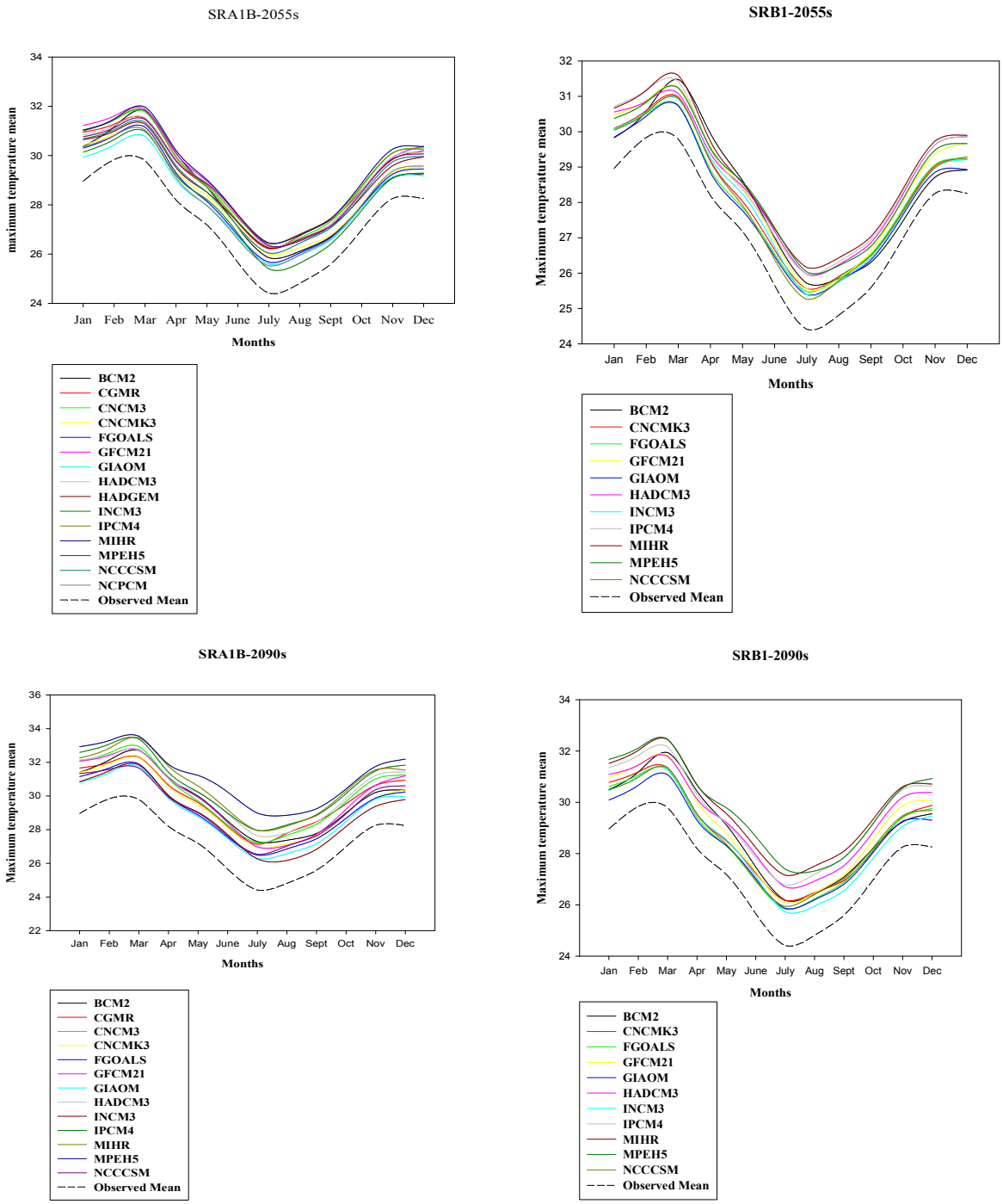

Figure 2: Monthly 15 GCMs model output of Simulated Versus Observed maximum temperature under two emission scenarios and three time periods. The solid lines show mean of each 15GCMs output and short dash black line is observed historical mean.

SRA1B-2020s

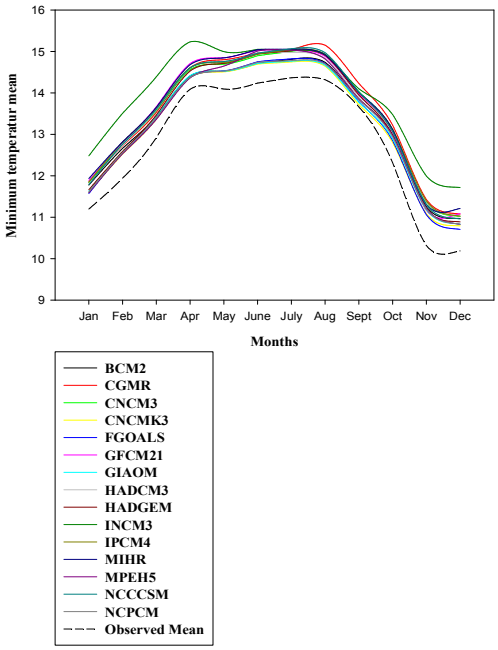

SRB1-2020s

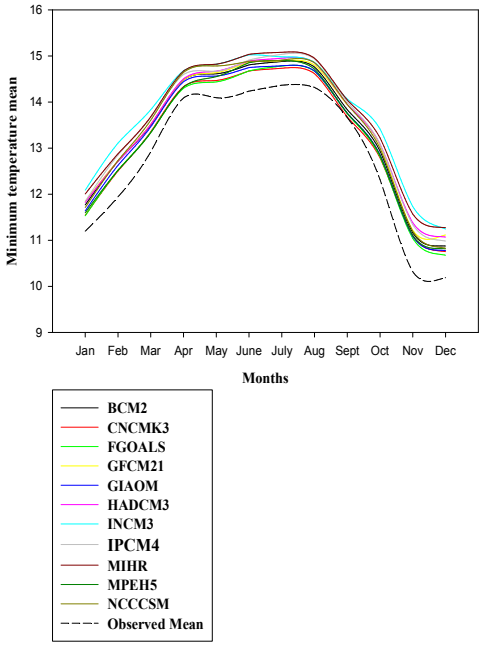

SRA1B-2055s

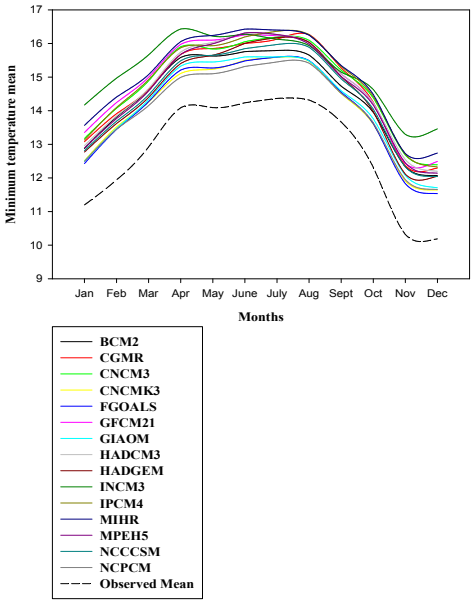

SRB1-2055s

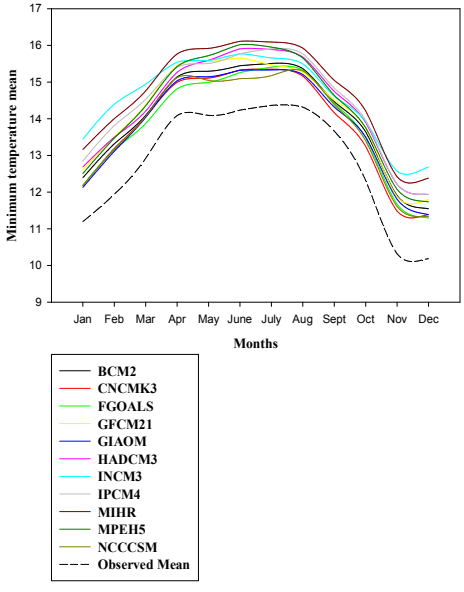

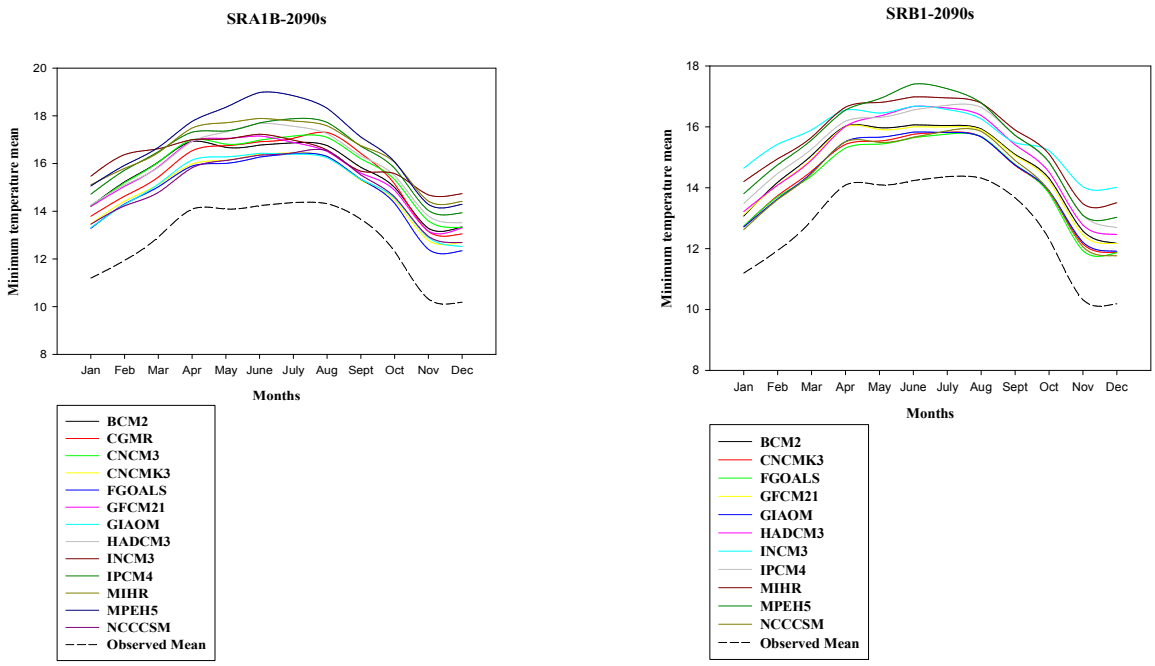

Figure 3: Monthly 15 GCMs model output of Simulated Versus Observed minimum temperature under two emission scenarios and three time periods. The solid lines show mean of each 15GCMs output and short dash black line is observed historical mean.